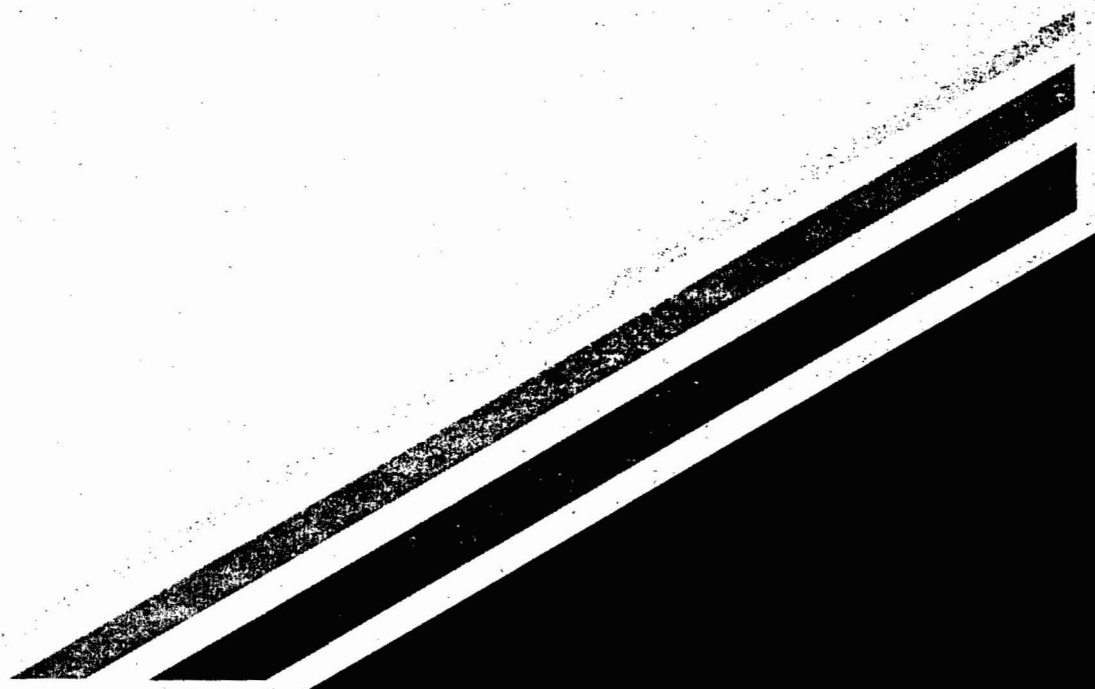




CONTRACT NO. A132-149  
FINAL REPORT  
MARCH 1994

# Regional Estimates of Acid Deposition Fluxes in California



**CALIFORNIA ENVIRONMENTAL PROTECTION AGENCY**



**AIR RESOURCES BOARD  
Research Division**



# Regional Estimates of Acid Deposition Fluxes in California

Final Report

Contract No. A132-149

*Prepared for:*

California Air Resources Board  
Research Division  
2020 L Street  
Sacramento, California 95814

*Prepared by:*

Charles L. Blanchard  
Harvey Michaels

Envair  
956 Kains Avenue  
Albany, California 94706

March 1994



## **DISCLAIMER**

The statements and conclusions in this report are those of the contractor and not necessarily those of the California Air Resources Board. The mention of commercial products, their source, or their use in connection with material reported herein is not to be construed as either an actual or implied endorsement of such products.



## ABSTRACT

Acidic deposition occurs via precipitation, fog, cloud water, and dry deposition. Each of these processes is potentially important in California. The specific objectives of this project were to (1) evaluate the quality of the available deposition data; (2) compute estimates of the deposition of each species of interest, by mode of deposition, at each monitoring location in California having sufficient data available; (3) generalize the estimated deposition amounts to larger regions of interest, to the extent possible; (4) compare wet with dry deposition; and (5) identify measurement and methodological requirements for improving the results.

Sulfate and nitrate deposition via precipitation were each less than 8 kilograms per hectare per year ( $\text{kg ha}^{-1} \text{ yr}^{-1}$ ); excess sulfate (i.e., excluding sea-salt sulfate), ammonium, and calcium deposition were less than  $3 \text{ kg ha}^{-1} \text{ yr}^{-1}$ . Wet deposition uncertainties were less than 20 percent in the South Coast Air Basin, which has a large number of monitors; uncertainties can be up to 100 percent in portions of northeastern and southeastern California, where little monitoring has been done.

The dry-deposition flux estimates are subject to uncertainties on the order of 50 percent. Estimated dry deposition of nitric acid ( $\text{HNO}_3$ ) at the 10 monitoring sites ranged from 1 to  $87 \text{ kg ha}^{-1} \text{ yr}^{-1}$ . At the 7 urban sites,  $\text{HNO}_3$  deposition accounted for 50 to 80 percent of the deposition of oxidized nitrogen species and 40 to 70 percent of the total nitrogen deposition.

At the three nonurban sites, wet nitrate and sulfate deposition approximately equalled or slightly exceeded dry deposition of oxidized nitrogen and sulfur species. In contrast, dry sulfur deposition at the urban sites was approximately 1 to 3 times the magnitude of wet sulfur deposition; dry deposition of oxidized nitrogen species at the urban sites ranged from about 5 to 30 times the magnitude of wet nitrate deposition. At all sites, dry deposition of reduced nitrogen species (ammonia and particulate ammonium) was about a factor of 2 greater than wet ammonium deposition.

## ACKNOWLEDGMENTS

Many people assisted us in this project. We thank J. Gardner for assistance with the data bases and M. Blanchard and S. Tanenbaum for assistance with the kriging analyses. S. Golding edited a draft version of this report. T. Meyers provided computer programs and much helpful advice. L. Dolislager obtained ozone data and compiled 12-hour average ozone concentrations for us. R. Rothacker and M. Redgrave provided us with data for particulate matter (PM10), sulfur dioxide (SO<sub>2</sub>), and nitrogen oxides (NO<sub>x</sub>). We also benefitted from conversations with P. Solomon and S. Hering. Finally, we wish to thank N. Motallebi, our contract manager, who obtained data, located missing information, provided advice, and, in numerous other ways, facilitated this project.

This report was submitted in fulfillment of contract number A132-149, "Regional Estimates of Acid Deposition Fluxes in California," under the sponsorship of the California Air Resources Board. Work was completed as of 31 March 1994.

## TABLE OF CONTENTS

GLOSSARY .....	-vii-
SUMMARY .....	S-1
INTRODUCTION .....	S-1
OBJECTIVES .....	S-1
APPROACH .....	S-2
PRINCIPAL FINDINGS .....	S-2
Wet Deposition .....	S-2
Dry Deposition .....	S-3
Comparison of Wet and Dry Deposition .....	S-3
Comparison of Deposition and Emissions .....	S-4
Limitations .....	S-4
RECOMMENDATIONS .....	S-5
PART I: WET DEPOSITION .....	I-1
INTRODUCTION .....	I-1
Objectives .....	I-1
Overview of Part I .....	I-1
METHODS .....	I-1
Use of Kriging for Spatial Interpolation of Acidic Deposition ...	I-1
Data Availability .....	I-7
Data Quality .....	I-11
Specification of Variables of Interest .....	I-16
Temporal and Spatial Resolution .....	I-17
Procedures for Uncertainty Analysis .....	I-18
Implementation of Kriging Procedures .....	I-18
RESULTS .....	I-21
Evaluation of the Methods .....	I-21
Summary Results .....	I-28
PART II: DRY DEPOSITION .....	II-1
INTRODUCTION .....	II-1
Objectives .....	II-1
Overview of Part II .....	II-1
METHODS .....	II-1
Use of the Inferential Method .....	II-1
Data Availability .....	II-4
Data Quality .....	II-6
Specification of Variables of Interest .....	II-19
Calculation of Deposition Velocities: The Oak Ridge/EPA Dry- deposition Program .....	II-19
Calculation of Deposition Velocities and Fluxes: Outline of the	

<b>Program Flow</b> .....	II-20
<b>RESULTS</b> .....	II-31
<b>Summary Results</b> .....	II-31
<b>Sensitivity Analyses</b> .....	II-35
<b>PART III: SYNTHESIS</b> .....	III-1
<b>SUMMARY</b> .....	III-1
<b>Wet Deposition</b> .....	III-1
<b>Dry Deposition</b> .....	III-3
<b>Comparison of Wet and Dry Deposition</b> .....	III-4
<b>Comparison of Deposition and Emissions Estimates</b> .....	III-5
<b>LIMITATIONS</b> .....	III-6
<b>RECOMMENDATIONS</b> .....	III-6
<b>REFERENCES</b> .....	R-1
<b>APPENDIX: DEPOSITION AND UNCERTAINTY MAPS FOR PRECIPITATION AND PRECIPITATION CHEMISTRY</b> .....	A-1

## LIST OF TABLES

1.	Replicability of wet-deposition measurement parameters . . . . .	I-12
2.	Accuracy estimates for CADMP wet-deposition data . . . . .	I-13
3.	Comparison of measurements taken at collocated CADMP and NADP/NTN samplers. . . . .	I-15
4.	Distribution of fractional cross-validation errors for precipitation amount . .	I-22
5.	Distribution of kriging coefficients of variation for precipitation amount . . .	I-23
6.	Distribution of fractional cross-validation errors for nitrate deposition . . . .	I-24
7.	Distribution of kriging coefficients of variation for nitrate deposition . . . . .	I-25
8.	Sites having the largest fractional cross-validation errors for nitrate deposition . . . . .	I-26
9.	Distribution of fractional cross-validation errors for nitrate deposition kriged directly . . . . .	I-27
10.	Distribution of kriging coefficients of variation for nitrate and sulfate deposition, water year 1984-1985 . . . . .	I-27
11.	Annual nitrate deposition ( $\text{kg ha}^{-1} \text{ yr}^{-1}$ ) by site and CARB sample year . . .	I-29
12.	Mean annual wet deposition of nitrate, sulfate (not adjusted for sea salt), ammonium, and calcium . . . . .	I-30
13.	Results for regression of denuder-difference $\text{HNO}_3$ and filter-pack nitrate against ozone . . . . .	II-13
14.	Percentage of usable dry-deposition samples . . . . .	II-16
15.	Percentage of samples exceeding minimum detection limits for all sites and selected chemical species. . . . .	II-17
16.	Percentage of samples exceeding limits of quantification for all sites and selected chemical species. . . . .	II-18
17.	Mean quarterly and annual dry deposition at Azusa . . . . .	II-32
18.	Mean quarterly and annual dry deposition at Bakersfield . . . . .	II-32
19.	Mean quarterly and annual dry deposition at Fremont . . . . .	II-32
20.	Mean quarterly and annual dry deposition at Gasquet . . . . .	II-33
21.	Mean quarterly and annual dry deposition at Los Angeles . . . . .	II-33
22.	Mean quarterly and annual dry deposition at Long Beach . . . . .	II-33
23.	Mean quarterly and annual dry deposition at Sacramento . . . . .	II-34
24.	Mean quarterly and annual dry deposition at Sacramento collocated monitor . . . . .	II-34
25.	Mean quarterly and annual dry deposition at Santa Barbara . . . . .	II-34
26.	Mean quarterly and annual dry deposition at Sequoia . . . . .	II-35
27.	Mean quarterly and annual dry deposition at Yosemite . . . . .	II-35
28.	Parameters affecting canopy resistance, by species . . . . .	II-37
29.	Sensitivity of dry deposition estimates at Azusa to surface . . . . .	II-38
30.	Sensitivity of dry deposition estimates at Bakersfield to surface . . . . .	II-38
31.	Sensitivity of dry deposition estimates at Fremont to surface . . . . .	II-38
32.	Sensitivity of dry deposition estimates at Gasquet to surface . . . . .	II-39
33.	Sensitivity of dry deposition estimates at Los Angeles to surface . . . . .	II-39

34.	Sensitivity of dry deposition estimates at Long Beach to surface . . . . .	II-39
35.	Sensitivity of dry deposition estimates at Sacramento to surface . . . . .	II-40
36.	Sensitivity of dry deposition estimates at Santa Barbara to surface . . . . .	II-40
37.	Sensitivity of dry deposition estimates at Sequoia to surface . . . . .	II-40
38.	Sensitivity of dry deposition estimates at Yosemite to surface . . . . .	II-41
39.	Mean annual dry deposition ( $\text{kg ha}^{-1}$ ) using 12-hour and 24-hour deposition velocity and concentration averages . . . . .	II-43
40.	Sensitivity of mean annual dry deposition ( $\text{kg ha}^{-1}$ ) to ten percent decreases and increases in $\sigma_{\Theta}$ . . . . .	II-47
41.	Mean annual wet deposition of sulfate (as S, not adjusted for sea salt), nitrate (as N), ammonium (as N), total nitrogen, and calcium . . . . .	III-2
42.	Mean annual dry deposition of sulfur and nitrogen . . . . .	III-4

## LIST OF ILLUSTRATIONS

1.	Example variograms calculated from National Weather Service (NWS) precipitation amount data .....	I-4
2.	Locations of CADMP and NADP/NTN monitoring sites .....	I-8
3.	Locations of NWS precipitation stations .....	I-10
4.	Depth-weighted annual nitrate concentration vs. annual precipitation amount .....	I-20
5.	Locations of CADMP dry-deposition monitoring sites. ....	II-5
6.	Denuder difference HNO <sub>3</sub> and filter-pack nitrate vs. time .....	II-7
7.	PM10 and denuded particulate nitrate concentrations at four sites. ....	II-9
8.	Example comparison of CADMP to routine CARB PM10 data .....	II-11
9.	Time series of daytime NO <sub>2</sub> at four CADMP sites. ....	II-12



## GLOSSARY

°C	degrees Celsius
Ca <sup>2+</sup>	calcium ion
CADMP	California Acid Deposition Monitoring Program
CARB	California Air Resources Board
Cl <sup>-</sup>	chloride ion
cm	centimeter
CV	coefficient of variation
DRI	Desert Research Institute
EPA	Environmental Protection Agency
eq	equivalent
g	gram
H <sup>+</sup>	hydrogen ion
ha	hectare
HNO <sub>3</sub>	nitric acid
K <sup>+</sup>	potassium ion
kg	kilogram
km	kilometer
L	liter
m	meter
M	molar
mb	millibar
Mg <sup>2+</sup>	magnesium ion
ml	milliliter
mm	millimeter
μg	microgram
μg m <sup>-3</sup>	micrograms per cubic meter
μeq L <sup>-1</sup>	micro-equivalents per liter (a unit of concentration)
μS cm <sup>-1</sup>	micro-Siemen per cm (a unit of conductance)
N	nitrogen
Na <sup>+</sup>	sodium ion
NADP/NTN	National Atmospheric Deposition Program/National Trends Network
NH <sub>3</sub>	ammonia
NH <sub>4</sub> <sup>+</sup>	ammonium ion
NO <sub>x</sub>	nitrogen oxides
NO <sub>3</sub> <sup>-</sup>	nitrate ion
NWS	National Weather Service
O <sub>3</sub>	ozone
pH	negative base 10 logarithm of the hydrogen ion concentration
PM10	particulate matter 10 microns and smaller
PM2.5	particulate matter 2.5 microns and smaller
pNH <sub>4</sub> <sup>+</sup>	particulate ammonium
pNO <sub>3</sub> <sup>-</sup>	particulate nitrate

pSO <sub>4</sub> <sup>2-</sup>	particulate sulfate
ppb	parts per billion
pphm	parts per hundred million
ppm	parts per million
QA/QC	quality assurance/quality control
S	sulfur
SoCAB	South Coast Air Basin
SO <sub>2</sub>	sulfur dioxide
SO <sub>4</sub> <sup>2-</sup>	sulfate ion
TDLAS	Tunable Diode Laser Absorption Spectroscopy
USGS	U.S. Geological Survey
V <sub>d</sub>	deposition velocity
VOC	volatile organic compound
W	Watt
xSO <sub>4</sub> <sup>2-</sup>	excess sulfate: sulfate concentration with estimated sea-salt sulfate concentration removed
yr	year

## SUMMARY

### INTRODUCTION

Acidic deposition occurs via precipitation, fog, cloud water, and dry deposition. Each of these processes is potentially important in California.

The California Acid Deposition Monitoring Program (CADMP) was established to provide information about the concentrations and mass fluxes of acidic species delivered by precipitation, fog, cloud water, and dry deposition. The CADMP has four objectives:

- To identify the range of chemical concentrations and mass deposition occurring in California;
- To provide data to be used as inputs for studies of the effects of acidic deposition in California;
- To provide data that may be useful in establishing relationships between regions that are sources of precursor emissions and regions that receive acidic deposition;
- To identify possible time trends in concentration or deposition amounts.

This project addresses the first objective.

The measurement and calculation of mass fluxes at any one location requires appropriate monitoring methods and, in the case of dry deposition, an appropriate model to be applied to the monitoring data. After concentrations or fluxes have been measured (or computed) at specific sites, it is usually necessary to generalize the results to larger regions. The problem addressed by this work is thus twofold. First, we compute estimates of the deposition of each species of interest, by mode of deposition, at each monitoring location in California having sufficient data available. Second, we generalize the estimated deposition amounts to larger regions of interest, to the extent possible.

### OBJECTIVES

The specific objectives of this project are to

1. Evaluate the quality of the available deposition data;
2. Compute estimates of the deposition of each species of interest, by mode of deposition, at each monitoring location in California having sufficient data available;
3. Generalize the estimated deposition amounts to larger regions of interest, to the

- extent possible;
4. Compare wet with dry deposition;
  5. Identify measurement and methodological requirements for improving the results.

## APPROACH

We used precipitation-chemistry data from the CADMP and the National Atmospheric Deposition Program/National Trends Network (NADP/NTN) to calculate the fluxes of chemical species delivered via precipitation. We then interpolated from the monitoring sites to the state as a whole by using a statistical procedure, kriging, which quantifies both the interpolated values and the interpolation errors, thus yielding estimates for the uncertainties in isopleths. We carried out calculations for six years, 1985 through 1990.

The CADMP dry-deposition network was designed with the intent of implementing a procedure known as the inferential method. In this approach, the flux of a particular species is calculated as the product of its ambient concentration and a velocity, known as the deposition velocity,  $V_d$ . Deposition velocity generally depends on both the nature of the pollutant and the surface. We used a set of calculational procedures, developed at Oak Ridge National Laboratory, to carry out the calculations. The period of record began with the inception of the CADMP dry-deposition network in early 1988 and continued through September 1991.

We evaluated the quality of the CADMP data through a set of statistical analyses and by comparison of the CADMP dry-deposition data to collocated measurements of  $O_3$ , nitrogen dioxide ( $NO_2$ ), sulfur dioxide ( $SO_2$ ), particulate matter 10 microns and smaller (PM10), PM10-nitrate, PM10-sulfate, and PM10-ammonium, obtained from routine CARB aerometric monitoring sites.

## PRINCIPAL FINDINGS

### Wet Deposition

Sulfate and nitrate deposition were each less than  $8 \text{ kg ha}^{-1} \text{ yr}^{-1}$ ; excess sulfate (i.e., excluding sea-salt sulfate), ammonium, and calcium deposition were less than  $3 \text{ kg ha}^{-1} \text{ yr}^{-1}$ . For comparison, wet sulfate and nitrate deposition in portions of eastern North America exceed  $25$  and  $15 \text{ kg ha}^{-1} \text{ yr}^{-1}$ , respectively (Sisterson, 1991); ammonium and calcium deposition are less than about  $4$  and  $2.5 \text{ kg ha}^{-1} \text{ yr}^{-1}$  in almost all parts of eastern North America (Sisterson, 1991).

In most years, nitrate deposition was greater in the South Coast Air Basin (SoCAB) and the southern Sierra Nevada than in other parts of California.

Deposition uncertainties were less than 20 percent in the SoCAB, which has a large number of monitors; uncertainties can be up to 100 percent in portions of northeastern and southeastern California, where little monitoring has been done.

### **Dry Deposition**

This project has produced new estimates of dry-deposition fluxes at 10 sites in California. These estimates will help improve our understanding of the magnitude of dry deposition in California. However, the calculations are limited in numerous important respects and they could likely be improved over time with additional effort. The dry-deposition flux estimates are subject to uncertainties of approximately 50 percent.

CADMP samples are now collected over 12-hour intervals. Nitric acid ( $\text{HNO}_3$ ) fluxes would be underestimated by 30 to 40 percent at all sites except Gasquet if samples were collected as 24-hour averages rather than 12-hour averages (at Gasquet,  $\text{HNO}_3$  was frequently below detection limits).  $\text{O}_3$  fluxes would be underestimated by seven to 23 percent at all sites except Sequoia and Yosemite if samples were collected as 24-hour averages rather than 12-hour averages (Sequoia and Yosemite showed very weak diurnal variations in ozone concentration).

Estimated deposition of  $\text{HNO}_3$  at the 10 sites ranges from 1 to 87  $\text{kg ha}^{-1} \text{yr}^{-1}$ . At the urban sites,  $\text{HNO}_3$  deposition accounts for 50 to 80 percent of the deposition of oxidized nitrogen species and 40 to 70 percent of the total nitrogen deposition.

Annual rates of deposition of oxidized nitrogen species at the three rural sites (Gasquet, Sequoia, and Yosemite) are about one-tenth to one-half as great as the values reported by Meyers et al. (1991) for sites in the eastern United States. The deposition rates calculated for the rural CADMP sites are quite uncertain because many of the measurements were below the limits of quantification. The rates of nitrogen deposition at Azusa, Bakersfield, Long Beach, and Los Angeles exceed those reported by Meyers et al. (1991) by factors of 2 to 17.

### **Comparison of Wet and Dry Deposition**

At the three nonurban sites (Gasquet, Yosemite, and Sequoia), wet nitrate and sulfate deposition approximately equalled or slightly exceeded dry deposition of oxidized nitrogen and sulfur species. In contrast, dry sulfur deposition [ $\text{SO}_2$  and particulate sulfate ( $\text{pSO}_4^{2-}$ )] at the urban sites was approximately 1 to 3 times the magnitude of wet sulfur deposition. At the urban sites, dry deposition of oxidized nitrogen species [ $\text{HNO}_3$ ,  $\text{NO}_2$ , and particulate nitrate ( $\text{pNO}_3^-$ )] ranged from about 6 to 35 times the magnitude of wet nitrate deposition. At all sites, dry deposition of reduced nitrogen species [ammonia ( $\text{NH}_3$ )]

and particulate ammonium ( $\text{pNH}_4^+$ ) was about a factor of 2 greater than wet ammonium deposition.

Despite the large estimated uncertainties in the dry deposition estimates, dry deposition of sulfur and nitrogen can be seen to range from approximately equal to wet deposition to many times greater.

### **Comparison of Deposition and Emissions**

The calculated rates of deposition of oxidized nitrogen species at the SoCAB stations ranged from 22 to 52 percent of the SoCAB  $\text{NO}_x$  emission density, suggesting that a substantial portion of these emissions would be deposited within the basin. In contrast, the rate of dry deposition of oxidized nitrogen species at Fremont is about 13 percent of the rate of  $\text{NO}_x$  emissions within the San Francisco Bay area. However, deposition rates could be greater at some other locations within this area. The estimated oxidized nitrogen dry deposition rates at Bakersfield and Sacramento exceed the  $\text{NO}_x$  emissions rates in the San Joaquin and Sacramento air basins. However, these basins are large and include much rural or mountainous land; emissions would be more concentrated in the urban areas, where the monitoring sites were located.

### **Limitations**

Wet-deposition flux estimates are based on data obtained using a proven monitoring technique and a reasonably dense network of stations. The most significant source of potential bias is underestimation of precipitation amounts in alpine regions. We were unable to make use of data from the alpine network because its period of record barely overlapped that of the CADMP data; however, in future years, the alpine-network data will be available for use. The uncertainties in our regionalized estimates of wet deposition vary spatially and among chemical species; they are typically in the range of 20 to 50 percent for the species and areas of greatest interest.

In contrast, both the measurements and the model used to calculate dry deposition are subject to potentially large uncertainties. At present, outstanding questions remain regarding the accuracy of the denuder difference  $\text{HNO}_3$  concentrations. Moreover, the expected uncertainties in dry deposition flux estimates calculated according to the inferential method are on the order of 50 percent.

It is premature to attempt to regionalize the dry deposition estimates. Because 30 to 70 percent of the dry nitrogen deposition occurred via deposition of  $\text{HNO}_3$ , it is first necessary to establish the accuracy of the  $\text{HNO}_3$  measurements. Measurements of particulate sulfate and nitrate,  $\text{SO}_2$ , and  $\text{NO}_2$  are available from a large number of monitors in California; these measurements may be of use in generalizing the dry deposition estimates. The necessary meteorological measurements do not exist at routine monitoring sites; however, the available concentration data might be of use in bounding the dry

deposition of rates of these species. In contrast to these routinely available measurements, no routine measurements of  $\text{HNO}_3$  exist.

## RECOMMENDATIONS

We offer the following recommendations for consideration:

1. Particular effort should be devoted to resolving the questions pertaining to accurate measurement of nitric acid. At many locations, it is the largest component of total nitrogen deposition. Therefore, accurate measurement is critical.
2. The  $\text{HNO}_3$  fluxes calculated for 24-hour intervals were 30 to 40 percent lower than those calculated for 12-hour intervals at 9 of the 10 sites. If the CADMP dry-deposition sampling interval were increased from 12 to 24 hours, methods should be developed for correcting the resulting underestimation of  $\text{HNO}_3$  deposition.
3. Comparison of results obtained from application of the inferential method and from micrometeorological studies would be highly desirable. Lacking such a comparison, we cannot evaluate the accuracies of the calculated deposition amounts.
4. Approximately three additional years of wet and dry deposition data, now being validated, will become available soon. Consideration should be given to updating the wet deposition estimates and, pending resolution of measurement questions, the dry deposition estimates as well.
5. If analyses of trends are of interest, they should be carried out for the ambient air concentrations, rather than the calculated dry-deposition fluxes, because many uncertainties are introduced in the process of calculating fluxes.



# **PART I: WET DEPOSITION**

## **INTRODUCTION**

### **Objectives**

The specific objectives of this part of the project are to

1. Evaluate the quality of the available precipitation-chemistry data;
2. Compute estimates of the wet deposition of each species of interest at each monitoring location in California having sufficient data;
3. Generalize the estimated deposition amounts to larger regions of interest.

### **Overview of Part I**

We first summarize the methods used. We describe the interpolation procedure (kriging) in some detail; though it has been applied to acidic deposition by several workers in recent years, the approach is probably unfamiliar to most readers. We then briefly describe the data that are available and discuss the quality of these data. We identify the variables and the spatial and temporal scales of interest. Finally, we describe the methods used in uncertainty analysis and present summary results.

## **METHODS**

### **Use of Kriging for Spatial Interpolation of Acidic Deposition**

**Description of kriging procedures.** A number of possible procedures are available for interpolating the precipitation monitoring data. Both deterministic and stochastic (i.e., the variable of interest is generated by a random field) interpolation methods appear in the literature (Federov, 1989). For many environmental applications, stochastic procedures have proved quite useful (e.g., Ripley, 1981).

A particularly attractive option is kriging, which is a stochastic approach encompassing a family of procedures. These procedures were originally developed for geostatistical applications (Journel and Huijbregts, 1978). Kriging uses the similarities in the measurements taken at different sites to determine a set of weights; weighted averages of the observations are then used to generate the unknown point or regional estimates. Kriging is attractive because it quantifies the interpolation errors, thus yielding estimates for the uncertainties in isopleths. When the assumptions of the kriging methodology are fulfilled, kriging provides the best linear unbiased estimator in the sense that it minimizes

the variance of the estimation error (Journel and Huijbregts, 1978).

We briefly describe some key characteristics and limitations of kriging. All forms of kriging model the spatial correlation (or spatial covariance) in the data; the terms "spatial correlation" or "spatial covariance" simply refer to the degree of similarity of two measurements taken at two different locations. Several forms of kriging exist, which differ in some of the underlying assumptions.

"Simple kriging" assumes that a variable can be represented as:

$$Z(x,y) = \mu_Z + \epsilon(x,y) \quad , \quad (1)$$

where  $\mu_Z$  is fixed and  $\epsilon(x,y)$  is a stochastic component. Fixing  $\mu_Z$  implies that the spatial variation is entirely random in character, i.e., the true local means are identical to the global mean over the entire domain. For most environmental applications, this assumption is inappropriate (e.g., mean deposition in the Sierra is not the same as in Los Angeles). Although applying simple kriging to cases in which the mean is not constant over the domain will not give incorrect isopleths, it will inflate the uncertainties in the isopleths.

"Ordinary kriging" assumes that the mean varies spatially and therefore uses only samples in a local neighborhood of the point or area for which an estimate is needed. The interpolation estimates are usually generated by restricting the area in which data are used to an ellipse centered on the point or area. In this way, ordinary kriging allows for a nonstationary mean.

"Universal kriging" fits a so-called drift function to the spatial pattern. The drift function is assumed to be known (not estimated from the data). However, universal kriging is not commonly employed because it requires information to specify the drift function, which is usually unavailable.

A further useful distinction is that between point kriging and block kriging. Point kriging is used to estimate the value at a point from nearby sample values. It would be of use, for example, in filling in missing grid points. Block kriging estimates the value for a block (i.e., an area or grid cell) from a set of nearby points. Block kriging is more appropriate for generating isopleths.

Journel (1989) summarizes kriging in terms of the following principal steps:

1. Define an area that is sufficiently homogeneous to warrant statistical averaging within it;
2. Use the data within this area to calculate the observed patterns of spatial variability (spatial correlation);

3. Develop a model of the observed spatial correlation;
4. Use the model along with traditional regression methods to interpolate.

Journel (1989) points out that all statistical methods (including kriging) involve the practice of discerning a domain over which stationarity (i.e., a constant mean) is appropriate. The size of the domain over which stationarity is an acceptable approximation determines the area over which the calculated averages will be considered representative.

Kriging models the spatial correlation in terms of the variogram, which is:

$$2\gamma(\mathbf{h}) = E\{[Z(\mathbf{x}) - Z(\mathbf{x} + \mathbf{h})]^2\} \quad , \quad (2)$$

where  $2\gamma(\mathbf{h})$  denotes the variogram (without the factor of 2, it is known as the semi-variogram),  $E$  signifies expected value,  $\mathbf{x}$  is the location vector,  $\mathbf{h}$  is a vector (which represents distance and direction), and  $Z$  is the variable to be interpolated. This model implies that the degree of similarity between two points is a function of the distance and direction between them, but not of their location.

In practice, the variogram is not known; it must be estimated from the data. The estimator is

$$\gamma_{Z(\mathbf{x}), Z(\mathbf{x} + \mathbf{h})} = [1/n(\mathbf{h})] \sum_{\alpha=1}^{n(\mathbf{h})} [z(x_{\alpha}) - z(x_{\alpha} + \mathbf{h})]^2 \quad , \quad (3)$$

where  $\mathbf{h}$  represents a binned distance and direction [e.g., distances from 0 to 10 kilometers (km) and directions from west-northwest to east-northeast] and  $n(\mathbf{h})$  is the number of site pairs within the category  $\mathbf{h}$ .

For illustration, Figure 1 shows a variogram obtained by us for precipitation amount. The variogram is expressed as a function only of distance (not direction) in this case.

Some key terms used in describing variograms are:

- **Nugget:** the y-intercept;
- **Sill:** the asymptotic value of the variogram;
- **Range:** the distance over which the variogram reaches a specified portion (e.g., 95 percent) of its sill.

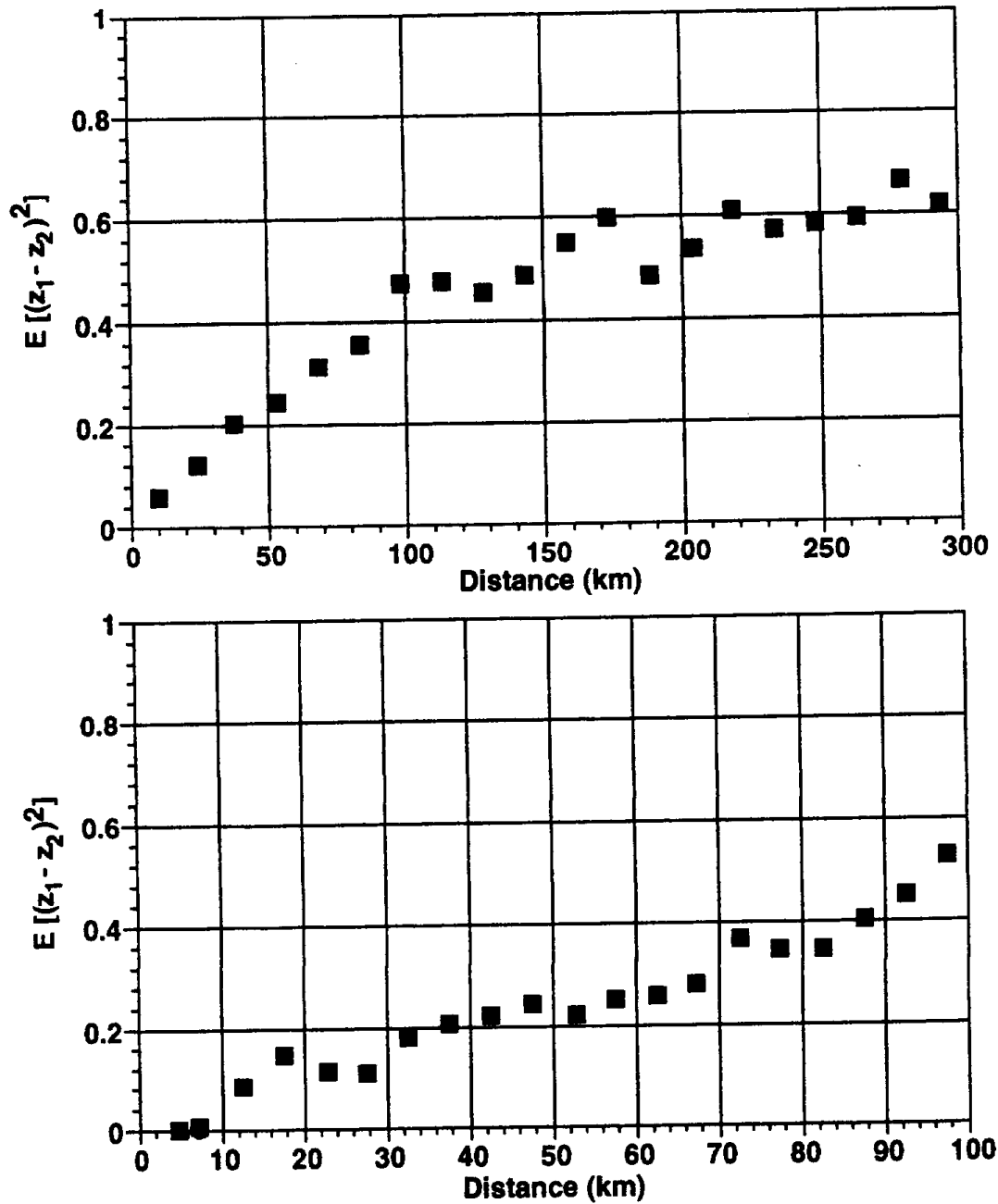


Figure 1. Example variograms calculated from National Weather Service (NWS) precipitation amount data (quarterly average, January-March 1988). Variogram units are squared differences of the log-transformed precipitation amounts (inches). Binned distances of 15 km (top) and 5 km (bottom) were used.

The simplest assumption that can be made regarding the covariance structure is that the covariance between any two stochastic terms  $\epsilon(x_1, y_1)$  and  $\epsilon(x_2, y_2)$  is a function only of the distance between them; in this case, the covariance structure is said to be homogeneous (independent of location) and isotropic (independent of direction). However, the covariance function need not be homogeneous and isotropic. For example, covariances can be stronger in one direction than another. All forms of kriging allow for inhomogeneity and anisotropy, though, in practice, the data may be inadequate for estimating complex variograms.

**Previous applications of kriging to acidic deposition.** A number of applications of kriging to acidic deposition data have been made (Seilkop and Finkelstein, 1987; Eynon, 1988; Venkatram, 1988; Guertin et al., 1988; Haas, 1990; Haas, 1992). We briefly summarize some of the key findings and criticisms that bear on the present study.

Seilkop and Finkelstein (1987) used simple kriging to estimate patterns and trends in the major ions found in precipitation in eastern North America for the period 1980-1984. The use of simple kriging implies a constant mean, as described above, which may inflate the estimated uncertainties. Eynon (1988) removed the spatial pattern, using a quadratic function, prior to kriging (i.e., he kriged the residuals), which substantially reduced the interpolation errors. Venkatram (1988) also reduced interpolation errors by removing the spatial pattern; he did so by using a simple long-range transport model. The Environmental Monitoring and Assessment Program (EMAP) of the U.S. Environmental Protection Agency (EPA) uses a moving-window kriging method (Haas, 1990; Haas, 1992).

Guertin et al. (1988) argued that deposition, but not depth-weighted concentration, could be kriged, because kriging regionalizes using linear combinations of the observations (i.e., it would generate an arithmetic, rather than a depth-weighted average, across stations). These researchers proposed that deposition (which is additive across stations) be used and that concentration isopleths be generated as the quotient of deposition and precipitation amount.

Federov (1989) critiqued the application of kriging to environmental studies. He notes that kriging cannot guarantee statistical optimality when the means and covariances are unknown and must therefore be estimated from the data (as is generally the case). He proposed alternative approaches, including the use of spatial-temporal models. The development of spatial-temporal models for acidic deposition is an area of active research (e.g., Oehlert, 1992).

Because some controversy exists in the literature concerning the adequacy of the uncertainty estimates of kriging (the kriging standard deviations), we devote particular attention to our uncertainty analyses.

**General approach.** In evaluating previous applications of kriging to acidic deposition data, it appears that isopleth uncertainties can be substantially reduced by

employing more sophisticated approaches than simple kriging. Several options are available for doing so. The use of ordinary kriging is one. A second is employment of a moving-window approach (Haas, 1990; Haas, 1992). A third is to remove the overall spatial pattern and kriging the residuals, following either the approach of Eynon (1988) or that of Venkatram (1988). Of the latter two, the approach followed by Eynon (1988) is much simpler and appears to be more effective: Eynon (1988) reduced the interpolation variances for sulfate, nitrate, and ammonium concentration by factors of 5-20; Venkatram (1988) reduced the interpolation variance for sulfate deposition by a factor of 2 (the comparison is complicated by the use of different sets of monitoring sites in the two studies). Moreover, Venkatram (1988) used a simple long-range transport model to generate a spatial pattern for sulfate deposition only. In California's complex terrain, the adequacy of the model would be questionable. In addition, using a model to predict the spatial patterns for some of the species of interest (e.g., wet ammonium deposition) appears highly problematic. We note that Federov (1989) raised some theoretical concerns regarding the approach taken by Eynon (1989).

We have attempted to adopt an approach that fulfills the basic kriging assumptions to the extent possible and makes use of as much data as possible. Rather than following the purely statistical procedures employed by Eynon (1988), Haas (1990), and Haas (1992), we have attempted to utilize known physical relationships and additional data bases, which, as we will show, reduces the interpolation uncertainties.

We interpolate average adjusted concentrations to one grid and precipitation amounts to another; we then combine these variables to obtain deposition. "Adjusted" refers to the residuals that result from regressing concentration against precipitation amount. In the discussion of results, we show that this approach yields lower uncertainties than would occur if we were simply to interpolate deposition amounts directly. Briefly, the rationale for our approach is the following:

1. Deposition amounts are influenced both by ambient air concentrations and by the amount of precipitation (which is, in turn, a function of frequency and intensity of precipitation). Most of the precipitation-chemistry data show a strong relationship between deposition (or concentration) and precipitation amount on quarterly to annual time scales. Spatial variations in precipitation amount partially explain the spatial variability of the acidic-deposition data. The variability in precipitation amount is, in turn, related to topographical and meteorological variability. The portion of the deposition variability that can be related to variations in precipitation amount should be represented deterministically, not stochastically, to the extent possible. The unexplained portion of the variability in concentrations at various stations can be modeled statistically, using the kriging methodology.
2. If the precipitation-amount field can be resolved well, we will better resolve the deposition fields. Whereas data from fewer than 40 precipitation chemistry sites are available to us, nearly 500 National Weather Service (NWS) stations monitor

precipitation amount (see also later discussion of data).

3. Data are never entirely complete. Incomplete sampling leads to underestimation of deposition amounts; within limits, however, it does not affect the average concentration too much. When average concentration is multiplied by total precipitation amount (from NWS sites), reasonably accurate estimates of deposition amount should result (most of the NWS stations record greater than 95 percent completeness of sampling).

Our method, in effect, combines deterministic and stochastic approaches. It allows for nonstationarity of the mean. Moreover, by removing the functional relationship between concentration and precipitation amount, our data should more closely satisfy the additivity requirements described by Guertin et al. (1988). Our procedure should also permit other kriging assumptions (e.g., homogeneity of the variogram) to be met more adequately. To the extent that the kriging assumptions are not fulfilled exactly, though, the interpolation uncertainties may be underestimated (Federov, 1989). In the section presenting the results, we attempt to evaluate the adequacy of the calculated uncertainties.

#### **Data Availability**

We have available to us CADMP data from July 1984 through June 1990. More recent CADMP data have not yet been validated by the California Air Resources Board (CARB). We also obtained monthly-average precipitation-chemistry data from the NADP/NTN for California and for selected sites in Oregon, Nevada, and Arizona (for 1979 through 1990). Figure 2 shows the locations of CADMP and NADP/NTN sites used in our analyses.

Both CADMP and NADP/NTN use automated Aerochem Metrics collectors, which open automatically with the onset of precipitation and close when precipitation ceases. However, these collectors, which are now widely used for monitoring precipitation chemistry, fail to collect snow well under conditions of large snowfall or moderate-to-heavy winds. Consequently, the CADMP monitors are of limited accuracy at high elevations of the Sierra Nevada. To remedy this shortcoming, the CARB funded a special four-year project to measure wet-deposition fluxes at 10 alpine sites between the Lake Tahoe basin and the region near Mt. Whitney. We have data from the alpine network for the period February 1990 through September 1991. Although there is little overlap between our CADMP and alpine-network data at present, future updates of our calculations would be able to make use of CADMP, NADP/NTN, and alpine-network data.



Figure 2. Locations of CADMP and NADP/NTN monitoring sites.

Both the Pacific Gas and Electric Company (PG&E) and the Southern California Edison Company (SCE) operated precipitation-chemistry networks during periods since the CADMP began functioning (Zeldin and Ellis, 1984; Collins et al., 1987; Saxena et al., 1987). We were unable to obtain the PG&E data, which had been archived. At the time of our inquiry, the SCE data of interest to us were undergoing review, including a comparison with CADMP data. Precipitation-chemistry measurements are available from a number of studies, for limited areas and time periods, prior to the beginning of the CADMP network. However, we have limited our analyses to the period for which CADMP data are available.

We also obtained NWS precipitation-amount data from 492 stations in California, Arizona, Nevada, and Oregon (see Figure 3). Although the large number of stations provides good coverage of California, portions of the alpine Sierra and southeastern desert are not as well covered.

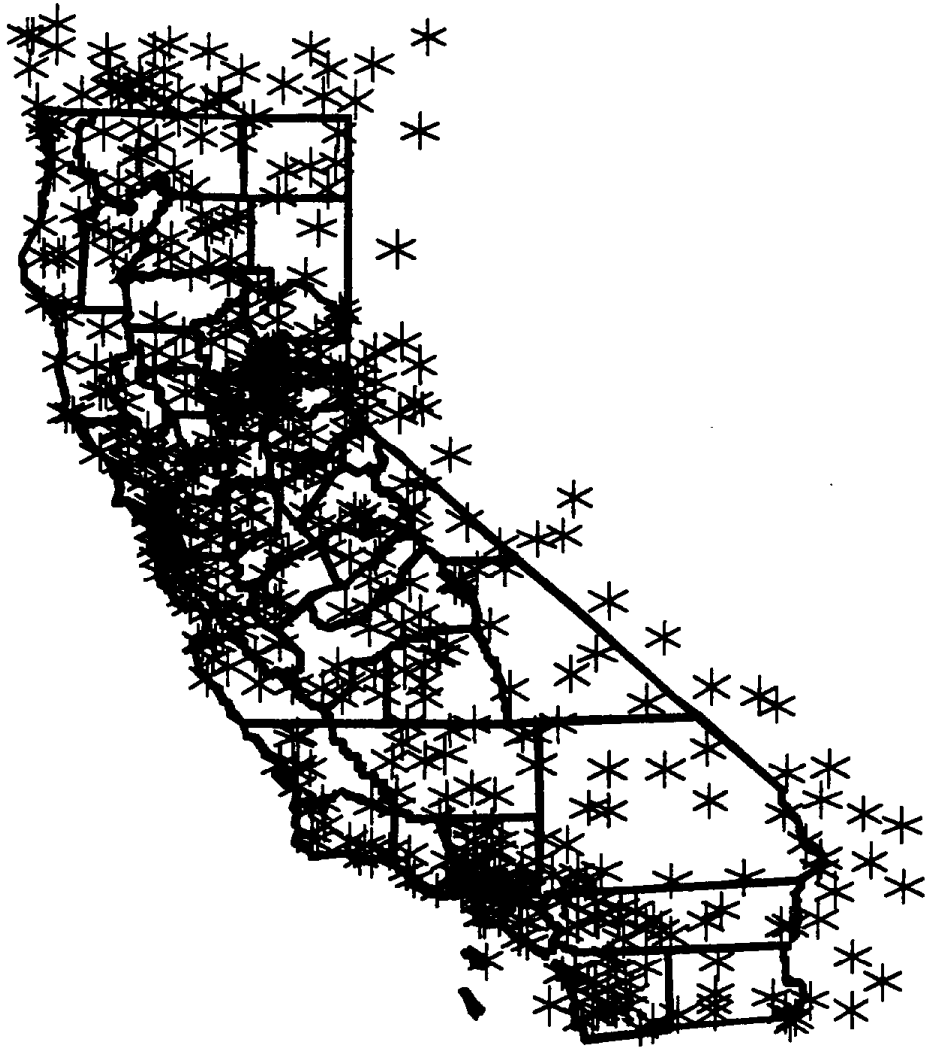


Figure 3. Locations of NWS precipitation stations.

## Data Quality

The CADMP data we used had been carefully reviewed, first by the CARB's El Monte laboratory (Horrocks and Kowalski, 1987) and, second, by that agency's Technical Services Division (TSD), which compiled the CADMP data base. Samples failing to meet quality assurance/quality control (QA/QC) checks were reanalyzed (Horrocks and Kowalski, 1987). The NADP also follows rigorous QA/QC procedures (e.g., Bigelow, 1986; Lockard, 1987; Peden, 1988), which include external audits by the U.S. Geological Survey (USGS) (e.g., See et al., 1989).

**Replicability.** Blanchard and Tonnessen (1993) computed the precisions of individual weekly samples for each of the four pairs of CADMP collocated wet-deposition samplers for the period 1 July 1985 to 30 June 1990 (see Table 1). Sampling variance was calculated as

$$\sigma^2 = \frac{1}{N} \sum_{i=1}^N \frac{(X_i - Y_i)^2}{2} \quad (4)$$

where N precipitation samples have been taken and  $X_i$  and  $Y_i$  denote the  $i$ 'th measurement from the primary and collocated samplers. It is often more useful to express replicability in percentages; we did so, using the following formula to calculate mean coefficients of variation (CVs)

$$\overline{CV} = \frac{1}{N} \sum_{i=1}^N \frac{\sqrt{2(X_i - Y_i)^2}}{X_i + Y_i} \quad (5)$$

The mean CVs, shown in Table 1, vary widely among ion species. Table 1 shows the replicability of weekly measurements; the precisions of quarterly or annual averages would be significantly better (i.e., typically by a factor of 2-3 in the wet season, because quarters might then show up to 10 weeks of precipitation). Thus, for sulfate and nitrate, the precision of quarterly averages would generally be better than 5 percent; for calcium, however, quarterly precision would seldom be better than 10 percent.

**Accuracy.** We obtained QA/QC audit results from the CARB Technical Services Division; they are summarized in Table 2. The audits indicate that any given batch of analyses is subject to an unknown bias of varying magnitude. Calcium measurements appear to have been particularly problematic during some portions of the record. Biases are known to exist for some of those measurements (Blanchard and Tonnessen, 1993).

Table 1. Replicability of wet-deposition measurement parameters for individual samples collected at four monitoring sites with collocated collectors.<sup>(a,b)</sup> Measurement parameters are volume of precipitation collected in the sampler (volume), electrical conductance (Conduct.), and concentrations of inorganic ion species (see "Glossary" for abbreviations of chemical species). Units are fractional coefficients of variation for precision, dimensionless units for number of samples (N), milliliters (ml) for mean volume, micro-Siemen per cm ( $\mu\text{S cm}^{-1}$ ) for mean conductance, and micro-equivalents per liter ( $\mu\text{eq L}^{-1}$ ) for mean concentration for all ion species.

Parameter	Precision (by site)				Mean (by site) <sup>(c)</sup>			
	Sac.	Mon.	G.F.	T.F.	Sac.	Mon.	G.F.	T.F.
N	-	-	-	-	30	89	80	68
Volume	0.04	0.08	0.05	0.05	1666	620	1836	1980
Conduct.	0.04	0.07	0.03	0.05	11.9	7.4	9.0	21.2
Ca <sup>2+</sup>	0.26	0.37	0.34	0.32	8.4	10.9	11.0	17.1
Mg <sup>2+</sup>	0.20	0.24	0.11	0.16	2.6	3.8	2.4	6.5
Na <sup>+</sup>	0.12	0.21	0.22	0.14	7.9	5.1	5.2	19.9
K <sup>+</sup>	0.38	0.38	0.33	0.34	0.8	1.4	1.3	1.3
Cl <sup>-</sup>	0.09	0.17	0.16	0.10	8.9	5.1	5.6	23.3
NO <sub>3</sub> <sup>-</sup>	0.05	0.11	0.06	0.09	22.6	13.9	20.6	39.9
SO <sub>4</sub> <sup>2-</sup>	0.06	0.13	0.05	0.08	18.3	9.8	13.3	25.3
xSO <sub>4</sub> <sup>2-(d)</sup>	0.07	0.14	0.05	0.08	17.3	9.2	12.7	22.9
H <sup>+</sup>	0.13	0.16	0.14	0.13	7.2	7.2	7.2	25.0
NH <sub>4</sub> <sup>+</sup>	0.11	0.18	0.09	0.17	39.6	12.0	25.4	28.2

Notes:

- (a) Based on samples collected from two collectors at each site during sample years 1986 through 1989, computed as the mean coefficient of variation (Equation 5 in the text).
- (b) Sites are Sacramento (Sac.), Montague (Mon.), Giant Forest - Sequoia National Park (G.F.), and Tanbark Flat (T.F.).
- (c) Means were obtained by averaging the primary and secondary weekly measurements, which were then averaged over the sampling period by weighting by precipitation amount.
- (d) Excess sulfate: sulfate concentration with estimated sea-salt sulfate concentration removed. Adjusted using the ratio of sulfate to sodium contained in ocean waters (Stumm and Morgan, 1981).

Table 2. Accuracy estimates for CADMP wet-deposition data by audit date<sup>(a)</sup>.

	Concentration <sup>(b)</sup>		Accuracy (mean percent error) by date <sup>(c)</sup>								
	min	max	1985	1986		1987		1988		1989	
			Oct	Apr	Oct	Apr	Oct	Apr	Oct	Jul	
pH <sup>(d)</sup>	3.19	4.53	+4	<+1	<+1	<+1	<+1	+1	+1	+1	
Conduct.	15.9	322.2	-12	-2	-2	>-1	-3	+3	-2	<-1	
SO <sub>4</sub> <sup>2-</sup>	33.1	356.2	+1	<+1	>-1	+3	+6	-3	+5	+3	
NO <sub>3</sub> <sup>-</sup>	7.9	258.0	-10	-3	-4	>-1	+33	-2	-11	+16	
Cl <sup>-</sup>	8.1	578.2	<1	+3	-6	-3	-7	-18	<-1	+94	
Na <sup>+</sup>	7.3	121.6	+23	-25	+5	+3	-3	-6	+5	+9	
K <sup>+</sup>	1.9	138.9	+18	-4	+19	>-1	-1	-1	+4	+11	
Mg <sup>2+</sup>	0.4	21.6	+23	+27	-1	+5	-8	-0	-7	+9	
Ca <sup>2+</sup>	0.4	311.9	+28	+74	+138	+14	-7	+18	+4	-5	
NH <sub>4</sub> <sup>+</sup>	5.5	258.0	+9	-7	+4	+10	+11	-23	ND	+8	

Notes:

- (a) Obtained from California Air Resources Board (1987), California Air Resources Board (1988), California Air Resources Board (1989), and California Air Resources Board (1990).
- (b) Units are pH units for pH, uS cm<sup>-1</sup> for conductance, and ueq L<sup>-1</sup> for ion concentrations.
- (c) Accuracy estimates are based on EPA performance audits using two to six audit samples on each occasion. For each sample on each occasion, the relative error was computed as the difference between reported and expected concentration divided by the expected concentration, expressed as a percentage. For each ion on each occasion, the relative errors were averaged over the individual audit samples, yielding the tabled values.
- (d) Laboratory pH.

**Comparability of CADMP and NADP data.** The two principal data sets used here are the CADMP and NADP/NTN data.

Table 3 (Blanchard and Tonnessen, 1993) compares the CADMP and NADP/NTN data for the four locations where both networks operate samplers. Although conductance, hydrogen ion, ammonium, and sulfate concentrations are statistically different for depth-weighted means, the differences are small in absolute terms (about 1-3  $\mu\text{eq/L}$  for the three species). The NADP/NTN samples are known to have a fixed bias of about  $-7 \mu\text{eq L}^{-1}$  (Bigelow et al., 1989), which easily accounts for the difference in hydrogen ion shown in Table 3.

One method of handling systematic differences between networks is to establish one as the standard and apply additive or multiplicative adjustment factors to measurements from the other networks. We have decided not to use this method because (1) the differences are small, and (2) CADMP and NADP sites are interspersed, so no gradient will result from systematic differences between them. The differences between the networks will be reflected in our estimates of interpolation uncertainty.

Table 3. Comparison of measurements taken at collocated CADMP and NADP/NTN samplers.<sup>(a)</sup>

Parameter	Unweighted means <sup>(b)</sup>		Depth-weighted means <sup>(c)</sup>		
	Mean Diff. <sup>(d)</sup>	Sig. Prob. <sup>(e)</sup>	CADMP Mean Conc. <sup>(f)</sup>	Mean Diff. <sup>(d)</sup>	Sig. Prob. <sup>(e)</sup>
Amount <sup>(g)</sup>	0.05	0.11	-	-	-
Conduct.	1.49	0.0017	6.08	2.87	0.0046
Ca <sup>2+</sup>	4.7	0.015	3.8	1.1	0.13
Mg <sup>2+</sup>	0.1	0.79	1.9	-0.2	0.34
K <sup>+</sup>	0.5	0.074	0.7	0.1	0.57
Na <sup>+</sup>	0.4	0.70	6.2	0.2	0.65
NH <sub>4</sub> <sup>+</sup>	3.8	0.0001	10.0	2.9	0.0001
NO <sub>3</sub> <sup>-</sup>	2.4	0.16	10.2	0.8	0.12
Cl <sup>-</sup>	1.6	0.02	7.2	0.6	0.069
SO <sub>4</sub> <sup>2-</sup>	-1.2	0.040	6.6	-0.9	0.0003
H <sup>+</sup> <sup>(h)</sup>	4.4	0.0001	7.3	1.5	0.0046

Notes:

- (a) Comparisons are based on paired values of CADMP and NADP/NTN samples that were collected over identical time intervals. Paired differences were computed as CADMP-NADP/NTN; positive differences therefore indicate species for which CADMP values are on average larger. All available paired data from each of the four collocated CADMP-NADP/NTN sites were used (n=206).
- (b) Mean and variance were computed as  $C = (\sum c_i)/n$  and  $\text{var} = [\sum (c_i - C)^2]/(n-1)$ , where  $c_i$  refers to the concentration difference of the  $i$ 'th sample.
- (c) The depth-weighted mean and variance were computed as  $C = (\sum c_i d_i)/\sum d_i$  and  $\text{var} = \{\sum [d_i (c_i - C)^2]\}/\sum d_i$ , where  $c_i$  refers to the concentration difference and " $d_i$ " refers to the depth of the  $i$ 'th sample.
- (d) Mean difference (mean diff.) between CADMP and NADP/NTN. Units are cm for amount,  $\mu\text{S cm}^{-1}$ , for conductance, and  $\mu\text{eq L}^{-1}$  for ion concentrations.
- (e) Significance probability (sig. prob.) refers to a t-test of the hypothesis that the paired difference is zero.
- (f) Mean concentration (mean conc.) determined from the CADMP samples.
- (g) Precipitation amount as determined by the volume of sample in the collector.
- (h) From laboratory measurements of pH.

**Sampling completeness.** Sampling is seldom complete over periods such as a quarter. Most networks rely on measures of sampling completeness to determine the representativeness of period averages. We use the following four measures of sampling completeness, which are employed by NADP/NTN. In describing these measures, "samplers" or "collectors" refer to the devices that collect precipitation samples for chemical analysis:

- CI1 Portion of time that acceptable samples were taken for chemical analysis. Times when the sampler was broken or when the sample was contaminated would be excluded.
- CI2 Portion of time with precipitation depth measurements available. These measurements would normally be from rain gauges, but if a rain gauge were broken, depth measurements would be recorded from samplers.
- CI3 Portion of total recorded precipitation depth for which acceptable samples were taken.
- CI4 Portion of precipitation depth included in collectors relative to depth recorded by rain gauges for periods during which both were operational.

These indicators can be computed from the CADMP weekly data (Blanchard and Tonnessen, 1993) and are included in the monthly data provided by NADP/NTN. In compiling monthly, seasonal, or annual averages from weekly data, NADP requires criterion (2) to be at least 0.90 and the other three criteria to be 0.75. The CARB excludes any week in which the weekly CI4 is less than 0.70.

Sirois (1990) related CI1 and CI3 to the bias of monthly, seasonal, and annual average concentrations. The expected bias of annual average depth-weighted sulfate and nitrate concentrations were less than 6 and 10 percent, respectively, if indicators (1) and (3) were each greater than 80 percent.

### Specification of Variables of Interest

Discussions with CARB staff indicated that the principal variables of interest were sulfate, nitrate, ammonium, calcium, and hydrogen ion deposition. Because hydrogen ion is not conservative, we prefer to base our calculations on acidity. In a carbonate system, mineral acidity is (Stumm and Morgan, 1981)

$$[H\text{-Acidity}] = [H^+] - [HCO_3^-] - 2[CO_3^{2-}] - [OH^-] \quad , \quad (6)$$

where all concentrations are in moles L<sup>-1</sup>. We calculated acidity from pH, K<sub>H</sub> (Henry's constant), and p<sub>CO2</sub> = 10<sup>-3.45</sup> atm [350 parts per million (ppm) at 1 atmosphere]. For ease of comparison with other monitoring programs, we report results in units of kg ha<sup>-1</sup> yr<sup>-1</sup> for

all species except acidity, which we report in grams (g) ha<sup>-1</sup> yr<sup>-1</sup>.

### Temporal and Spatial Resolution

For both temporal and spatial resolution, a trade-off exists between resolution and uncertainty. Temporally, we have used both quarterly and annual averages. We believe that the uncertainties are unacceptably large for anything less than annual resolution (see, also, discussion under "Results"). However, we have attempted to preserve flexibility by creating grid-cell averages on a quarterly basis and then combining them to make annual averages. In this way, the CARB could recombine the quarterly files however desired.

We use the following periods to define quarters:

1. Winter: January - March;
2. Spring: April - June;
3. Summer: July - September;
4. Fall: October - December.

This scheme permits results to be easily combined into calendar years, or USGS water years (1 October - 30 September), or the CARB's sampling years (1 July - 30 June). In this report, we present annual results using CARB sampling years only.

It is difficult to incorporate the alpine network using the temporal aggregation described here because the alpine-network data are based on sampling of the snow pack at the time of maximum accumulation. Rain samples are also collected for analysis at the alpine stations, and results are compiled as water-year averages (1 October - 30 September). Thus, analyses may need to be recomputed according to water year to incorporate the alpine-network data (we did not do so here because the CADMP and alpine-network data barely overlap: alpine-network data commence with water year 1990, but the CADMP does not have a complete water year for 1990).

We created a 40 km by 40 km grid for the state of California. This choice was a compromise between too much and too little resolution. For most of the state, we have insufficient data to adopt a finer resolution (the Los Angeles and San Francisco areas may be exceptions). At the same time, grids coarser than about 40 km seemed likely to be too coarse.

For comparison, other studies involving the interpolation of acid-deposition data have used coarser grids than ours: Seilkop and Finkelstein (1987) used a 4° grid (about 300 to 400 km per side), Guertin et al. (1988) used a grid size of 127 km, Oehlert used rectangles of 1° latitude by 1.5° longitude (about 100 km per side), Haas (1990) and Haas (1992) used

hexagons spaced approximately 150 to 200 km, and the National Acid Precipitation Program (NAPAP) used hexagons with 64 km spacing (Sisterson, 1991). Our network is somewhat denser than those used in the cited studies.

The projection method that we used was a modification of the standard procedure for converting latitude-longitude coordinates to Universal Transverse Mercator (UTM) coordinates. Because California spans two UTM zones, and because UTM zones cannot be aligned and combined, we projected a 12°-width strip (instead of the usual 6° width). It is centered at 120° W longitude (i.e., the California-Nevada border north of Lake Tahoe). The advantage of using UTM coordinates is that the distance scale is the same east-west as north-south.

### **Procedures for Uncertainty Analysis**

We use two approaches to quantify the estimation uncertainties: cross-validation and kriging standard deviations. Cross-validation is a "leave-one-out" method for evaluating accuracy, which is carried out as follows. First, select one station, leave it out, and interpolate its measurement from other stations using the kriging procedures. Repeat this process for each station. Then, generate a file of residuals (observed measurement minus predicted measurement). Finally, summarize key statistics for the residuals, such as the mean error or range of errors.

Cross-validation yields straightforward estimates of the accuracy of the procedure when it is used to estimate point averages. However, because we are estimating cell averages, rather than point measurements, another procedure is also needed. We use the kriging standard deviation for this purpose. The kriging standard deviation is an estimate of the uncertainty of a cell average, which is generated from the set of kriging equations along with the kriging estimate of the cell average. It is analogous to the standard deviation of the mean of a set of numbers; however, it is a function of the sample locations and the variogram only.

Because the data do not fulfill the assumptions of the kriging methodology exactly, the kriging standard deviation could be biased, as previously discussed. We evaluate the adequacy of the kriging standard deviations by comparing them with the cross-validation errors.

### **Implementation of Kriging Procedures**

Precipitation amounts were kriged from the quarterly data files. We compiled these quarterly files from NWS daily data. We included a site in the kriging analysis only if at least 95 percent of the days in the quarter had a valid precipitation amount (including zero). The data were log-transformed because this transformation yielded distributions that were very close to normal.

We used annual data to kriging precipitation-chemistry variables. We included a site in the kriging analysis only if both CI1 and CI3 were at least 75 percent.

As described in greater detail under "Results," we compared the results obtained by kriging concentration, deposition, and residual concentration. We will show that the uncertainties can be reduced by first accounting for the functional relationship between concentration (or deposition) and precipitation amount, then kriging residual concentration, and, finally, recombining the results with kriged precipitation amounts.

Both annual concentration and deposition vary spatially as functions of precipitation amount. Thus, neither concentration nor deposition normalizes for the variations in precipitation. For example, Figure 4 shows annual depth-weighted nitrate concentration for all sites and water years (provided CI3  $\geq$  75 percent) vs. precipitation amount; the approximately inverse relationship is obvious. In contrast, deposition varies in proportion to precipitation amount. We removed the functional relationship according to the following equations:

$$\ln(C_i) = \alpha + \beta \ln(P_i) + e_i \quad , \quad (7)$$

or

$$D_i = a + bP_i + e_i \quad , \quad (8)$$

where  $P_i$  represents precipitation amount for the  $i$ 'th sample,  $C_i$  is concentration,  $D_i$  is deposition, and  $e_i$  is the error term, or residual. We used Equation 7 for all variables except acidity and kriged the residuals (retaining the log scale). Because acidity sometimes takes on negative values, we used Equation 8.

We used ordinary block kriging to interpolate station data to the grid. We utilized the GEO-EAS package developed by the EPA (Englund and Sparks, 1991). Ordinary kriging requires specification of a search ellipse, which is centered on each cell. For each cell, only stations within the ellipse are used in estimated the cell average. We used a circle of radius 300 km; we found no differences in the results to suggest that an ellipse was more appropriate. We also examined the station weights that were computed by the program for selected grid cells. In general, the grid-cell averages were largely determined by sites within about 100 km of the cell center.

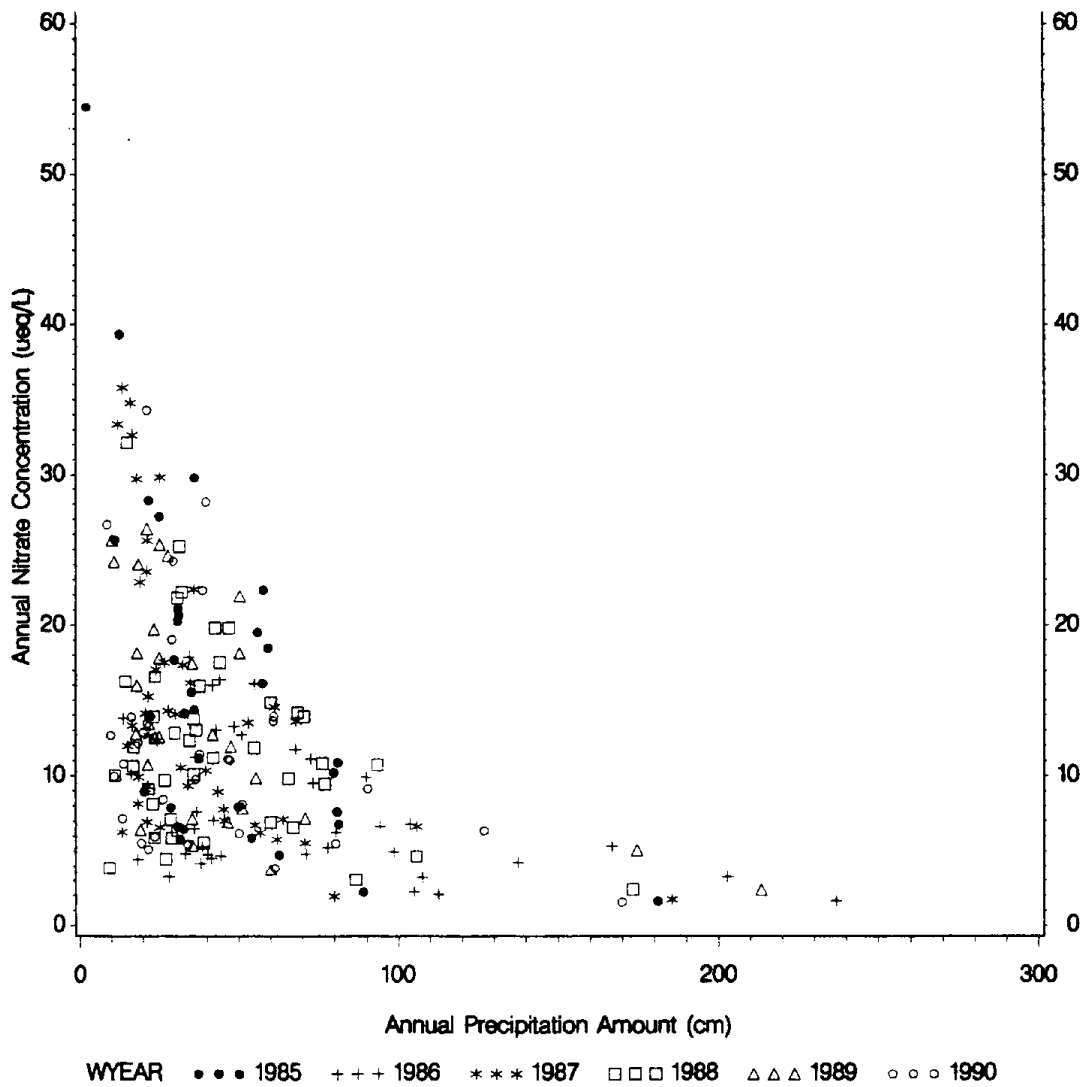


Figure 4. Depth-weighted annual nitrate concentration vs. annual precipitation amount for all monitoring sites and water years.

Variograms were calculated up to 300 km using about 15 km lag spacing. In all cases, we fit an exponential function to the observed variogram, with nugget (i.e., y-intercept) of zero. The zero nugget reflects our belief that monitors that are moved sufficiently close to each other (e.g., collocated samplers) would produce identical values (within the sampling error). When the lag spacing is reduced sufficiently (e.g., to 5 km), the variograms do show a zero nugget (see, e.g., Figure 1). We fit the observed variograms by adjusting the range and sill of the exponential functions. We tested for directional dependence, but found no evidence for it.

The variogram is a very simplified model of potentially complex spatial covariance. In areas where the concentration or deposition fields exhibit steep gradients, the variogram is likely to underestimate uncertainty. We discuss this topic in more detail under below.

## RESULTS

### Evaluation of the Methods

**Comparison of methods for quantifying uncertainties.** We first evaluate our methods for quantifying uncertainties. To illustrate the findings, we will present more detailed results for precipitation amount and nitrate concentration than for other variables.

We computed both cross-validation errors and kriging standard deviations. To make units of precipitation, concentration, and deposition comparable, we have used absolute cross-validation errors on a fractional basis (defined as  $|\text{observed-predicted}|/\text{observed}$ ) and have converted kriging standard deviations to coefficients of variation, defined as kriging standard deviation/kriging prediction.

Log-transformed precipitation amounts were kriged quarterly. From the cross-validation files, we converted both predicted and observed values from logarithmic units to the original scale [centimeters (cm)]. Predicted and observed values were then summed over each sample year. Fractional errors were then determined from the annual files. Sites were included only if all four quarters were complete. Table 4 shows the distribution of cross-validation errors for precipitation amount by water year. The number of sites, 343-364 per year, represents the number having data available for four quarters, each exhibiting 95 percent sampling completeness. The results show that over 75 percent of the cross-validation errors are less than 33 percent. A few sites (generally less than five per year) exhibit errors exceeding 100 percent.

Table 4. Distribution of fractional cross-validation errors for precipitation amount.

Water No.		Percentile					
Year	Sites	5	25	50	75	95	100
84-85	363	0.015	0.066	0.148	0.281	0.559	1.874
85-86	364	0.011	0.064	0.161	0.323	0.562	3.695
86-87	358	0.015	0.070	0.167	0.288	0.564	4.297
87-88	343	0.013	0.065	0.164	0.286	0.553	2.641
88-89	354	0.011	0.074	0.184	0.334	0.790	3.922
89-90	352	0.019	0.085	0.173	0.312	0.648	8.836

We next show the distribution of kriging standard deviations (expressed as CVs) for precipitation amount for all grid cells within California (see Table 5). Again, we converted the log-scale kriging estimates back to precipitation amounts (centimeters). To convert the log-scale kriging standard deviations to centimeters, we used the following formula (Kokoska and Nevison, 1989), which is appropriate for log-normal distributions:

$$\sigma_p^2 = (e^{2\mu_L + \sigma_L^2})(e^{\sigma_L^2} - 1), \quad (9)$$

where  $\mu_L$  is the log-scale kriging estimate,  $\sigma_L$  is the log-scale kriging standard deviation, and  $\sigma_p$  is the kriging standard deviation converted to the original measurement scale.

A comparison of Tables 4 and 5 shows that the kriging CVs are larger than the cross-validation errors up to the 75th percentile (i.e., most of the kriging CVs are larger than most of the cross-validation errors). Above this percentile, the cross-validation errors are larger. It is customary to use  $2\sigma$  confidence limits for most applications; twice the kriging standard deviation would be larger than all but the very largest cross-validation errors. From this comparison, we conclude that the kriging standard deviations do not underestimate the true uncertainties in the case of precipitation amount, with the exception of a few locations.

Table 5. Distribution of kriging coefficients of variation for precipitation amount. N=265 grid cells.

Water Year	Percentile					
	5	25	50	75	95	100
84-85	0.093	0.124	0.172	0.249	0.490	0.938
85-86	0.105	0.136	0.177	0.246	0.323	0.447
86-87	0.115	0.156	0.211	0.299	0.461	0.655
87-88	0.084	0.114	0.150	0.200	0.273	0.350
88-89	0.119	0.164	0.231	0.330	0.676	1.479
89-90	0.126	0.168	0.226	0.313	0.432	0.500

We next discuss the cross-validation errors and kriging standard deviations for nitrate deposition. We again wish to determine if the cross-validation errors are comparable to the kriging standard deviations. If they are, we have more confidence that the kriging standard deviations reflect the true interpolation uncertainties reasonably well.

In this set of calculations, we kriged the residuals from Equation 7 and the log-transformed precipitation amounts. We again carried out cross-validation calculations and examined the results. Table 6 shows the distribution of fractional cross-validation errors for nitrate deposition, by water year. To compute the values in Table 6, we calculated observed and predicted nitrate deposition (in units of kg/ha-yr) as the product of precipitation amount and Equation 7.

Table 6. Distribution of fractional cross-validation errors for nitrate deposition (computed from precipitation and adjusted concentration).

Water No.		Percentile					
Year	Sites	5	25	50	75	95	100
84-85	33	0.001	0.068	0.189	0.375	1.159	1.468
85-86	39	0.008	0.037	0.230	0.520	1.725	3.858
86-87	46	0.036	0.087	0.213	0.378	0.969	3.013
87-88	41	0.010	0.126	0.242	0.514	1.314	1.924
88-89	28	0.033	0.179	0.285	0.382	1.137	1.195
89-90	32	0.016	0.127	0.297	0.567	1.019	1.848

Table 7 shows the kriging coefficients of variation for nitrate deposition (computed from precipitation and adjusted concentration). We calculated the standard deviations of the estimated nitrate deposition as follows:

$$\sigma_D = CF(e^{\alpha+R})\sqrt{P^{2(1+\beta)}\sigma_R^2 + (1+\beta)^2 P^{2\beta}\sigma_P^2} \quad (10)$$

where  $\sigma_D$  is the deposition uncertainty, CF is a conversion factor (needed to obtain units of  $\text{kg ha}^{-1} \text{yr}^{-1}$ ), P is precipitation amount,  $\sigma_P$  is the kriging standard deviation for precipitation amount,  $\alpha$  and  $\beta$  are the coefficients appearing in Equation 7, R is the residual log concentration ( $e_i$  of Equation 7), and  $\sigma_R$  is the kriging standard deviation for the residual log concentration. We derived this equation by applying standard error propagation techniques (Bevington and Robinson, 1992) to the product of Equation 7 with precipitation amount.

Comparison of Tables 6 and 7 shows that the range of cross-validation errors is larger than that of the kriging coefficients of variation, i.e., the kriging uncertainties probably overestimate the true uncertainties in some areas and underestimate them in others. However, most of the cross-validation errors are less than about  $2\sigma$ , where  $\sigma$  is the kriging standard deviation. As was the case for precipitation amount, we conclude that the kriging standard deviations do not underestimate the true uncertainties for nitrate deposition, with the exception of a few locations. We examine these sites next.

Table 7. Distribution of kriging coefficients of variation for nitrate deposition (computed from precipitation and adjusted concentration). (N = 265 grid cells).

Water Year	Percentile					
	5	25	50	75	95	100
84-85	0.166	0.291	0.380	0.479	0.573	0.636
85-86	0.198	0.337	0.434	0.502	0.621	0.702
86-87	0.148	0.238	0.305	0.371	0.456	0.515
87-88	0.200	0.339	0.419	0.482	0.526	0.560
88-89	0.158	0.266	0.341	0.399	0.462	0.567
89-90	0.253	0.426	0.554	0.654	0.776	0.880

**Locations of areas of higher uncertainty.** In Table 8, we have listed for each year the sites exhibiting the five largest fractional cross-validation errors for nitrate deposition. Typically, large cross-validation errors occur at sites near the boundaries of our study domain, e.g., San Nicolas Island, Smith Valley (NV), Palomar, and Nipomo (and, particularly, sites that are generally upwind of the principal anthropogenic emission source areas). Other sites, such as Mt. Wilson, appear to exhibit large cross-validation errors due to elevation effects (concentration and/or deposition differ from nearby sites as a consequence of elevation, despite our incorporating the variation due to precipitation amount). The kriging standard deviations therefore do not appear to be completely reflective of the true interpolation uncertainties close to the boundaries and in some areas exhibiting particularly steep deposition gradients (for comparison, see the maps presented later in this section). Thus, some caution must be exercised in using the kriging standard deviations or the kriging CVs.

Table 8. Sites having the largest fractional cross-validation errors for nitrate deposition.

Water Year	Sites
84-85	San Nicolas, S. Lake Tahoe, Nipomo, NADP Yosemite, Ash Mountain
85-86	San Nicolas, Smith Valley, Mt. Wilson, Anaheim, Nipomo
86-87	San Nicolas, Mt. Wilson, Eureka, Palomar, Mammoth Mountain,
87-88	Victorville, San Nicolas, Lake Isabella, Nipomo, Palomar
88-89	Hopland, San Jose, Mt. Wilson, Chuchupate, Escondido
89-90	Lake Isabella, Smith Valley (NV), Chuchupate, Hopland, San Jose

**Evaluation of the effects of using precipitation data.** In this section, we compare our results with those we would have obtained had we simply kriged nitrate or sulfate deposition directly and had we not used the NWS precipitation data.

Table 9 shows the distribution of the fractional cross-validation errors for nitrate deposition, which was kriged directly without adjustment for precipitation amount or use of the NWS precipitation data. Comparison of this table to Table 6 shows that we have considerably reduced the largest fractional cross-validation errors by using precipitation amount data.

Table 10 compares our kriging CVs for sulfate and nitrate deposition to those we would have obtained had we kriged deposition directly without the precipitation data. The comparison shows that we have reduced the largest CVs by about a factor of 3.

These comparisons show the value of using the NWS precipitation data. The resulting reduction in interpolation uncertainty is probably greater than any that could have been obtained had the CADMP network been much denser than it is.

Table 9. Distribution of fractional cross-validation errors for nitrate deposition kriged directly without adjustment for precipitation amount.

Water No. Year	Sites	Percentile					
		5	25	50	75	95	100
84-85	33	0.05	0.16	0.32	0.57	2.02	5.93
85-86	39	0.03	0.20	0.34	0.66	4.61	5.15
86-87	46	0.03	0.14	0.25	0.45	0.88	3.95
87-88	41	0.02	0.13	0.32	0.55	1.96	3.94

Table 10. Distribution of kriging coefficients of variation for nitrate and sulfate deposition, water year 1984-1985 (N=263 grid cells).

Percentile	Sulfate Deposition	Nitrate Deposition	Sulfate deposition Calculated from Concentration and Precipitation	Nitrate deposition Calculated from Concentration and Precipitation
100	1.863	2.040	0.560	0.636
95	1.105	1.270	0.457	0.573
75	0.514	0.876	0.367	0.479
50	0.362	0.525	0.286	0.380
25	0.226	0.303	0.222	0.291
5	0.084	0.109	0.138	0.166
0	0.028	0.042	0.074	0.084

## Summary Results

Our results are shown in the maps in the appendix. For each species, one map shows deposition and one shows the kriging CV.

Sulfate and nitrate were each less than eight  $\text{kg ha}^{-1} \text{yr}^{-1}$ ; excess sulfate, ammonium, and calcium deposition were less than 3  $\text{kg ha}^{-1} \text{yr}^{-1}$ . For comparison, wet sulfate and nitrate deposition in portions of eastern North America exceed 25 and 15  $\text{kg ha}^{-1} \text{yr}^{-1}$ , respectively (Sisterson, 1991); ammonium and calcium deposition are less than about 4 and 2.5  $\text{kg ha}^{-1} \text{yr}^{-1}$  in almost all parts of eastern North America (Sisterson, 1991).

Comparison of the maps showing sulfate deposition with those showing excess sulfate deposition shows that in some areas where sulfate deposition is highest (e.g., the northwest coast), much of the sulfate had its origin as sea salt.

In most years, nitrate deposition was greater in the SoCAB and the southern Sierra Nevada than in other parts of California.

Deposition uncertainties are less than 20 percent in the SoCAB, which has a large number of monitors; uncertainties can be up to 100 percent in portions of northeastern and southeastern California, where little monitoring has been done.

The value of each grid cell represents a spatial average and thus can differ from the value for a particular station that might be located in the grid cell. For example, the network maximum nitrate deposition is located at Tanbark Flat. For each year, this maximum exceeds the grid cell average because other monitors, recording lower deposition amounts, are also located within or close to the same grid cell. A finer grid would help resolve particular maxima. For comparison, Table 11 lists nitrate deposition by station (site) and year. Table 12 lists mean deposition of nitrate, sulfate, ammonium, and calcium over all available years.

Grid cells can be summed or averaged to yield either basin totals or averages.

Table 11. Annual nitrate deposition ( $\text{kg ha}^{-1} \text{ yr}^{-1}$ ) by site and CARB sample year. Only years in which CI1 and CI3 were at least 75 percent are shown. NADP sites are indicated in capital letters.

Site	Year					
	1985	1986	1987	1988	1989	1990
Anaheim	.	1.74	1.81	2.43	2.75	1.38
Ash Mountain	6.76	5.51	4.98	5.76	3.30	6.92
Bakersfield	1.76	1.02	2.97	2.95	1.59	1.41
Berkeley	2.45	3.11	2.18	2.92	.	1.91
Bethel Island	1.93	2.54	1.72	2.00	1.82	1.37
CHUCHUPATE RANGER STATION	4.00	.	2.04	2.23	1.43	0.60
DAVIS	3.21	.	1.86	2.95	.	2.21
El Monte	4.04	4.00	3.07	4.41	2.85	3.43
Escondido	3.27	1.28	2.48	2.64	1.78	1.77
Eureka	1.22	1.45	0.95	1.63	.	.
Gasquet	1.77	2.38	1.97	2.54	3.11	1.62
GIANT FOREST	.	4.37	4.43	4.51	.	5.13
Giant Forest	.	5.47	5.52	5.11	3.14	5.26
HOPLAND	1.83	1.45	2.19	2.73	1.38	1.44
Lake Isabella	.	1.44	2.54	1.26	1.85	0.66
Lakeport	1.96	2.12	1.98	2.57	.	.
Lindcove	.	4.13	3.36	4.16	.	.
Lynwood	3.87	3.46	2.68	2.38	2.03	1.59
Mammoth Mountain	.	.	2.81	.	.	.
MONTAGUE	.	0.98	0.91	1.26	1.18	1.13
Montague	.	1.26	1.23	1.05	1.57	1.15
Mt Wilson	5.74	2.52	2.55	6.20	3.38	3.21
Napa	.	3.87	2.41	4.02	3.52	2.58
Nipomo	1.12	1.16	1.97	1.22	.	.
ORGAN PIPE CACTUS NAT. MON.	2.59	1.15	1.12	0.22	1.95	0.92
PALOMAR MOUNTAIN	5.46	3.01	2.21	1.34	.	.
Pasadena	6.68	5.48	4.68	5.23	4.23	4.41
Quincy	.	3.61	2.42	.	.	2.73
RED ROCK CANYON	0.66	.	3.30	1.45	1.62	.
Reseda	3.79	4.47	3.42	4.79	3.45	1.40
S Lake Tahoe	1.31	2.11	2.08	1.16	2.00	2.67
SILVER LAKE RANGER STATION	.	0.99	0.93	0.75	.	0.68
SMITH VALLEY	.	0.50	1.36	0.69	1.40	0.76
Sacramento	3.38	4.94	2.62	3.73	3.84	3.23
Salinas	1.27	1.18	1.03	1.23	.	.
San Bernardino	4.22	3.84	2.47	4.90	3.94	4.48
San Jose	1.40	1.83	1.14	1.61	0.76	0.87
San Nicolas	1.13	0.56	0.52	0.86	.	.
San Rafael	3.80	.	2.29	5.52	.	.
Santa Barbara	2.89	4.01	2.90	3.05	2.76	0.66
Soda Springs	.	4.07	4.34	3.03	5.46	4.98
TANBARK FLAT	6.78	4.33	3.48	6.01	5.66	.
Tanbark Flat	7.98	5.01	3.49	6.07	6.84	5.35
Victorville	3.03	1.18	3.34	1.11	.	.
YOSEMITE NATIONAL PARK	3.42	.	.	.	.	5.12
Yosemite	5.04	.	5.73	3.99	2.49	.

Table 12. Mean annual wet deposition of nitrate, sulfate (not adjusted for sea salt), ammonium, and calcium by site ( $\text{kg ha}^{-1} \text{yr}^{-1}$ ). Years were included only if CI1 and CI3 were each at least 75 percent. NADP sites are capitalized.

Site	Years	Species			
		Nitrate	Sulfate	Ammonium	Calcium
Anaheim	5	2.02	1.87	0.85	0.39
Ash Mountain	6	5.54	2.25	2.06	0.64
Bakersfield	6	1.95	1.92	1.10	0.41
Berkeley	5	2.52	2.83	0.60	0.69
Bethel Island	6	1.90	1.22	1.15	0.35
CHUCHUPATE	5	2.06	1.30	0.38	0.27
DAVIS	5	2.17	1.35	1.31	0.16
El Monte	6	3.63	3.08	1.34	0.51
Escondido	6	2.20	2.29	0.66	0.80
Eureka	4	1.31	4.93	0.46	1.21
Gasquet	6	2.23	6.70	0.77	1.94
GIANT FOREST	5	4.42	2.17	1.48	0.39
Giant Forest	5	4.90	2.47	1.91	0.77
HOPLAND	7	1.68	1.69	0.37	0.23
Lake Isabella	5	1.55	0.89	0.41	0.33
Lakeport	4	2.16	1.69	0.95	0.41
Lindcove	3	3.89	1.60	1.96	0.50
Lynwood	6	2.67	3.34	1.02	0.44
Mammoth Mountain	1	2.81	2.04	0.89	0.67
MONTAGUE	6	1.00	0.60	0.27	0.12
Montague	5	1.25	0.70	0.40	0.26
Mt Wilson	6	3.93	2.60	0.90	0.68
Napa	5	3.28	3.43	1.01	0.49
Nipomo	4	1.37	1.71	0.50	0.42
ORGAN PIPE CACTUS	7	1.59	1.70	0.43	0.34
PALOMAR MOUNTAIN	4	3.01	3.07	0.54	0.51
Pasadena	6	5.12	3.48	1.35	0.64
Quincy	3	2.92	1.99	0.64	0.67
RED ROCK CANYON	5	1.76	0.97	0.35	0.71
Reseda	6	3.55	2.30	0.92	0.43
S Lake Tahoe	6	1.89	1.17	0.46	0.41
SILVER LAKE	4	0.84	0.64	0.15	0.16
SMITH VALLEY	6	0.94	0.59	0.34	0.16
Sacramento	6	3.62	2.21	2.14	0.41
Salinas	4	1.18	1.36	0.65	0.33
San Bernardino	6	3.98	2.06	2.01	0.71
San Jose	6	1.27	1.61	0.64	0.45
San Nicolas	4	0.77	1.96	0.16	0.60
San Rafael	3	3.87	5.00	1.38	0.97
Santa Barbara	6	2.71	1.86	0.44	0.40
Soda Springs	5	4.38	2.75	1.05	0.90
TANBARK FLAT	6	4.67	2.82	0.86	0.37
Tanbark Flat	6	5.79	3.03	1.31	0.67
Victorville	4	2.17	1.08	0.65	0.89
YOSEMITE	2	4.27	2.80	1.21	0.42
Yosemite	4	4.31	2.11	1.26	0.71

## PART II: DRY DEPOSITION

### INTRODUCTION

#### Objectives

The specific objectives of this part of the project are to

1. Evaluate the quality of the CADMP dry-deposition data;
2. Compute estimates of the dry deposition of each species of interest at each monitoring site having sufficient data;
3. Generalize the estimated deposition amounts to larger regions of interest.

#### Overview of Part II

We first summarize the methods used. We describe the approach for calculating deposition fluxes (the inferential method) in some detail. We then briefly describe the data that are available and discuss the quality of these data. We discuss the structure of the program that is used for calculating deposition. Following the description of the methods, we present sensitivity analyses and summary results.

### METHODS

#### Use of the Inferential Method

**Description.** The CADMP dry-deposition network was designed with the intent of implementing the inferential method. In this approach, the flux of a particular species is calculated as the product of its ambient concentration and its deposition velocity,  $V_d$  (Hicks et al., 1987). Deposition velocity generally depends on both the nature of the pollutant and the surface. The inferential method is strictly applicable to cases in which the flux is unidirectionally toward the surface, i.e., no surface source exists. This assumption might prove questionable for ammonia gas at some sites (e.g., in rural locations) or  $\text{NO}_x$  at some urban locations.

At the CADMP monitors, deposition of a particular species  $i$  to surface  $j$  during a specified time interval (e.g., one hour) is computed as

$$F_{ij} = C_i V_{d_j} \quad , \quad (11)$$

where  $C$  is concentration and  $V_d$  is deposition velocity. (Actually, we have 12-hour

concentration averages and 1-hour averages of the meteorological parameters from which  $V_d$  is calculated).

The flux of pollutant  $i$  over an area that includes several different types of plants or surfaces is

$$F_i = \sum_j C_i V_d A_j \quad , \quad (12)$$

where  $A_j$  is the portion of the area covered by surface type  $j$ . The fact that most surface types have a true surface area larger than the horizontal plane they cover is included in  $V_d$  by the use of adjustment factors such as leaf area index (LAI). The LAI is the ratio of the area of one side of all the leaves to the area of the ground underneath the plant.

Deposition velocity for gases is calculated as the inverse of total resistance to deposition,  $V_d = 1/R_T$ , where  $R_T$  is calculated as a combination of resistances to dry deposition:

$$V_d = \frac{1}{R_a + R_b + R_t} \quad , \quad (13)$$

where  $R_a$  = aerodynamic resistance (determined by turbulent exchange),  $R_b$  = quasi-laminar boundary resistance (determined by molecular diffusivity of the pollutant and the thickness of the quasi-laminar boundary layer in contact with receptor surfaces), and  $R_t$  = transfer, or canopy resistance (determined by the uptake processes of a given surface for the species in question).

Aerodynamic resistance,  $R_a$ , is species-independent and reflects turbulent transport through the atmospheric surface layer. Quasi-laminar boundary layer resistance,  $R_b$ , is both species- and turbulence-dependent and reflects the importance of molecular diffusivity within about a millimeter (mm) or less of the surface. Transfer resistance,  $R_t$ , depends on both the species and the surface and reflects adsorption and uptake mechanisms of all types.

In calculating deposition velocity for large particles, settling velocity becomes important and requires the inclusion of another term in addition to the inverse resistance.

The terms  $R_a$  and  $R_b$  can be determined as described by Hicks et al. (1987) and Meyers and Yuen (1987) from the meteorological measurements taken at each of the CADMP sites (Watson et al., 1991). In brief, the resistance  $R_a$  can be approximated from field measurements as

$$R_a \sim \frac{4}{u \sigma_\theta^2} \quad (\text{neutral and stable conditions}) \quad , \quad (14)$$

$$R_a \sim \frac{9}{u \sigma_\theta^2} \quad (\text{unstable conditions}) \quad ,$$

where  $u$  = mean wind speed and  $\sigma_\theta$  = standard deviation of horizontal wind direction. The standard deviation of the horizontal wind direction contains information related to both stability and surface roughness. If net radiation is positive and  $\sigma_\theta$  exceeds some critical value, conditions are unstable. Although the critical value is site-specific, it is presently assumed by the EPA to be  $\sigma_\theta = 10^\circ$  (Hicks et al., 1987).

$R_b$  is obtained from (Hicks et al., 1987):

$$R_b = \frac{2}{k u_*} \left( \frac{Sc}{Pr} \right)^{2/3} \quad , \quad (15)$$

where  $k$  = von Karman's constant (0.4),  $u_*$  = friction velocity,  $Sc$  = Schmidt number (for gases or particles), and  $Pr$  = Prandtl number for air ( $\approx 0.72$ ). Once  $R_a$  has been determined, it is possible to determine  $R_b$  because  $u_*$  can be determined from the approximation (Hicks et al., 1987):

$$R_a \sim u u_*^{-2} \quad , \quad (16)$$

In the computer programs developed by Oak Ridge Laboratory for carrying out the calculations of deposition, the ratio of the Schmidt to Prandtl numbers is approximated by the ratio of the molecular diffusivity of water in air to that of the gaseous pollutant in air. Thus  $R_b$  is calculated as

$$R_b = \frac{2}{k u_*} \left( \frac{D_{H_2O}}{D_{\text{pollutant}}} \right)^{2/3} \quad . \quad (17)$$

In the current version of the program from Oak Ridge, which has a 21-layer canopy, a separate  $R_b$  is calculated for each layer, on the basis of the work of Cionco (1972, 1978) and of Shaw and Pereira (1982). The resistance at the top of the canopy is slightly greater than that calculated by the preceding equation. This outcome is expected because areas within the canopy are more protected than is the top and because one factor damping canopy turbulence is the flexibility of leaves.

$R_t$  is specific to particular species-surface combinations. For some reactive species, such as nitric acid,  $R_t$  can be assumed to be zero (Hicks et al., 1987). For other species,  $R_t$

is nonzero. In general,  $R_1$  consists of parallel resistance terms for water, soil, leaf, and other surfaces. The leaf surface resistance, in turn, consists of resistances for stomata, cuticle, and mesophyll.

**Limitations.** The method described here represents a model of deposition processes. As is the case with any model, it is important to recognize key limitations. For example, the surface resistance terms are highly simplified parameterizations of complex physical processes. Moreover, for  $\text{NH}_3$ , which can be emitted from the surface, and possibly for  $\text{NO}_2$ , which can be produced from  $\text{NO}$  below the height of the monitoring instruments, the assumption of strictly downward transfer is not always correct (Hicks et al., 1991). Few comparisons of the results from the inferential method to micrometeorological estimates of deposition are available. Uncertainties in the deposition velocities of  $\text{SO}_2$  and ozone ( $\text{O}_3$ ) calculated by the inferential method at sites located away from major emission sources, having uniform vegetation, and located in uncomplicated terrain, are thought to be about 30 percent (McMillen, 1990; Hicks et al., 1991; Clarke et al., 1992). Uncertainties for  $\text{HNO}_3$  and particulate nitrate or sulfate are thought to be in the range of 30 to 50 percent (McMillen, 1990; Clarke et al., 1992).

### Data Availability

The CADMP dry-deposition network consists of 10 sites (see Figure 5); a collocated sampler is situated at the Sacramento site. Two measurements are made every sixth day: one from 6:00 a.m. to 6:00 p.m. and one from 6:00 p.m. to 6:00 a.m. Sampling methods, species monitored, and initial results are described in Watson et al. (1991).

Briefly, the CADMP dry-deposition data base includes gases (sulfur dioxide, nitrogen dioxide, ammonia, ozone, and nitric acid) and total mass for particles (PM) in the  $\text{PM}_{2.5}$  and  $\text{PM}_{10}$  size ranges. The particle mass has been further analyzed for sulfate, nitrate, chloride, ammonium, sodium, magnesium, potassium and calcium.

We were provided with data from the program's inception (early 1988) through September 1991. As noted earlier, more recent measurements are undergoing review and validation by the CARB.

In addition to the CADMP data, CARB aerometric data are available for a limited number of species at a many more monitoring sites. These measurements consist of  $\text{O}_3$ ,  $\text{NO}_2$ ,  $\text{SO}_2$ ,  $\text{PM}_{10}$ -nitrate,  $\text{PM}_{10}$ -sulfate,  $\text{PM}_{10}$ -ammonium, and  $\text{PM}_{10}$ -chloride ( $\text{HNO}_3$  is not measured at CARB aerometric sites). The CARB's routine  $\text{PM}_{10}$  samples are collected every sixth day (on the same schedule as the CADMP samples); however, samples are collected as 24-hour averages (from midnight to midnight). We obtained hourly  $\text{NO}_2$  and  $\text{SO}_2$  data,  $\text{PM}_{10}$  data (speciated), and 12-hour  $\text{O}_3$  data from all monitors in California from 1989 through 1991.



Figure 5. Locations of CADMP dry-deposition monitoring sites.

## Data Quality

**Data accuracy.** We carefully reviewed the CADMP dry-deposition chemical data. We were provided with two data bases. The first had been prepared by Desert Research Institute (DRI), which implemented the CADMP dry-deposition network, and consisted of measurements from April 1988 through September 1989. The second had been prepared by the El Monte laboratory, which was responsible for sample analysis from October 1989 through September 1991.

The initial version of the El Monte laboratory's data base exhibited some unusual sample concentrations, including a large number of very negative  $\text{HNO}_3$  concentrations. The denuder difference (DD)  $\text{HNO}_3$  is a linear combination of three measurements: two are added and one is subtracted. Thus, the calculated  $\text{HNO}_3$  can be negative, but only within the sampling errors of its three constituent measurements. We located a systematic bias occurring in the data, which had to do with the extraction of the samples (in specified volumes of deionized water) from the filters. Species mass per filter [microgram ( $\mu\text{g}$ )/filter] is obtained by multiplication of aqueous concentration [ $\mu\text{g}/\text{milliliter (ml)}$ ] by a conversion factor (CF)

$$\text{CF} = \text{extractant volume (ml)}/\text{fraction of filter used} \quad .$$

We determined that extractant volumes had been modified from those specified in the standard operating procedures (SOPs); however, CF had not been correspondingly revised. Hence, many concentration values were incorrect by amounts ranging from 20 percent up to a factor of 2. Because the actual extractant volumes had been recorded in the data base, it was possible to recalculate all concentrations using the correct CFs. The El Monte laboratory corrected the data base and provided us with a revised version.

After reviewing the revised data base, we determined that the ambient air sampling volumes had inadvertently been corrected to standard temperature and pressure (STP). Because the ambient air concentrations are computed as the quotient of sample mass by sample volume, the concentrations were thus incorrect for ambient conditions (i.e., they had also been converted to STP-equivalent concentrations). The two sites most affected were Yosemite and Sequoia, whose concentrations were approximately 20 percent too high. We obtained the necessary correction factors from DRI and converted sample volumes and concentrations to ambient conditions.

**Potential biases in nitric acid measurements.** Unresolved questions still remain regarding the accuracy of the  $\text{HNO}_3$  data. We identified a diminution of the denuder difference  $\text{HNO}_3$  at Azusa and Los Angeles; in contrast, no trend occurred in the filter-pack nitrate (see Figure 6). At the remaining CADMP sites, the DD  $\text{HNO}_3$  and filter-pack nitrate curves were essentially parallel.

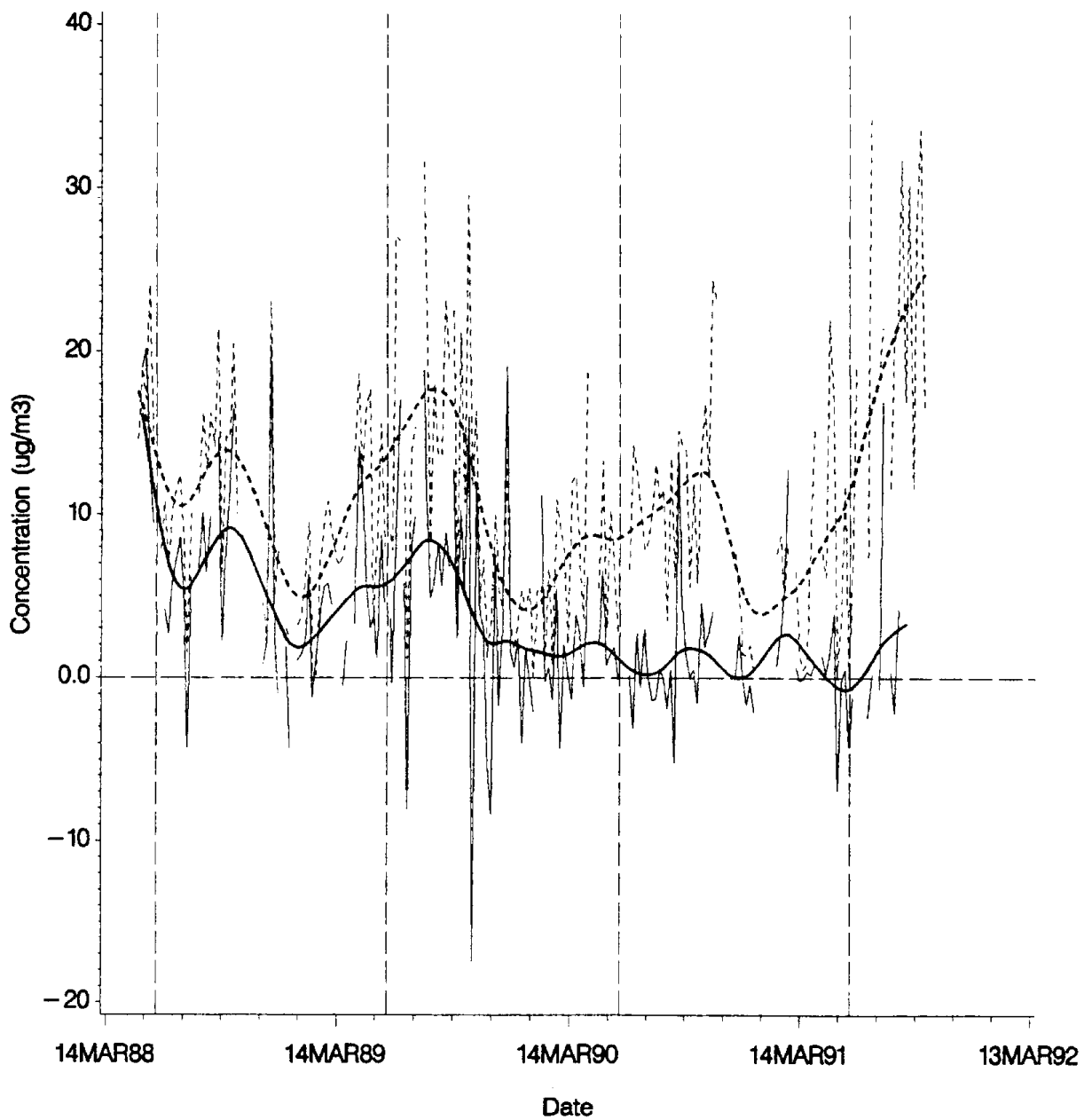


Figure 6. Denuder difference HNO<sub>3</sub> and filter-pack nitrate vs. time (day samples only) at Los Angeles. DD HNO<sub>3</sub> is shown by solid lines with a solid smoothed curve superimposed. Filter-pack nitrate is shown by dashed lines with a dashed smoothed curve superimposed. Vertical lines are placed at 1 June.

We also determined that PM10 and denuded particulate nitrate concentrations were similar to each other at all sites except Azusa and Los Angeles, where they diverged over time (see Figure 7). At all sites except Azusa and Los Angeles, the PM10 and denuded particulate nitrate remained in phase and showed winter maxima. At Azusa and Los Angeles, though, the PM10 nitrate exhibited winter maxima, while the denuded particulate nitrate went out of phase with respect to the PM10 nitrate. The concentrations diverged during summers; this divergence increased each summer.

These patterns strongly suggest a deterioration in the performance of the denuders over the four years of sampler operation. Samples collected from a new monitor that the CARB collocated at Azusa appear to confirm this problem. From July through September, 1993, the primary collector recorded daytime concentrations of denuded particulate nitrate that were about half again as high to two times higher than those measured by the collocated collector [ $5-8 \mu\text{g}/\text{meter (m)}^3$ ]; nighttime concentrations were comparable (within  $1 \mu\text{g}/\text{m}^3$ ), however.

It appears that other sampler biases may also exist. Comparison of the measurements from the refurbished primary and collocated collectors to Unisearch's Tunable Diode Laser Absorption Spectroscopy (TDLAS) measurements in October 1993 indicated that the CADMP measurements were generally 40-50 percent lower. Thus, it appears likely that, at some point,  $\text{HNO}_3$  is being lost from the CADMP sampler. The CARB is planning further testing of the CADMP sampler. In addition, the Research Division is planning an in-house project to investigate the feasibility of estimating  $\text{HNO}_3$  concentrations using measurements of ozone, ammonia, particulate nitrate and ammonium, temperature, and relative humidity.

From our review, it is clear that the denuder-difference  $\text{HNO}_3$  measurements at Azusa and Los Angeles are incorrect beginning as early as the spring of 1989, probably as a result of deterioration of denuder efficiency. Although the CADMP samplers were tested when prototypes were developed, evidently  $\text{HNO}_3$  is currently being lost. We do not know, however, which of the  $\text{HNO}_3$  measurements, if any, are reasonably accurate.

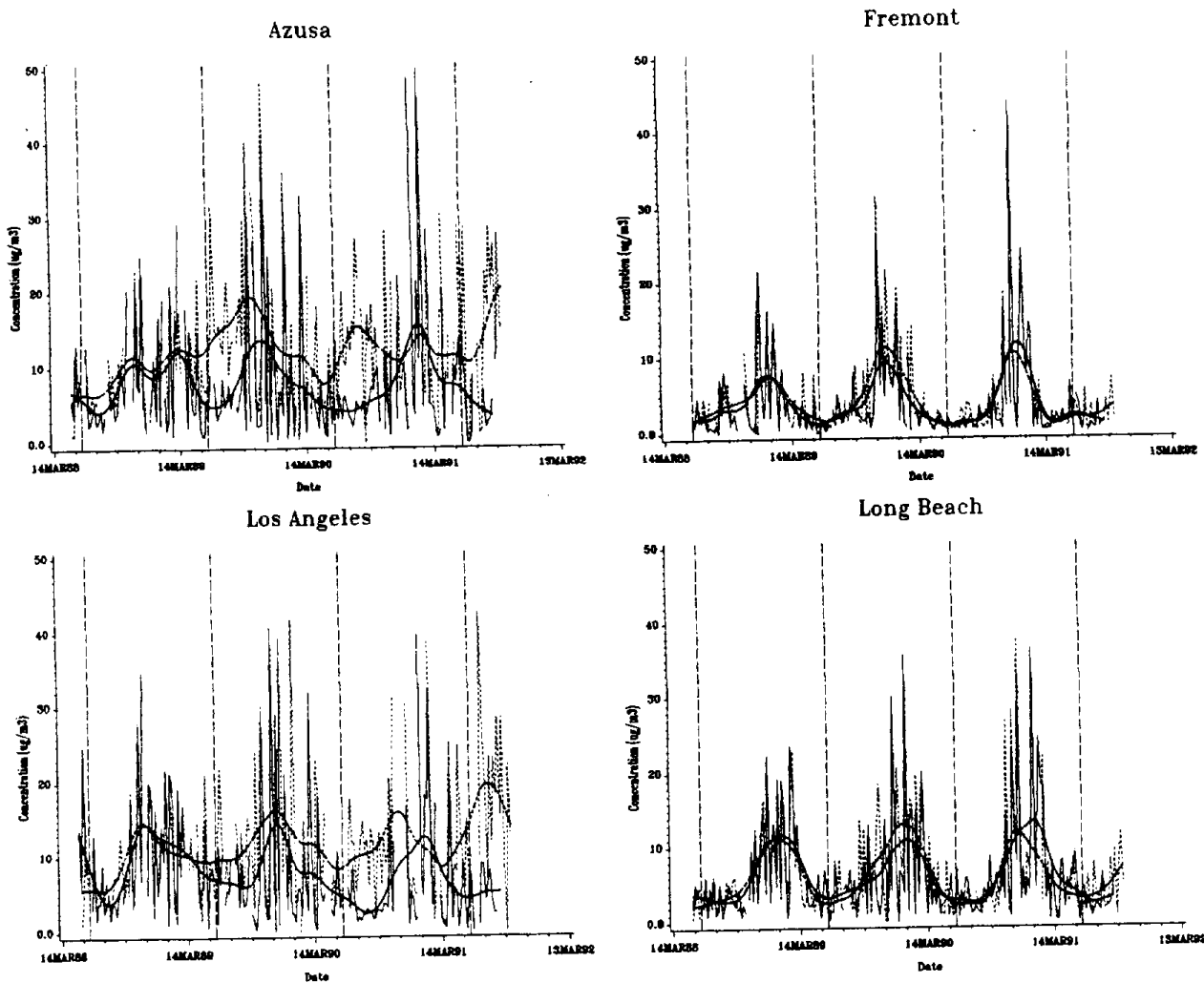


Figure 7. PM10 and denuded particulate nitrate concentrations at four sites. Denuded particulate nitrate is shown by dashed lines with dashed smoothed curves superimposed. PM10 nitrate is shown by solid lines with solid smoothed curves superimposed. Vertical lines are placed at 1 June.

**Comparison of CADMP data to other data bases.** We made a considerable number of comparisons of CADMP to other data: (1) collocated routine PM10 measurements, (2) O<sub>3</sub> measurements (for correlation with HNO<sub>3</sub>), (3) the 1986 CalTech study (Solomon et al., 1988). In this section, we briefly summarize the key findings.

Six CADMP sites are collocated with a routine PM10 monitor: Azusa, Bakersfield, Fremont, Los Angeles, Long Beach, and Sacramento. The CADMP and routine samples are not simultaneous (they overlap for 18 of 24 hours). We therefore do not expect exact agreement. Most comparisons showed a good level of agreement, though. Figure 8 shows one example. There is no evidence of a bias in the CADMP sampler's particulate measurements relative to those of the routine samplers.

We also compared CADMP NO<sub>2</sub> measurements to routine hourly measurements from collocated chemiluminescent monitors (we aggregated the hourly data to 12-hour averages). We found agreement during some periods of time; during others, however, the CADMP measurements were about a factor of 2 lower than those of the chemiluminescent data. Time series plots showed unusually low NO<sub>2</sub> values at all CADMP sites from late 1989 through early 1991 (see Figure 9). On further investigation, we learned that samples from October 1989 through about March 1991 had experienced up to a 14-month delay in analysis, had been transferred between two laboratories twice, and had not been stored according to SOP at some times. Because NO<sub>2</sub> can be converted to nitrate (and consequently not measured because the analysis is carried out for nitrite) (M. Poore, personal communication, 1993), we concluded that NO<sub>2</sub> data for approximately 18 months should be invalidated at all sites.

We also compared both filter-pack and denuder difference HNO<sub>3</sub> to collocated ozone concentrations. Regressions were computed by year and site, using all valid samples. Results are listed in Table 13. The slope and r<sup>2</sup> for the regression of denuder difference HNO<sub>3</sub> against ozone both decrease over time (with the exception of Azusa, 1991). By 1991, the correlation between denuder difference HNO<sub>3</sub> and ozone disappears at Los Angeles. Thus, the accuracy of the CADMP denuder difference HNO<sub>3</sub> appears to diminish over time.

In contrast, the regression of filter-pack nitrate against ozone shows consistently high correlations for all years at both Azusa (or Upland) and Los Angeles. These correlations are as high for the CADMP data as for the data of Solomon et al. (1988). The slopes of these regressions vary from year to year, but no trend is evident. At Azusa, the greatest slopes are for 1986 and 1991; at Los Angeles, the greatest slopes are for 1991, 1986, and 1989 (in that order). Although the mean 1986 filter-pack nitrate measurements (Solomon et al., 1988) are greater than the CADMP means, the slopes shown in Table 13 indicate that the ratio of filter-pack HNO<sub>3</sub> to ozone is as large for some of the CADMP data as it was in the 1986 study.

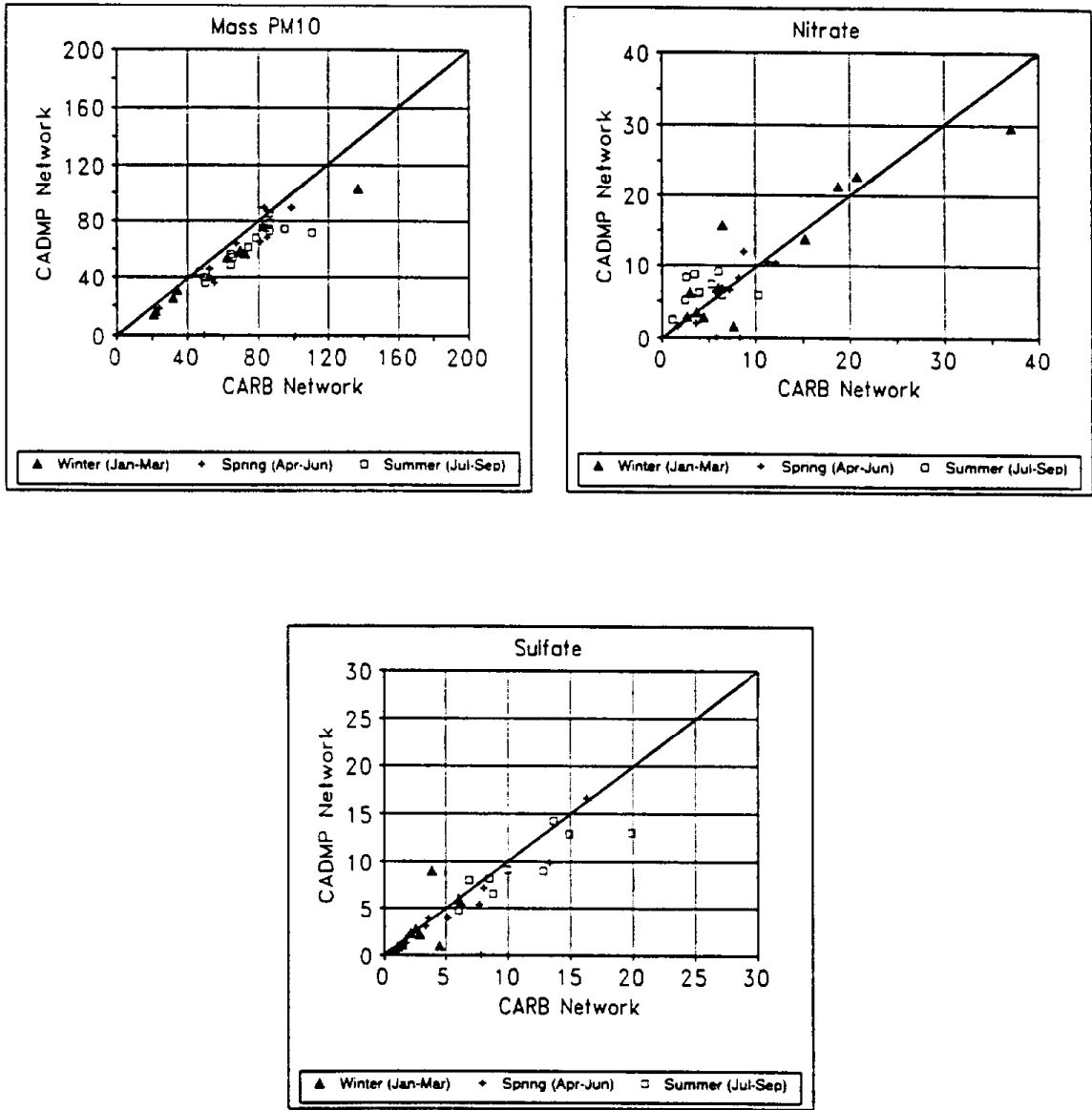


Figure 8. Example comparison of CADMP to routine CARB PM10 data, Azusa, January through September, 1991. Measurement units are  $\mu\text{g m}^{-3}$ .

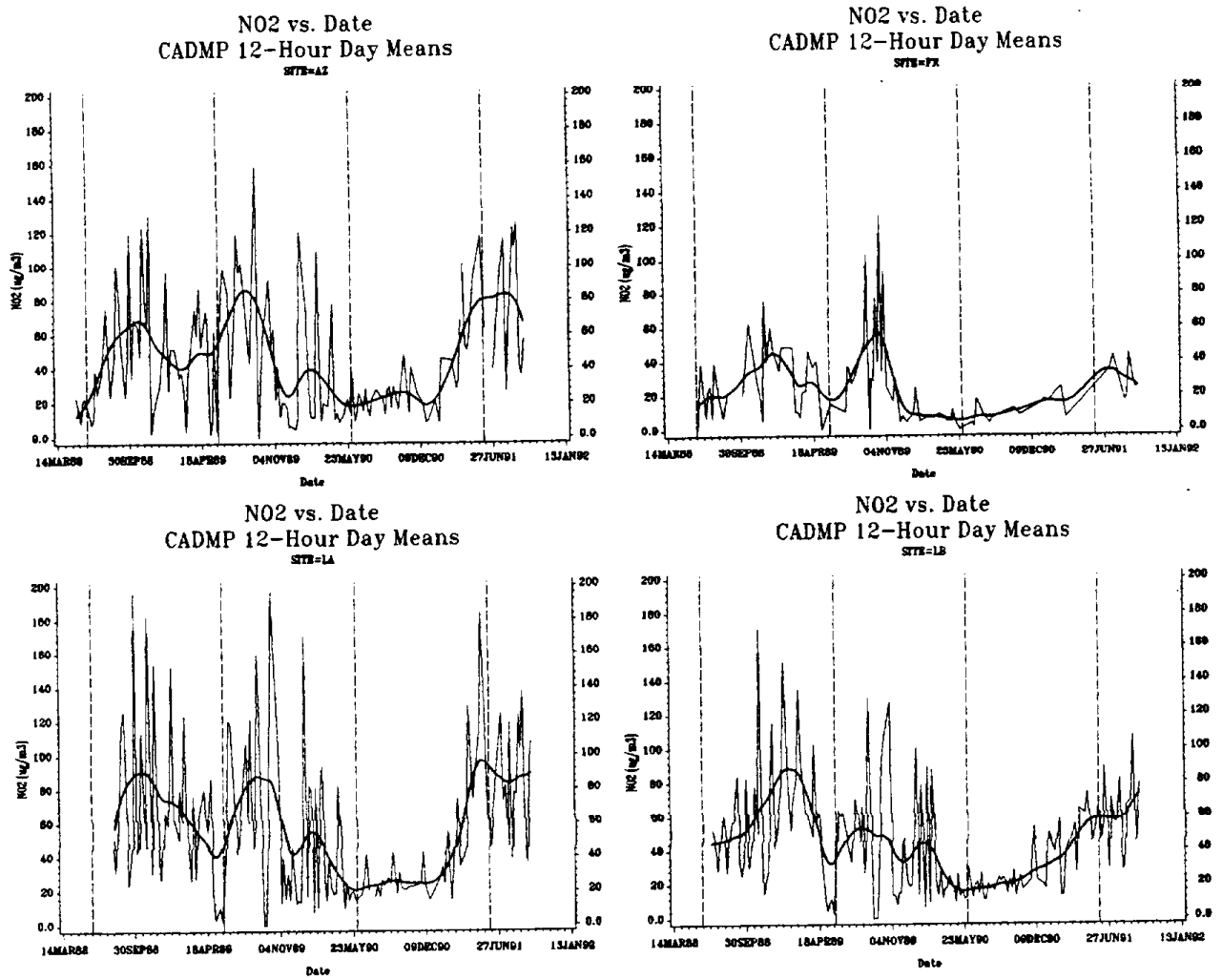


Figure 9. Time series of daytime NO<sub>2</sub> at four CADMP sites with smoothed curves superimposed.

Table 13. Results for regression of denuder-difference HNO<sub>3</sub> and filter-pack nitrate against ozone<sup>(a)</sup>.

Site	Year	Denuder-difference HNO <sub>3</sub>				Filter-pack HNO <sub>3</sub>			
		No.	Slope	S.E.	r <sup>2</sup>	No.	Slope	S.E.	r <sup>2</sup>
Azusa <sup>(b)</sup>	1986	58	2.0	0.2	0.73	58	3.6	0.2	0.82
	1988	30	1.3	0.2	0.57	36	1.8	0.2	0.69
	1989	86	1.3	0.2	0.39	89	2.7	0.2	0.66
	1990	89	0.5	0.1	0.22	90	2.1	0.1	0.73
	1991	53	1.7	0.3	0.40	65	3.5	0.2	0.83
Los Angeles	1986	56	2.1	0.3	0.53	57	3.5	0.5	0.52
	1988	15	1.7	0.3	0.67	17	2.3	0.3	0.82
	1989	83	1.6	0.3	0.22	84	3.3	0.3	0.63
	1990	70	0.7	0.4	0.05	71	2.0	0.1	0.75
	1991	26	-0.4	0.5	0.02	32	4.4	0.7	0.56

(a) Units for the slope are  $\mu\text{g m}^{-3}$  per parts per hundred million (pphm). To convert to parts per billion (ppb) per ppb, multiply by 0.04.

(b) The 1986 data were obtained from Solomon et al. (1988). Because these researchers did not operate a site at Azusa, we substituted results for Upland.

In summary, the regressions show that denuder difference HNO<sub>3</sub> concentrations at Azusa and Los Angeles diminished over time relative to ozone concentrations, whereas filter-pack nitrate did not. Coupled with the previously described comparisons, the regressions indicate that denuder difference HNO<sub>3</sub> at Los Angeles and Azusa should be considered suspect (perhaps invalid) after about early 1989. The regressions provide no indication that filter-pack nitrate concentrations were inaccurate.

**Data validation procedure.** After examining the data for systematic biases, as described above, we carried out a series of internal consistency checks:

1. Comparison of PM<sub>2.5</sub> to PM<sub>10</sub> mass.
2. Comparison of PM<sub>2.5</sub> to PM<sub>10</sub> species concentrations.

3. Comparison of total PM2.5 nitrate (teflon + nylon filters) to PM10 nitrate and denuded particulate nitrate.
4. Comparison of filter-pack HNO<sub>3</sub> to denuder difference HNO<sub>3</sub>.
5. Plotting time series of all species.
6. Checking for deviations from nominal sample volumes exceeding specified amounts (e.g., 15 percent).

We added four flags to the data base (one for each of the four filter packs). These flags take on values of "I" (invalid), "i" (some species invalid), "S" (suspect), "s" (some species suspect), "V" (valid), or "C" (charge balance failed). We used the flags initially in the data base and we incorporated the information from our consistency checks. We

1. Invalidated samples in which the following ratios exceeded  $1 + 2 \cdot \sigma_R$ , where  $\sigma_R$  represents the standard deviation of the ratios: (a) sum of PM2.5 species to PM2.5 mass, (b) sum of PM10 species to PM10 mass, and (c) PM2.5 mass to PM10 mass. (Note:  $\sigma_R$  is a function of the uncertainties associated with both the numerator and denominator of each ratio, which, in turn, are functions of the magnitudes of the concentrations). Failure to satisfy one or more of these ratio tests violates physical principles, so samples should be excluded. In the present data base, this criterion eliminated very few samples (generally because PM2.5 mass was greater than PM10 mass).
2. Invalidated measurements from any filter showing a deviation of sample volume in excess of 15 percent from nominal. This percentage represents a compromise between possible inaccuracy caused by incorrect sampling volume and loss of too much data. Failure to satisfy this criterion does not actually violate physical principles. At most sites, this rule eliminated about 5-7 percent of the total samples; some of these samples were void anyway and had no measurements. Thus, at most sites, about 2-3 percent of the actual data (i.e., samples having volumes greater than zero) were lost. This criterion eliminated all samples exhibiting grossly incorrect volumes. Application of this criterion to the current data base helped us identify a systematic error in the calculation of sample volumes (which has since been corrected).
3. Flagged as suspect all samples that failed charge balance for either the PM2.5 or PM10 size fractions (i.e., if  $|\Sigma(\text{Cations} - \text{Anions})| > 2 \cdot \sigma_\Sigma$ , where  $\sigma_\Sigma$  is the standard deviation of the sum). Failure to meet this criterion does not violate physical principles because some chemical species may not have been measured. Many samples failed to meet either (or both) the criteria for charge balance for PM2.5 and PM10. Violations involved excesses of both cations and anions in roughly equal numbers (except at Bakersfield, where most violations involved an excess of cations).

Thus, we invalidated only those measurements that were clearly incorrect on the basis of (1) comparisons with other data, (2) violation of criteria that must be met to satisfy physical principles (e.g., ratio of PM<sub>2.5</sub> to PM<sub>10</sub> mass), or (3) violation of sampling/analytical protocols. Measurements that were determined invalid or suspect were flagged without deleting them from the data base. If a filter pack carried more than one flag, the most serious was retained (e.g., if it earned an "S" for one reason and an "I" for another, the "I" was used).

Table 14 shows the percentage of usable samples by monitoring site and filter pack. Filter packs are designated as:

- GT - NO<sub>2</sub> measurements;
- TCK - all PM<sub>10</sub> species, SO<sub>2</sub>, and NH<sub>3</sub>;
- DN - PM<sub>2.5</sub> denuded particulate nitrate;
- TN - all PM<sub>2.5</sub> species.

Note that HNO<sub>3</sub> requires valid DN and TN.

Percentages are low for GT (i.e., NO<sub>2</sub>) because we flagged all samples from October 1989 through April 1991 as suspect (as described above). Percentages for DN are low for Los Angeles and Azusa because we flagged all samples collected after May 1989 as suspect. The TCK, DN, and TN percentages are low for Santa Barbara because most of the sample volumes for these filter packs exceed the nominal volume of 14.4 m<sup>3</sup>. We flagged these samples as suspect because we have found no explanation (we have discussed the problem with CARB staff, who are investigating the matter).

Table 14. Percentage of usable dry-deposition samples by monitoring site and filter pack. Samples were considered usable if they were flagged "V" (valid), "C" (charge balance not satisfied), or "s" (one or more individual species suspect). Samples were considered not usable if they were flagged "I" (invalid) or "S" (suspect).

Site	No.	GT	TCK	DN	TN
Azusa	443	47.2	93.2	23.7	91.7
Bakersfield	436	40.8	85.1	86.9	83.5
Fremont	429	47.8	96.5	96.0	95.6
Gasquet	353	31.4	83.7	87.0	89.9
Los Angeles	444	42.1	83.1	25.7	83.3
Long Beach	438	46.6	92.2	95.9	95.6
Sacramento	382	41.1	88.0	90.8	88.3
Santa Barbara	322	32.0	11.1	64.0	26.1
Sacramento collocated	326	32.5	86.8	88.3	82.6
Sequoia	422	37.4	84.1	81.0	85.3
Yosemite	417	37.2	79.9	83.2	60.0

**Samples falling below detection or quantification limits.** Many measurements fall below the detection limits or limits of quantification that are reported by Watson et al. (1991). Table 15 shows the percentage of samples exceeding detection limits for all sites and selected chemical species. Table 16 shows the percentage of samples exceeding limits of quantification for all sites and selected chemical species. It is clear that some measurements at some sites essentially constitute random noise, including NO<sub>2</sub> at Sequoia and Yosemite and HNO<sub>3</sub> at Gasquet.

Sample values falling below the limits of detection and quantification appear in the data base; they have not been censored. Censoring raises a number of difficulties with respect to most statistical analyses, and procedures are available for treating censored data (e.g., El-Shaarawi, 1989; Gilliom and Helsel, 1986). We neither censor nor exclude measurements that fall below detection or quantification limits. Such measurements will contribute little to total deposition over quarterly or annual time scales.

Table 15. Percentage of samples exceeding minimum detection limits for all sites and selected chemical species.

Site	Denuded		PM2.5 SO <sub>4</sub> <sup>2-</sup>	SO <sub>2</sub>	NH <sub>3</sub>	NO <sub>2</sub>	DD HNO <sub>3</sub>	Filter- Pack NO <sub>3</sub> <sup>-</sup>
	PM2.5 NO <sub>3</sub> <sup>-</sup>	PM2.5 NO <sub>3</sub> <sup>-</sup>						
Azusa	98.2	95.8	94.3	93.7	99.3	98.8	48.5	86.7
Bakersfield	83.0	79.8	80.5	79.8	86.2	89.2	53.2	84.4
Fremont	89.5	84.6	85.3	83.2	93.7	96.3	38.9	87.9
Gasquet	78.5	47.3	79.0	58.6	69.7	60.3	23.2	52.4
Los Angeles	79.5	78.8	77.7	73.9	81.3	84.0	42.1	79.5
Long Beach	90.9	87.7	87.9	84.9	91.6	94.5	49.5	90.0
Sacramento	85.9	76.7	79.1	81.2	86.1	88.0	48.7	82.2
Sacramento collocated	81.9	75.2	76.1	77.3	86.2	86.8	46.3	82.5
Santa Barbara	91.0	80.4	83.5	75.5	91.3	91.3	55.0	89.1
Sequoia	85.5	60.7	79.4	69.2	83.9	20.9	43.4	81.5
Yosemite	77.5	52.0	76.0	62.6	77.5	12.2	48.0	78.7

Table 16. Percentage of samples exceeding limits of quantification for all sites and selected chemical species.

Site	Denuded		PM2.5 SO <sub>4</sub> <sup>2-</sup>	SO <sub>2</sub>	NH <sub>3</sub>	NO <sub>2</sub>	DD HNO <sub>3</sub>	Filter Pack NO <sub>3</sub> <sup>-</sup>
	PM2.5 NO <sub>3</sub> <sup>-</sup>	PM2.5 NO <sub>3</sub> <sup>-</sup>						
Azusa	82.4	86.5	84.7	79.9	88.9	92.8	38.4	78.1
Bakersfield	80.3	78.9	79.4	79.1	86.2	89.2	45.4	69.5
Fremont	81.8	79.4	83.9	74.8	92.1	95.1	21.7	49.4
Gasquet	17.3	79.1	75.6	26.3	53.0	51.0	2.3	4.5
Los Angeles	76.1	86.2	77.5	72.5	80.4	83.8	34.5	70.0
Long Beach	86.1	75.1	87.9	84.0	91.1	94.5	40.4	69.9
Sacramento	77.2	76.7	77.0	75.9	85.6	88.0	35.1	51.3
Santa Barbara	78.3	75.8	82.0	59.3	87.6	91.0	35.4	53.7
Sacramento collocated	73.0	72.4	74.8	75.5	85.9	86.5	29.1	46.9
Sequoia	59.5	54.0	73.5	51.2	75.1	13.7	20.9	43.8
Yosemite	31.7	42.9	68.3	39.1	67.6	6.2	24.0	35.7

**Meteorological data.** We were provided with two meteorological data bases. One was prepared by DRI for the period up to September 1989. The second was prepared by the El Monte laboratory, using DRI's programs, for the period from October 1989 through September 1991. We found that level 1 validation of the CARB portion of the data base had not been completed. All the programs had been run and certain informational flags had been added to the data base. However, all data records were listed as validated at level 0, not level 1. The DRI programs require the user to examine the data and convert "0" to "1" (valid at level I), "8" (suspect), or "9" (invalid). This step had not been completed.

We compared frequency distributions of all meteorological variables in the DRI (level 1 valid records) and CARB (level 0 valid records) data bases and found no substantial differences.

We used records flagged as "0" and carrying no other validation flags in the CARB portion of the data base. We used all records flagged as "1" (regardless of other flags) in

the DRI portion of the meteorological data. We made one exception. At Gasquet, the dew-point temperature data in the DRI data base had been flagged suspect for all but 24 hours, apparently because dew-point temperature was reading about 5° Celsius (C) low (Watson et al., 1991). We chose to use values flagged "8" in this case.

### Specification of Variables of Interest

The variables of interest include the following species, which were treated in the Oak Ridge/EPA dry-deposition program (described in the next section):

- O<sub>3</sub> (g);
- SO<sub>2</sub> (g);
- HNO<sub>3</sub> (g);
- particulate sulfate;
- particulate nitrate.

The following species are also of interest, but were not treated in the Oak Ridge/EPA program:

- NH<sub>3</sub> (g);
- NO<sub>2</sub> (g);
- particulate ammonium.

Because particulates are differentiated by size only for deposition velocity calculations, particulate ammonium is treated identically to particulate sulfate and nitrate. Rough estimates of transfer resistances for ammonia and nitrogen dioxide gases were obtained by applying the algorithms of Wesely (1989). The resistance values we used [seconds per meter (s/m)] are shown in the tabulation below:

	NO <sub>2</sub>	NH <sub>3</sub>
Mesophyll	0	0
Cuticle	20,000	10,000
Soil	2000	2000

### Calculation of Deposition Velocities: The Oak Ridge/EPA Dry-deposition Program

The theoretical basis and practical implementation of the inferential method have been developed by a number of workers at Oak Ridge National Laboratory and at EPA (e.g., Hicks et al., 1987; McMillen, 1990; Hicks et al., 1991; Meyers et al., 1991). We requested and received two versions of the computer program developed by the Oak Ridge group; we denote them DD1 and DD2 (dry deposition 1 and 2). The dry-deposition algorithms we use are essentially those of DD2. We use a version that we modified to handle our data and output needs - DD3. In this section, we first document the overall

program flow, which includes preprocessing of data, calculation of deposition velocities (DD3), and postprocessing of deposition velocities. The multiplication of deposition velocities by concentrations to produce fluxes is a postprocessing step, which we carry out using programs written for the SAS software system. We next present the algorithms of the latest version of the Oak Ridge program, indicating any modifications we made. We present the overall structure of the program, the inputs required by the model, a discussion of the manner in which the model calculates the resistance terms, and a description of the way in which they are combined to generate deposition velocities for gases and particles. (This discussion is detailed and technical; it is intended for readers having a particular interest in the computational procedures.)

Insofar as possible, we have used the original Oak Ridge/EPA algorithms. At the current level of development of the inferential method, judgment necessarily plays a significant role as one moves from the theoretical concept to detailed parameterization. In using this program, we have relied on those researchers at the forefront of the field.

### Calculation of Deposition Velocities and Fluxes: Outline of the Program Flow

**Preprocessing.** Daily meteorological data from the NWS sites closest to the CADMP sites are used to generate hourly rainfall by dividing rainfall among hours in proportion to the wetness parameter in the CADMP data. Daily rain files are first edited to convert M (missing) to -9 and S (total in following day) to a split between days. Next, our FORTRAN program PRE.FOR rewrites the NWS files into columnar sets easy to input into other programs. Then, MET.FOR combines the data with the CADMP meteorological data to produce the variable "RAIN" needed by DD3. Rainfall data were not available as part of the CADMP data set, but were obtained from the nearest available sites, as shown in the following tabulation:

CADMP Site	Precipitation Site	Distance Difference (km)	Elevation Difference (m)
Gasquet	GASQUET R S	2.2	-82.0
Fremont	NEWARK	7.0	-15.0
Sacramento	SACRAMENTO WSO CI	.0	5.0
Yosemite	YOSEMITE PARK HDQ	11.5	-1212.0
Sequoia	LODGEPOLE	6.0	-1240.0
Bakersfield	BAKERSFIELD WSO AP	7.0	-70.0
Santa Barbara	SANTA BARBARA FAA AP	.0	-19.0
Long Beach	LONG BEACH WSO AP	3.8	-24.0
Los Angeles	LOS ANGELES CIVIC CTR	2.2	-63.0
Azusa	SAN GABRIEL CANYON P H	3.1	-113.0

MET.FOR also generates relative humidity from dew point and ambient temperatures. Finally, an output file is produced that is readable by DD3.

**DD3.FOR.** The program produces a "canopy" resistance for stomata, cuticle, and soil resistance for each plant for each hour. This canopy resistance is the sum of boundary layer and transfer resistances, which are calculated and summed separately for each of 21 canopy layers and then combined as parallel resistances. The resulting overall canopy resistances are then combined as parallel resistances and the total is summed with aerodynamic resistance. We have added a subroutine to the program to disaggregate these resistances so that it is possible, for each plant, to look at the contribution of three separate surfaces: stomatal, cuticular, and soil. For each of these, or for their combination, the approximate contribution of  $R_a$ ,  $R_b$ , and  $R_t$  can be determined, and an aggregate  $R_a$ ,  $R_b$ ,  $R_t$  for the entire plant can also be determined. A "plant" includes deposition to the soil underneath the plant. Although the disaggregations are approximate, they were carried out such that reaggregation always equals the values generated by the program for the total canopy. The outputs are hourly values, plant by plant, with separate  $R_a$ ,  $R_b$ , and  $R_t$  for each surface. Thus, nine resistances are produced for each pollutant for each plant for each hour. These represent the most disaggregated set of outputs. The original program output a single deposition velocity for each species; however, this approach presupposes accurate knowledge of the areal distribution of plant species for a site, information that we do not have. We merge combinations of plants at sites as a postprocessing step using SAS programs. The disaggregation of resistance terms allows us to examine the contributions of various surfaces and resistance terms.

The CADMP meteorological data also contains hourly  $O_3$  in ppb by volume (ppbv). DD3 converts this value to  $\mu\text{g m}^{-3}$ . Pressure is estimated at the site from altitude and ambient temperature and by assuming 1013 millibars (mb) at sea level and a lapse rate of  $6.5^\circ\text{C km}^{-1}$ . Site ambient temperature and estimated pressure are then used to convert ppbv to  $\mu\text{g m}^{-3}$ .

Because of the large volume of output from DD3, it is output into a FORTRAN-readable binary file for postprocessing.

**Postprocessing.** To merge DD3 results with the CADMP chemistry data sets, the first postprocessing step produces ASCII output files suitable for easy reading by SAS from the binary files. The first postprocessing program is POST1.FOR. Total deposition velocities are obtained by summing  $R_a$ ,  $R_b$ , and  $R_t$  for each surface and then combining them in a parallel manner to produce the  $V_d$  for each pollutant for each plant for each hour. Bare ground is treated as a plant lacking either a stomatal or cuticular surface. Total deposition velocities for each plant are then averaged over the day (6:00 a.m. to 6:00 p.m.) and night (6:00 p.m. to 6:00 a.m.) periods.

$O_3$  concentrations are multiplied by  $V_d$  on an hourly basis and the resulting deposition value is averaged for comparison with deposition values calculated using 12-hour

averages. Thus, two values per day are produced for all days having data available.

**SAS.** The output from POST1.FOR is read into a SAS data set, which is then merged with the once-per-week day and night chemical data. Fluxes are produced by multiplying 12-hour  $V_d$  averages by the 12-hour pollutant concentration averages. Site totals are produced by summing across area-weighted plant fluxes.

**Structure of DD3.** The calculation of deposition velocities is carried out by the Oak Ridge program, which has been modified to make the input/output procedures more compatible with our data, but which implements the scientific algorithms substantially the same manner as does the original program. Each run considers one site only. Each site has a short informational data file (latitude, longitude, elevation, plant species, etc.) and a meteorological data file. The meteorological data is preprocessed by MET.FOR, which generates an ASCII file with extension .MET. The main program DD3, reads the control file and all non-site-specific plant data. It then calls MEYERS, which reads site-specific data and enters the main program loop. This loop consists of reading one line of hourly met data and calling a sequence of subroutines.

**Inputs.** Below, we list the input files and the input variables. (The variables used by the program are in capital letters, followed in parentheses by the symbols used in our description of the algorithm.)

Data read from control file:

- RUNID = Run ID, 10 character max
- NOTE = Descriptive title
- Names and paths of all input and output files
- Some miscellaneous program options, mostly diagnostic.

Data read from PLANT.DAT, one line for each type:

- TYPE = Character string name of plant
- RSTOM = ( $R_{Stom}$ ) Minimal stomatal resistance, single leaf, both sides, converted to RSMIN in program (s/m)
- BSTOM = Coefficient used to determine stomatal resistance [Watts (W)  $m^{-2}$ ], converted to B in program
- OPT = Optimal temperature, converted to TOPT in program ( $^{\circ}C$ )
- MAX = Maximum temperature, converted to TMAX in program ( $^{\circ}C$ )
- MIN = Minimum temperature, converted to TMIN in program ( $^{\circ}C$ )
- PROF = Option (1,2, or 3) for vertical profile of leaf area, converted to IPROF in program, used to select data in the PADPROF(1, 2, or 3).20 files
- CANHT = Canopy height (not used; read instead from STATION.DAT)
- IFR = 1 = forest, 2 = not forest.

Data read from LANG.SPH, a nine-record file having two real fields per record:

- LF(I) = Portion of leaves in each of 9 classes of leaf angle
- CSNL(I) = Cosine of the angle between the leaf normal vector and the zenith.

Data read from STATION\_NAME.DAT (e.g., GA8990.DAT) by MEYERS:

- SITECODE = Two-character site identifier
- STATION = Character string name of the station
- LAT = Decimal latitude
- LONG = Decimal longitude
- ZONE = Time zone (used by ZENGEN)
- NSTPLNTS = Number of plants at the site
- ZMET = Height of the met instruments above the ground (m)
- IAVGS = Averaging scheme for computing canopy resistance: 0 = "canopy mix", 1 = "area weighting"
- ELEVN = Elevation above mean sea level (m).

For each of NSTPLNTS the following:

- PNAME = Name of plant
- PRCNT = Percentage of the area covered by PLANT(1)
- LAII = Maximum LAI of plant
- LAIW = Winter LAI (not used)
- CANHT = Canopy height
- Z0 = Roughness length
- IPER = The number of periods in the year for which fractional LAI's are defined.

For each IPER:

- IBEG = Starting day of the period
- IEND = Ending day of the period
- RPCT = Percentage of maximum LAI for each plant during the period.

Data read from STATION.MET (e.g., GA8990.MET):

- YR\_JDAY = Julian Day (in YYDDD format)
- TIME = Time (in HHMM format)
- UMH = (u) Mean wind speed ( $\text{m s}^{-1}$ )
- STHETA = ( $\sigma_{\Theta}$ ) Standard deviation of horizontal wind direction (deg)
- RG = Global radiation ( $\text{watts m}^{-2}$ )
- TA = Air temperature ( $^{\circ}\text{C}$ )

- RH = Relative humidity (percent)
- CWET = Canopy wetness (0-1)
- RAIN = Rainfall (mm)
- O3PPBV = Concentration of O<sub>3</sub> in ppbv.

**Initializations.** The program reads station information from STATION.DAT: latitude, longitude, time zone, averaging scheme for computing canopy resistance, the plant types, and LAI. It looks up the data for the plant types from PLANT.DAT.

For each plant type, the program reads one of three vertical-leaf-profile files: PADPROF1.20, PADPROF2.20, or PADPROF3.20. Each consists of 21 lines containing a series of positive real numbers that sum to one. Each line is read into the variable NLAI, and a new variable is created - MLAI = NLAI\*LAI, thus breaking each LAI into 21 parts that sum to the old LAI. For algorithmic analysis, layer index 2 corresponds to the bottom and layer index 21 to the top of the canopy; index 1 is not used.

Next, a nine-record, two-field file, LANG.SPH, defines "the constants representative of a spherical leaf angle distribution" (as indicated in the program). The variables are LF and CSNL. The angles range from 5° to 85° in 10° intervals. LF and CSNL are passed via a common statement to subroutines CANRES and ZENGEN.

**Meteorological Data.** The main loop begins by reading a line of meteorological input for a particular day and hour. The variables are Julian day (JDAY), time, mean wind speed ( $u$ ), standard deviation of wind direction ( $\sigma_{\Theta}$ ), global radiation (RG), air temperature ( $T$ ), relative humidity (RH), canopy wetness (CWET), and rainfall (RAIN).

If  $u$ ,  $\sigma_{\Theta}$ ,  $T$ , RH, CWET, or RG are missing,  $V_d$  is set to missing and is not calculated.

Bounds are then assigned to  $\sigma_{\Theta}$ . If this value is less than 1°, it is set to 1°; if it is greater than 0.6 radians, it is set to 0.6 radians.

**Soil Resistance.** Subroutine SOILRES is called with input variables SNOW,  $T$ , and AVSW (average soil water), and returns the variable RSOIL (soil resistance). SNOW and AVSW have been initialized in the main program to 0 and 120 respectively. Air temperature is a meteorological variable. (In calculating  $V_d$ , the program does not put RSOIL in series with  $R_b$ .) The values of RSOIL are a function of the values of SNOW,  $T$ , and AVSW, as shown in the tabulation below.

Input			RSOIL for three gases		
AVSW	SNOW	Air Temp (°C)	SO <sub>2</sub>	O <sub>3</sub>	HNO <sub>3</sub>
≥ 75	0	-	350	2000	1
< 75	0	-	700	2000	1
-	1	≥ -2	100	600	100
-	1	< -2	100+E	600+E	100+E
Program DD1 values			1500	1500	1000

The enhancement factor, E, of snow resistance below -2°C is as follows:

$$E = 1000 \times \exp(-\text{air temp } ^\circ\text{C} - 4) \quad (18)$$

This factor has a value of 18 at 0°C, 135 at -2°C, 1000 at -4°C, 2700 at -5°C, and 20,000 at -7°C. The practical effect is that at air temperatures below -7°C, snow has an infinite resistance to gaseous deposition.

**Computation of the Aerodynamic Resistance,  $R_a$ .** If global radiation is greater than 10,

$$R_a = 9/\sigma_0^2 u \quad (19)$$

Otherwise,

$$R_a = 4/\sigma_0^2 u + 300 \quad (20)$$

Then friction velocity,  $u_*$ , is calculated as a function of  $R_a$  and  $u$ :

$$u_* = \sqrt{u/R_a} \quad (21)$$

**Canopy resistance.** Subroutine WETRES is called to determine cuticular resistance. Input values are CWET, RAIN, and IWET. RCUT (s/m) is returned. CWET and RAIN are meteorological inputs. IWET is set to zero in the main program, apparently as an initialization. RAIN is rainfall in mm/hr. CWET, range 0-1, is the portion of the hour during which a wetness sensor detects that surfaces are wet. The following tabulation indicates the manner in which these variables are combined to produce RCUT:

Input			RCUT for three gases		
RAIN	CWET	State	SO <sub>2</sub>	O <sub>3</sub>	HNO <sub>3</sub>
0	< 0.5	Dry	15,000	15,000	0.01
	≥ 0.5	Dew	5,000	8,000	0.01
> 0	< 0.5	Dry	15,000	15,000	0.01
	≥ 0.5	Rain	10,000	3,000	0.01

The tabulated values imply that:

- The cuticular resistance of HNO<sub>3</sub> is unaffected by wetness;
- The driest condition occurs when CWET is less than .5, regardless of whether it is raining or not, implying that the CWET input is more reliable than the RAIN input. This condition might be called "dry;"
- For the cases in which CWET is ≥0.5, and it is also raining, the conditions are clearly wetter than if it is not raining. The two cases might be called "dew" and "rain;"
- For ozone, we see the resistance decreasing from 15,000 to 8,000 to 3,000 as the conditions become wetter;
- For SO<sub>2</sub>, the resistance decreases from 15,000 to 5,000 as the conditions change from dry to dew. It increases to 10,000 as conditions change from dew to rain. This algorithm accommodates the findings of Wesely and Lesht (1989): "dew is particularly effective in increasing SO<sub>2</sub> deposition for short periods of time".

Because the CADMP network does not report rainfall, we used daily NWS precipitation data and divided daily rainfall among hours in proportion to the values for CWET. This procedure is implemented in MET.FOR. The effect of rain could be bounded by the two conditions of "always raining" and "never raining."

Subroutine ZENGEN is called to produce the zenith angle, ZEN. Inputs are Julian day, time, latitude, longitude, and time zone.

Day is indicated by the flag IDAY=1, night by IDAY=0. Night is defined by global radiation less than 10 W m<sup>-2</sup> or by a zenith angle greater than 90°. If night is indicated, RBVD (visible beam radiation) and RVD(2-21) (diffuse visible radiation) are set to 0.001 W m<sup>-2</sup> and FSL(2-21) (fraction of sunlit leaves) are set to zero.

Subroutine WSTRESS is called to calculate a water stress correction (FW) to minimal stomatal resistance, RSMIN, based on the soil water deficit in the top 60 cm of soil. Inputs are global radiation (RG) average soil water (AVSW) time interval of the data (TINT) and day/night status (IDAY). The time interval is set in the main program to be one hour.

**Canopy averaging.** There are two averaging schemes for computing canopy resistance: canopy mix (AVER = 0) and area weighting (AVER = 1). AVER is set in the STATION.DAT file; the user must exercise some judgment in choosing the appropriate averaging scheme for a given station.

Averaging scheme 0 (AVER = 0: canopy mix) for computing canopy resistance is performed as follows. For the first plant type, call WNDPROF and, if daytime, CANRAD2. For each plant type ( $j=1, nstplnts$ ), call TSTRESS and CANRES.

WNDPROF is called once with these input variables: the sum of the two LAIs, LAITOT, and the canopy height and leaf profile of plant 1. WNDPROF returns the array RB ( $R_b$ ). This scheme reflects a mixed forest canopy containing a dominant species and a secondary species. The resulting RB ( $R_b$ ) values are slightly greater than those that would occur in considering the dominant species alone.

CANRAD2 is also called once. It uses MLAITOT, the array of LAIs summed over both species, zenith angle, and global radiation, and returns the array FSL (portion of sunlit leaves), the array RVD (diffuse visible radiation), and RBVD (visible beam radiation at the top of the canopy not corrected for zenith angle). These three parameters are transferred to subroutine CANRES in COMMON /NUMBERS/.

Then, TSTRESS and CANRES are called for each species using the specified LAI. This averaging scheme explains the reason for specifying LAI for the plants separately for each station and the reason that this averaging scheme ignores the PRCNT variable. It allows the calculation of a single wind profile and sunlight regime. The LAIs thus do not reflect a monoculture, but a mixed forest.

Subroutine WNDPROF is called to calculate the mean wind speed vertical profile within the canopy. Inputs are  $u_*$ , the sum of the two species LAI, LAITOT, canopy height for the first plant type, HC(1), and vertical profile of leaf area option for first plant type, IPROF(1). Returned is an array of 21 leaf boundary layer resistances, RB ( $R_b$ ).

If it is daytime (IDAY = 1), subroutine CANRAD2 is called to compute the vertical profile of both beam and diffuse components of photosynthetically active radiation for a 21-layer canopy. Inputs are

- MLAITOT, a 21 element array consisting of the sum of the two MLAI arrays, one for each species;
- ZEN, zenith angle;

- RG, global radiation.

Outputs are:

- FSL(21), fraction of sunlit leaves;
- RVD(21), array of diffuse visible radiation;
- RBVD, visible beam radiation (not an array).

For each plant type ( $j = 1, 2$ ), call the following subroutines: TSTRESS and CANRES.

Calculate  $V_d$  for the gaseous species  $i=1,2,3$ :

$$V_{d_i} = \frac{100}{R_a + R_{c_u} \parallel R_{c_g} \parallel R_{soil_i}} \quad (22)$$

Averaging scheme 1 (AVER = 1: area weighting) for computing canopy resistance is performed as follows. For each plant type ( $j = 1, 2$ ), call the following subroutines:

- WNDPROF. Returns RB(21), boundary layer resistance uncorrected for varying diffusivities;
- If daytime, CANRAD2. Returns FSL(21) and RBVD;
- TSTRESS. Returns temperature stress correction for stomatal resistance;
- CANRES. Returns a total canopy resistance (boundary layer plus transfer) for each chemical species. We modified this routine to return boundary layer and transfer components of stomatal and cuticular conductivities for each species as well.

Calculate  $R_t$  for the gaseous species  $i = 1, 2, 3$  and plant types  $j = 1, 2$ :

$$R_{t_{ij}} = R_{L_{ij}} \parallel R_{soil_i} \quad (23)$$

Calculate  $V_d$  for the gaseous species  $i = 1, 2, 3$ :

$$V_{d_i} = \frac{A_1}{R_a + R_{c_u}} + \frac{A_2}{R_a + R_{c_g}} \quad (24)$$

Equation 24 can also be written as

$$V_{d_i} = A_1 V_{d_{i1}} + A_2 V_{d_{i2}} \quad , \quad (25)$$

where the deposition velocities are calculated as if the two plants are the only ones being considered, but are then area-weighted.

**Comparison of canopy averaging schemes.** Canopy mix is intended for the case in which the plants are mixed together and the wind profile is controlled by one of them. In this case, LAI is the LAI of the species within the mix, the multiple of total unit area that one side of the leaves of that species makes up. If the species is a small proportion of the mix, its LAI could be a small number, even for a very leafy species. PRCNT, the area percentage specified in STATION.DAT, is not used in this scheme. WNDPROF (which returns RB) is called using LAITOT, the sum of all LAIs in the mix, but the canopy height and the vertical profile of the leaf area of the first species only. Therefore, the data need to be arranged so that the wind-controlling species in the mix (probably the tallest and most common tree) is listed first in STATION.DAT.

Area weighting is intended for the case in which the plants occupy separate regions of a unit area. An agricultural region would constitute the simplest case; however, an oak grassland biome would be another example. In area weighting, the LAI specified in STATION.DAT must be that of the species alone, and PRCNT is used to weight the various additional plants. WNDPROF is called separately for each species, so that RB is different for each species, depending on the canopy height and LAI of that species alone.

We ran a pair of test cases, which produced almost identical results, indicating that the calculated deposition velocities are not particularly sensitive to the choice of averaging schemes.

In practice, the actual meteorological monitors are likely to be placed in open areas, a condition likely to be uncharacteristic of most of the surrounding area. For example, the monitors at Gasquet are located in a grassy field at the Gasquet Airport; however, the surrounding land is forested. For this reason, the adjustments to windspeed and friction velocity suggested by Wesely (1989) and used in the RADM module are appropriate. We use the area-weighting scheme. We do not have information on LAI and speciation; however, it seems possible to obtain the LAI of individual species and the percentage of the ground area that those species cover. The algorithms do not seem to be particularly sensitive to the choice of canopy averaging.

**Subroutine CANRES.** CANRES is the 21-layer canopy resistance subroutine. It begins by calculating the stomatal resistance for shaded and sunlit leaves for each layer, without regard for the portions that are sunlit.

Stomatal resistance is added to boundary layer resistance and mesophyll resistance (considered to be zero) within each layer and sublayer. These resistances are then inverted

to form conductances. The conductances are weighted by the portions of both sunlit and shaded leaves and by the percentage of the sum that each layer and sublayer makes up; they are then summed.

**Particle deposition velocity.** For submicron particles (the program does not deal with larger ones),

$$V_d = \frac{1}{\frac{1}{0.002u_*} + R_a} \quad (26)$$

However, if  $\sigma_\Theta$  is greater than 0.175 radians and global radiation is greater than  $250 \text{ W m}^{-2}$ , then (apparently to prevent the boundary layer resistance from becoming too small),

$$V_d = \frac{1}{\frac{1}{0.01u_*} + R_a} \quad (27)$$

Settling velocity for submicron particles can be ignored. The CADMP data suggest that species formed primarily from condensation processes, such as sulfate, nitrate, and ammonium, are principally of submicron size (PM2.5 concentrations typically make up a large portion of PM10 concentrations of these species). Although the program deals with sulfate and nitrate particles only, adding others is a straightforward procedure because canopy (or transfer) resistance is absent (i.e., deposition velocity does not depend on the adsorptive or chemical interaction of the species and surface) (Seinfeld, 1986).

It is possible to determine deposition velocities for larger particles, for which settling velocity is important or even dominant. The expression would be (Hicks et al. 1987) as follows:

$$V_d = V_s + \frac{1}{R_a + R_b + R_a R_b V_s} \quad (28)$$

The only new term is settling velocity,  $V_s$ , which critically depends on particle size. However, because the CADMP data do not include a complete size distribution, one must either postulate a distribution or simply generate only upper and lower bounds for fluxes of large particles.

## RESULTS

### Summary Results

For each 12-hour period having valid data available, we used the program to calculate deposition of  $\text{SO}_2$ ,  $\text{O}_3$ ,  $\text{HNO}_3$ ,  $\text{NO}_2$ ,  $\text{NH}_3$ , particulate nitrate, particulate sulfate, and particulate ammonium. Because a large amount of the data was flagged as suspect or invalid, we utilized alternative measurements wherever possible. For particulate ammonium and sulfate, we used the  $\text{PM}_{2.5}$  measurement whenever it was present and substituted the  $\text{PM}_{10}$  measurement when necessary. For particulate nitrate, we used the denuded particulate nitrate measurement; if this measurement was not valid on a particular day, we first substituted the  $\text{PM}_{2.5}$  nondenuded nitrate, then the  $\text{PM}_{10}$  nitrate. For  $\text{HNO}_3$ , we used denuder difference  $\text{HNO}_3$ , substituting filter-pack nitrate when necessary. In the cases of Azusa and Los Angeles, we flagged as suspect all denuder difference  $\text{HNO}_3$  measurements after May 1989, so most of the calculations for these two sites were based on filter-pack nitrate.

We show summary results in Tables 17 through 27. Quarterly averages were produced by averaging separately day and night fluxes and then taking the unweighted mean of these two averages for all samples falling within each of the four seasons. The calculation was done in this way so as not to bias results if more day samples than night samples were available (or vice versa). We chose not to pair the day and night samples within each 24 hour period because the resulting 24-hour average would be missing whenever either the day or night subsample was missing (which occurred with some frequency).

Annual averages were produced by multiplying the unweighted mean of the quarterly averages by four. This procedure is equivalent to summing the quarters when all four quarterly averages are available. In some cases, one or more quarterly averages were missing, generally because we invalidated some portion of the measurements (see Table 14 and associated text). Results are also available for individual time periods.

Table 17. Mean quarterly and annual dry deposition at Azusa (kg ha<sup>-1</sup>).

Species	Q1	Q2	Q3	Q4	Annual
SO <sub>2</sub>	0.400	0.523	0.681	0.329	1.934
O <sub>3</sub>	3.701	6.674	7.386	3.189	20.950
HNO <sub>3</sub>	8.847	24.132	40.158	14.500	87.636
NO <sub>2</sub>	3.767	4.201	6.420	.	19.185
NH <sub>3</sub>	0.581	0.536	0.666	0.311	2.094
pNO <sub>3</sub> <sup>-</sup>	0.601	0.324	0.164	0.426	1.516
pSO <sub>4</sub> <sup>2-</sup>	0.156	0.482	0.707	0.204	1.549
pNH <sub>4</sub> <sup>+</sup>	0.183	0.192	0.233	0.145	0.753

Table 18. Mean quarterly and annual dry deposition at Bakersfield (kg ha<sup>-1</sup>).

Species	Q1	Q2	Q3	Q4	Annual
SO <sub>2</sub>	0.460	0.769	0.813	0.684	2.725
O <sub>3</sub>	3.085	5.959	6.327	3.312	18.683
HNO <sub>3</sub>	1.907	11.321	14.428	4.518	32.174
NO <sub>2</sub>	1.788	2.093	2.454	2.966	9.301
NH <sub>3</sub>	0.947	0.880	1.004	0.964	3.796
pNO <sub>3</sub> <sup>-</sup>	0.786	0.413	0.461	1.294	2.955
pSO <sub>4</sub> <sup>2-</sup>	0.159	0.308	0.367	0.263	1.097
pNH <sub>4</sub> <sup>+</sup>	0.215	0.094	0.115	0.350	0.773

Table 19. Mean quarterly and annual dry deposition at Fremont (kg ha<sup>-1</sup>).

Species	Q1	Q2	Q3	Q4	Annual
SO <sub>2</sub>	0.170	0.134	0.238	0.191	0.734
O <sub>3</sub>	1.769	4.338	3.537	1.470	11.114
HNO <sub>3</sub>	0.303	1.632	2.991	1.064	5.990
NO <sub>2</sub>	1.795	1.576	2.130	1.804	7.305
NH <sub>3</sub>	0.320	0.237	0.328	0.252	1.137
pNO <sub>3</sub> <sup>-</sup>	0.192	0.216	0.239	0.513	1.160
pSO <sub>4</sub> <sup>2-</sup>	0.051	0.184	0.223	0.086	0.543
pNH <sub>4</sub> <sup>+</sup>	0.041	0.032	0.052	0.079	0.204

Table 20. Mean quarterly and annual dry deposition at Gasquet (kg ha<sup>-1</sup>).

Species	Q1	Q2	Q3	Q4	Annual
SO <sub>2</sub>	0.071	0.079	0.046	0.035	0.231
O <sub>3</sub>	4.603	7.718	5.703	3.558	21.582
HNO <sub>3</sub>	0.190	0.094	0.434	0.228	0.946
NO <sub>2</sub>	0.662	0.358	0.179	.	1.599
NH <sub>3</sub>	0.083	0.541	0.051	0.047	0.722
pNO <sub>3</sub> <sup>-</sup>	0.015	0.033	0.041	0.017	0.105
pSO <sub>4</sub> <sup>2-</sup>	0.028	0.093	0.142	0.035	0.298
pNH <sub>4</sub> <sup>+</sup>	0.003	0.013	0.028	0.009	0.053

Table 21. Mean quarterly and annual dry deposition at Los Angeles (kg ha<sup>-1</sup>).

Species	Q1	Q2	Q3	Q4	Annual
SO <sub>2</sub>	0.463	0.560	0.448	0.487	1.958
O <sub>3</sub>	1.401	4.036	4.576	2.201	12.214
HNO <sub>3</sub>	3.049	17.409	22.989	15.475	58.922
NO <sub>2</sub>	2.443	4.807	6.239	.	17.985
NH <sub>3</sub>	0.467	0.520	0.618	0.506	2.111
pNO <sub>3</sub> <sup>-</sup>	0.164	0.217	0.144	0.575	1.100
pSO <sub>4</sub> <sup>2-</sup>	0.099	0.409	0.617	0.327	1.454
pNH <sub>4</sub> <sup>+</sup>	0.090	0.176	0.210	0.221	0.697

Table 22. Mean quarterly and annual dry deposition at Long Beach (kg ha<sup>-1</sup>).

Species	Q1	Q2	Q3	Q4	Annual
SO <sub>2</sub>	0.881	0.688	0.821	0.705	3.096
O <sub>3</sub>	2.077	3.471	3.481	1.558	10.587
HNO <sub>3</sub>	2.549	4.635	8.602	5.448	21.235
NO <sub>2</sub>	6.027	3.540	3.999	.	18.087
NH <sub>3</sub>	0.597	0.393	0.381	0.566	1.937
pNO <sub>3</sub> <sup>-</sup>	0.577	0.285	0.441	0.730	2.033
pSO <sub>4</sub> <sup>2-</sup>	0.217	0.358	0.690	0.309	1.573
pNH <sub>4</sub> <sup>+</sup>	0.170	0.125	0.224	0.207	0.726

Table 23. Mean quarterly and annual dry deposition at Sacramento (kg ha<sup>-1</sup>).

Species	Q1	Q2	Q3	Q4	Annual
SO <sub>2</sub>	0.225	0.340	0.455	0.204	1.224
O <sub>3</sub>	2.706	4.826	4.103	1.159	12.795
HNO <sub>3</sub>	2.656	3.116	5.758	2.324	13.853
NO <sub>2</sub>	.	2.221	2.104	.	8.650
NH <sub>3</sub>	0.770	0.807	0.731	0.484	2.791
pNO <sub>3</sub> <sup>-</sup>	0.492	0.163	0.187	0.596	1.439
pSO <sub>4</sub> <sup>2-</sup>	0.120	0.160	0.184	0.092	0.557
pNH <sub>4</sub> <sup>+</sup>	0.145	0.035	0.055	0.150	0.384

Table 24. Mean quarterly and annual dry deposition at Sacramento collocated monitor (kg ha<sup>-1</sup>).

Species	Q1	Q2	Q3	Q4	Annual
SO <sub>2</sub>	0.243	0.238	0.408	0.248	1.136
O <sub>3</sub>	2.701	4.826	4.117	1.164	12.808
HNO <sub>3</sub>	2.230	3.348	6.443	3.541	15.562
NO <sub>2</sub>	.	1.961	1.873	.	7.669
NH <sub>3</sub>	0.748	0.602	0.761	0.470	2.580
pNO <sub>3</sub> <sup>-</sup>	0.429	0.145	0.174	0.560	1.308
pSO <sub>4</sub> <sup>2-</sup>	0.109	0.167	0.208	0.104	0.587
pNH <sub>4</sub> <sup>+</sup>	0.130	0.039	0.083	0.163	0.415

Table 25. Mean quarterly and annual dry deposition at Santa Barbara (kg ha<sup>-1</sup>).

Species	Q1	Q2	Q3	Q4	Annual
SO <sub>2</sub>	0.108	.	.	0.132	0.479
O <sub>3</sub>	3.665	4.810	5.097	3.544	17.116
HNO <sub>3</sub>	.	1.488	4.706	3.167	12.482
NO <sub>2</sub>	.	0.978	1.259	.	4.474
NH <sub>3</sub>	0.118	.	.	0.110	0.455
pNO <sub>3</sub> <sup>-</sup>	0.070	0.095	0.123	0.121	0.409
pSO <sub>4</sub> <sup>2-</sup>	0.128	0.266	0.417	0.214	1.024
pNH <sub>4</sub> <sup>+</sup>	0.030	0.066	0.136	0.090	0.321

Table 26. Mean quarterly and annual dry deposition at Sequoia ( $\text{kg ha}^{-1}$ ).

Species	O1	O2	O3	O4	Annual
SO <sub>2</sub>	0.024	0.112	0.166	0.035	0.336
O <sub>3</sub>	5.195	9.182	10.218	5.226	29.822
HNO <sub>3</sub>	0.053	0.914	1.540	0.208	2.715
NO <sub>2</sub>	0.000	0.013	0.022	.	0.047
NH <sub>3</sub>	0.059	0.146	0.232	0.075	0.513
pNO <sub>3</sub> <sup>-</sup>	0.070	0.076	0.068	0.105	0.318
pSO <sub>4</sub> <sup>2-</sup>	0.034	0.121	0.140	0.026	0.321
pNH <sub>4</sub> <sup>+</sup>	0.014	0.045	0.046	0.029	0.133

Table 27. Mean quarterly and annual dry deposition at Yosemite ( $\text{kg ha}^{-1}$ ).

Species	O1	O2	O3	O4	Annual
SO <sub>2</sub>	0.052	0.053	0.084	0.044	0.233
O <sub>3</sub>	.	.	10.123	6.433	33.113
HNO <sub>3</sub>	0.215	0.534	1.092	.	2.455
NO <sub>2</sub>	.	0.002	0.002	.	0.007
NH <sub>3</sub>	0.063	0.071	0.114	0.033	0.282
pNO <sub>3</sub> <sup>-</sup>	0.006	0.035	0.034	0.026	0.101
pSO <sub>4</sub> <sup>2-</sup>	0.060	0.092	0.119	0.023	0.295
pNH <sub>4</sub> <sup>+</sup>	0.010	0.020	0.033	0.010	0.073

The fluxes of HNO<sub>3</sub> are of particular interest because of their magnitude. Estimated deposition of HNO<sub>3</sub> ranges from 1 to 87  $\text{kg ha}^{-1} \text{ yr}^{-1}$ . A distinct gradient of HNO<sub>3</sub> deposition exists in the SoCAB, from Long Beach (21  $\text{kg ha}^{-1} \text{ yr}^{-1}$ ) to downtown Los Angeles (59  $\text{kg ha}^{-1} \text{ yr}^{-1}$ ) to Azusa (87  $\text{kg ha}^{-1} \text{ yr}^{-1}$ ). At Azusa, Bakersfield, Los Angeles, and Sacramento, HNO<sub>3</sub> accounts for approximately 60 to 70 percent of the deposition of oxidized nitrogen species. At Fremont, Long Beach, and Santa Barbara, HNO<sub>3</sub> accounts for approximately half the deposition of oxidized nitrogen species.

### Sensitivity Analyses

The sensitivity analyses that we carried out do not encompass the full range of uncertainties associated with the inferential method and with the data. As noted previously,

the accuracy of the inferential method is considered to be no better than about 30 to 50 percent, depending upon the chemical species involved, for stations located in uncomplicated terrain and having uniform surroundings.

**Plant Parameters.** Plants are important in dry deposition of gases for two reasons: they generally have greater leaf surface area than an equivalent portion of plain ground and they absorb gases through their stomata, where, once inside, the leaf tissue transfer resistance to mesophyll is quite low. The stomatal characteristics of plants are important in the deposition of  $\text{SO}_2$ ,  $\text{O}_3$ ,  $\text{NO}_2$ , and  $\text{NH}_3$ . However, the transfer resistance of nitric acid is so low on any surface that the additional area of leaves makes little difference. As parameterized, the deposition of particles is not dependent on either leaf area or stomata.

The two factors of greatest significance are the lowest stomatal resistance that can be generated under the most favorable circumstances (RSTOM), and the leaf area index (LAI). Thus, given optimum temperature and light, grass, exhibiting an RSTOM of 50 and an LAI of 2.5, could stomatally absorb about 7 times the amount of pollutants as do ponderosa and lodgepole pine, which exhibit an RSTOM of 500 and an LAI of 3.5.

Canopy height is not an especially significant factor; it is used primarily to generate profiles of boundary layer resistances. One of three vertical leaf profiles (PROF) is chosen. This is the vertical distribution of leaf area. It affects the wind profile in the canopy.

The range in parameters characteristic of various plant types is about a factor of 2, depending on species, maturity, soil, and moisture conditions, (see Table 28).

For the sites in the CADMP, we know neither the species nor their areal distribution. The range of plant parameters, fortunately, is not enormous. We have somewhat arbitrarily selected and apportioned typical species (on the basis of an examination of photos of each site). We assigned all of the urban sites 15 percent grass, 15 percent "tree" (a sort of typical representative tree), and 70 percent bare ground. We assigned 100 percent spruce to Gasquet (the Gasquet forest is likely young redwood; because parameters were unavailable for redwood, we used spruce as a surrogate species). For Sequoia, we used one-third each of ponderosa pine, spruce, and white pine. For Yosemite, we assigned the same species 30 percent each and assigned 10 percent as bare ground.

Tables 29 through 38 show annual dry deposition calculated using these assigned values and several single surface types. The deposition values of the particulate species are invariant because particulate deposition is not a function of surface type. The tabled values show that deposition of nitric acid is not sensitive to surface type. The other gas-phase species ( $\text{O}_3$ ,  $\text{SO}_2$ ,  $\text{NO}_2$ , and  $\text{NH}_3$ ) are sensitive to the type of surface. To obtain accurate estimates for such species, it would be desirable to determine the distributions of surfaces within the immediate vicinity of each of the CADMP stations.

Table 28. Parameters affecting canopy resistance, by species.

Species	RSTOM	BSTOM	OPT	MAX	MIN	PROF	CANHT	LAI
Spruce	225	40	9	35	-5	2	23	3.7
Ponderosa/ lodgepole pine	500	40	25	5	40	3	23	3.5
Loblolly pine	200	55	25	40	5	3	23	3.6
White oak	100	50	25	45	5	2	23	4.5
Chestnut/ northern red oak	100	40	25	45	5	2	23	4.5
Maple	100	50	25	45	5	2	20	4.5
White birch	300	40	25	40	5	2	23	4.5
Beech	100	50	25	40	5	2	20	4.5
Maize	250	65	25	45	5	1	2.5	5.5
Wheat	100	25	25	40	5	1	1	3.0
Soybean	100	50	25	45	10	1	1	3.5
Grass	50	20	25	45	5	1	0.5	2.5
Blue grass	150	50	30	40	5	1	0.5	2.5
White pine	100	50	25	45	5	2	20	3.6
"Tree"	200	50	25	40	0	2	20	3.5

Table 29. Sensitivity of dry deposition estimates at Azusa to surface ( $\text{kg ha}^{-1} \text{ yr}^{-1}$ ).

Species	Assigned Split	Bare Ground	"Tree"	Chestnut/ N. Red Oak	Grass
SO <sub>2</sub>	1.934	1.393	2.379	3.200	4.010
O <sub>3</sub>	20.950	8.628	31.194	49.927	68.211
HNO <sub>3</sub>	87.636	87.496	87.977	88.031	87.949
NO <sub>2</sub>	19.185	9.798	26.643	40.780	55.534
NH <sub>3</sub>	2.094	0.797	3.250	5.157	6.988
pNO <sub>3</sub> <sup>-</sup>	1.516	1.516	1.516	1.516	1.516
pSO <sub>4</sub> <sup>2-</sup>	1.549	1.549	1.549	1.549	1.549
pNH <sub>4</sub> <sup>+</sup>	0.753	0.753	0.753	0.753	0.753

Table 30. Sensitivity of dry deposition estimates at Bakersfield to surface ( $\text{kg ha}^{-1} \text{ yr}^{-1}$ ).

Species	Assigned Split	Bare Ground	"Tree"	Chestnut/ N. Red Oak	Grass	Maize
SO <sub>2</sub>	2.725	2.119	3.299	4.167	4.982	3.442
O <sub>3</sub>	18.683	8.416	27.229	42.468	58.047	28.662
HNO <sub>3</sub>	32.174	32.094	32.369	32.398	32.352	32.452
NO <sub>2</sub>	9.301	5.581	13.022	18.186	22.939	13.666
NH <sub>3</sub>	3.796	1.709	5.909	8.807	11.422	6.386
pNO <sub>3</sub> <sup>-</sup>	2.955	2.955	2.955	2.955	2.955	2.955
pSO <sub>4</sub> <sup>2-</sup>	1.097	1.097	1.097	1.097	1.097	1.097
pNH <sub>4</sub> <sup>+</sup>	0.773	0.773	0.773	0.773	0.773	0.773

Table 31. Sensitivity of dry deposition estimates at Fremont to surface ( $\text{kg ha}^{-1} \text{ yr}^{-1}$ ).

Species	Assigned Split	Bare Ground	"Tree"	Chestnut/ N. Red Oak	Grass
SO <sub>2</sub>	0.734	0.549	0.897	1.167	1.434
O <sub>3</sub>	11.114	5.096	16.461	25.238	33.850
HNO <sub>3</sub>	5.990	5.979	6.018	6.022	6.016
NO <sub>2</sub>	7.305	4.618	10.154	14.047	16.996
NH <sub>3</sub>	1.137	0.483	1.787	2.708	3.543
pNO <sub>3</sub> <sup>-</sup>	1.160	1.160	1.160	1.160	1.160
pSO <sub>4</sub> <sup>2-</sup>	0.543	0.543	0.543	0.543	0.543
pNH <sub>4</sub> <sup>+</sup>	0.204	0.204	0.204	0.204	0.204

Table 32. Sensitivity of dry deposition estimates at Gasquet to surface ( $\text{kg ha}^{-1} \text{ yr}^{-1}$ ).

Species	Assigned	Bare Ground	"Tree"	Spruce	Grass
SO <sub>2</sub>	0.231	0.150	0.237	0.231	0.359
O <sub>3</sub>	21.582	5.718	22.122	21.582	40.657
HNO <sub>3</sub>	0.946	0.936	0.946	0.946	0.945
NO <sub>2</sub>	1.599	0.616	1.651	1.599	3.165
NH <sub>3</sub>	0.722	0.117	0.734	0.722	1.695
pNO <sub>3</sub> <sup>-</sup>	0.105	0.105	0.105	0.105	0.105
pSO <sub>4</sub> <sup>2-</sup>	0.298	0.298	0.298	0.298	0.298
pNH <sub>4</sub> <sup>+</sup>	0.053	0.053	0.053	0.053	0.053

Table 33. Sensitivity of dry deposition estimates at Los Angeles to surface ( $\text{kg ha}^{-1} \text{ yr}^{-1}$ ).

Species	Assigned Split	Bare Ground	"Tree"	Chestnut/ N. Red Oak	Grass
SO <sub>2</sub>	1.958	1.540	2.330	2.954	3.538
O <sub>3</sub>	12.214	5.764	17.857	27.601	36.670
HNO <sub>3</sub>	58.922	58.809	59.197	59.239	59.175
NO <sub>2</sub>	17.985	9.583	24.997	38.039	50.180
NH <sub>3</sub>	2.111	0.976	3.271	4.891	6.249
pNO <sub>3</sub> <sup>-</sup>	1.100	1.100	1.100	1.100	1.100
pSO <sub>4</sub> <sup>2-</sup>	1.454	1.454	1.454	1.454	1.454
pNH <sub>4</sub> <sup>+</sup>	0.697	0.697	0.697	0.697	0.697

Table 34. Sensitivity of dry deposition estimates at Long Beach to surface ( $\text{kg ha}^{-1} \text{ yr}^{-1}$ ).

Species	Assigned Split	Bare Ground	"Tree"	Chestnut/ N. Red Oak	Grass
SO <sub>2</sub>	3.096	2.291	3.781	* 4.982	6.167
O <sub>3</sub>	10.587	5.109	15.444	23.596	31.291
HNO <sub>3</sub>	21.235	21.194	21.335	21.351	21.327
NO <sub>2</sub>	18.087	7.822	25.904	41.426	58.172
NH <sub>3</sub>	1.937	0.808	3.014	4.628	6.128
pNO <sub>3</sub> <sup>-</sup>	2.033	2.033	2.033	2.033	2.033
pSO <sub>4</sub> <sup>2-</sup>	1.573	1.573	1.573	1.573	1.573
pNH <sub>4</sub> <sup>+</sup>	0.726	0.726	0.726	0.726	0.726

Table 35. Sensitivity of dry deposition estimates at Sacramento to surface ( $\text{kg ha}^{-1} \text{ yr}^{-1}$ ).

Species	Assigned Split	Bare Ground	"Tree"	Chestnut/ N. Red Oak	Grass
SO <sub>2</sub>	1.224	0.921	1.486	1.931	2.377
O <sub>3</sub>	12.795	5.554	18.643	29.467	40.737
HNO <sub>3</sub>	13.853	13.829	13.912	13.921	13.907
NO <sub>2</sub>	8.650	4.256	11.932	18.805	25.872
NH <sub>3</sub>	2.791	1.119	4.350	6.718	9.036
pNO <sub>3</sub> <sup>-</sup>	1.439	1.439	1.439	1.439	1.439
pSO <sub>4</sub> <sup>2-</sup>	0.557	0.557	0.557	0.557	0.557
pNH <sub>4</sub> <sup>+</sup>	0.384	0.384	0.384	0.384	0.384

Table 36. Sensitivity of dry deposition estimates at Santa Barbara to surface ( $\text{kg ha}^{-1} \text{ yr}^{-1}$ ).

Species	Assigned Split	Bare Ground	"Tree"	Chestnut/ N. Red Oak	Grass	Maize
SO <sub>2</sub>	0.479	0.400	0.569	0.677	0.759	0.600
O <sub>3</sub>	17.116	8.237	24.882	37.739	50.787	26.113
HNO <sub>3</sub>	12.482	12.461	12.531	12.539	12.527	12.553
NO <sub>2</sub>	4.474	2.204	6.230	9.663	13.316	6.377
NH <sub>3</sub>	0.455	0.219	0.708	1.017	1.303	0.770
pNO <sub>3</sub> <sup>-</sup>	0.409	0.409	0.409	0.409	0.409	0.409
pSO <sub>4</sub> <sup>2-</sup>	1.024	1.024	1.024	1.024	1.024	1.024
pNH <sub>4</sub> <sup>+</sup>	0.321	0.321	0.321	0.321	0.321	0.321

Table 37. Sensitivity of dry deposition estimates at Sequoia to surface ( $\text{kg ha}^{-1} \text{ yr}^{-1}$ ).

Species	Assigned Split	Bare Ground	"Tree"	Ponderosa/ Lodgepole	Spruce	White Pine
SO <sub>2</sub>	0.336	0.221	0.340	0.275	0.342	0.389
O <sub>3</sub>	29.822	11.235	30.254	20.760	32.812	35.715
HNO <sub>3</sub>	2.715	2.698	2.715	2.714	2.715	2.715
NO <sub>2</sub>	0.047	0.023	0.048	0.035	0.046	0.058
NH <sub>3</sub>	0.513	0.151	0.527	0.323	0.554	0.658
pNO <sub>3</sub> <sup>-</sup>	0.318	0.318	0.318	0.318	0.318	0.318
pSO <sub>4</sub> <sup>2-</sup>	0.321	0.321	0.321	0.321	0.321	0.321
pNH <sub>4</sub> <sup>+</sup>	0.133	0.133	0.133	0.133	0.133	0.133

Table 38. Sensitivity of dry deposition estimates at Yosemite to surface ( $\text{kg ha}^{-1} \text{ yr}^{-1}$ ).

Species	Assigned Split	Bare Ground	"Tree"	Ponderosa/ Lodgepole	Spruce	White Pine
SO <sub>2</sub>	0.233	0.168	0.262	0.213	0.262	0.300
O <sub>3</sub>	33.113	15.612	37.879	27.713	35.561	47.104
HNO <sub>3</sub>	2.455	2.709	2.728	2.727	2.728	2.728
NO <sub>2</sub>	0.007	0.005	0.007	0.007	0.008	0.008
NH <sub>3</sub>	0.282	0.089	0.326	0.183	0.347	0.410
pNO <sub>3</sub> <sup>-</sup>	0.101	0.112	0.112	0.112	0.112	0.112
pSO <sub>4</sub> <sup>2-</sup>	0.295	0.327	0.327	0.327	0.327	0.327
pNH <sub>4</sub> <sup>+</sup>	0.073	0.081	0.081	0.081	0.081	0.081

Duration of sample collection. Equation 11 can be rewritten in terms of averages (Hicks et al., 1985):

$$F = \bar{V}_d * \bar{C} + \sigma_{V_d} * \sigma_C * R_{V_d,C} \quad (29)$$

where the overbars denote averages,  $\sigma_{V_d}$  and  $\sigma_C$  are the standard deviations of  $V_d$  and  $C$ , respectively, and  $R_{V_d,C}$  is the correlation coefficient between  $V_d$  and  $C$ . From Equation 29, it is clear that if  $F$  is computed as the product of mean  $V_d$  by mean  $C$ , it will be underestimated when  $R_{V_d,C}$  is positive and overestimated when  $R_{V_d,C}$  is negative. The term  $R_{V_d,C}$  is likely to be nonzero if diurnal cycles exist in both  $V_d$  and  $C$ ; other periodicities, if present for both  $V_d$  and  $C$ , would also result in nonzero correlations.

The CADMP collects two 12-hour samples (6:00 a.m. to 6:00 p.m. and 6:00 p.m. to 6:00 a.m.). Because one daytime and one nighttime sample are collected, the correlation between  $V_d$  and  $C$  that might arise from diurnal cycles in both terms is lower than would be the case if samples were collected for 24 hours. Meyers and Yuen (1987) evaluated the need for day-night sampling at one dry-deposition site (near Oak Ridge, TN) for SO<sub>2</sub> and O<sub>3</sub>. They concluded that estimates of O<sub>3</sub> but not SO<sub>2</sub> flux were improved by day-night sampling and that errors decreased as the sampling time increased from one day to one week (O<sub>3</sub> showed positive correlation between  $V_d$  and concentration). Our expectation was that for sites near emission sources (e.g., the CADMP sites in the Los Angeles area), diurnal cycles in pollutant concentrations would be pronounced; this is in fact borne out by the mean day and night concentrations reported by Watson et al. (1990).

Table 39 compares fluxes calculated from 12-hour averages with fluxes calculated

from 24 hour averages. These fluxes were calculated as follows:

$$\begin{aligned}\text{flux}_{12} &= ((V_{\text{d-day}} * C_{\text{day}}) + (V_{\text{d-night}} * C_{\text{night}})) / 2 \\ \text{flux}_{24} &= (V_{\text{d-day}} + V_{\text{d-night}}) * (C_{\text{day}} + C_{\text{night}}) / 4\end{aligned}$$

Flux<sub>24</sub> is equivalent to the flux that would be calculated if the CADMP monitors collected 24-hour average samples. The annual averages were then calculated as described above. The annual averages do not agree exactly with those in Tables 17-27 and 29-38 because if any of the variables in the previous two equations were missing, the fluxes would be missing. The results show that HNO<sub>3</sub> fluxes would be underestimated by 30 to 40 percent at all sites except Gasquet if samples were collected as 24-hour averages rather than 12-hour averages (at Gasquet, HNO<sub>3</sub> was frequently below detection limits). Table 39 also shows that O<sub>3</sub> fluxes would be underestimated by seven to 23 percent at all sites except Sequoia and Yosemite if samples were collected as 24-hour averages rather than 12-hour averages (Sequoia and Yosemite showed very weak diurnal variations in ozone concentration).

Table 39. Mean annual dry deposition ( $\text{kg ha}^{-1}$ ) using 12-hour and 24-hour deposition velocity and concentration averages.

Site	Species	Sampling Duration	
		12-Hour	24-Hour
Azusa	SO <sub>2</sub>	1.886	1.697
	O <sub>3</sub>	20.948	16.858
	HNO <sub>3</sub>	88.050	53.668
	NO <sub>2</sub>	19.046	19.695
	NH <sub>3</sub>	2.056	1.828
	pNO <sub>3</sub> <sup>-</sup>	1.508	1.543
	pSO <sub>4</sub> <sup>2-</sup>	1.566	1.412
	pNH <sub>4</sub> <sup>+</sup>	0.760	0.760
Bakersfield	SO <sub>2</sub>	2.724	2.646
	O <sub>3</sub>	18.711	15.528
	HNO <sub>3</sub>	32.397	21.654
	NO <sub>2</sub>	9.362	10.783
	NH <sub>3</sub>	3.810	3.650
	pNO <sub>3</sub> <sup>-</sup>	2.898	2.620
	pSO <sub>4</sub> <sup>2-</sup>	1.112	1.103
	pNH <sub>4</sub> <sup>+</sup>	0.745	0.747
Fremont	SO <sub>2</sub>	0.742	0.663
	O <sub>3</sub>	11.181	9.660
	HNO <sub>3</sub>	6.037	3.793
	NO <sub>2</sub>	7.360	7.528
	NH <sub>3</sub>	1.140	1.026
	pNO <sub>3</sub> <sup>-</sup>	1.147	2.360
	pSO <sub>4</sub> <sup>2-</sup>	0.536	0.520
	pNH <sub>4</sub> <sup>+</sup>	0.200	0.216
Gasquet	SO <sub>2</sub>	0.230	0.232
	O <sub>3</sub>	22.124	20.441
	HNO <sub>3</sub>	0.837	0.926
	NO <sub>2</sub>	2.174	2.410
	NH <sub>3</sub>	0.750	0.593
	pNO <sub>3</sub> <sup>-</sup>	0.095	0.085
	pSO <sub>4</sub> <sup>2-</sup>	0.285	0.420
	pNH <sub>4</sub> <sup>+</sup>	0.053	0.063

Table 39. (continued)

Los Angeles	SO <sub>2</sub>	1.997	1.864
	O <sub>3</sub>	12.188	10.154
	HNO <sub>3</sub>	58.506	35.453
	NO <sub>2</sub>	17.532	17.156
	NH <sub>3</sub>	2.304	2.078
	pNO <sub>3</sub> <sup>-</sup>	1.085	1.139
	pSO <sub>4</sub> <sup>2-</sup>	1.310	1.260
	pNH <sub>4</sub> <sup>+</sup>	0.684	0.697
Long Beach	SO <sub>2</sub>	3.141	2.820
	O <sub>3</sub>	10.649	9.993
	HNO <sub>3</sub>	21.209	12.531
	NO <sub>2</sub>	17.931	16.954
	NH <sub>3</sub>	2.044	1.831
	pNO <sub>3</sub> <sup>-</sup>	2.116	1.797
	pSO <sub>4</sub> <sup>2-</sup>	1.607	1.443
	pNH <sub>4</sub> <sup>+</sup>	0.745	0.702
Sacramento	SO <sub>2</sub>	1.173	1.115
	O <sub>3</sub>	12.738	11.011
	HNO <sub>3</sub>	14.202	10.895
	NO <sub>2</sub>	8.654	9.199
	NH <sub>3</sub>	2.806	2.606
	pNO <sub>3</sub> <sup>-</sup>	1.443	1.286
	pSO <sub>4</sub> <sup>2-</sup>	0.564	0.574
	pNH <sub>4</sub> <sup>+</sup>	0.389	0.413
Sacramento collocated	SO <sub>2</sub>	1.126	1.068
	O <sub>3</sub>	12.748	11.039
	HNO <sub>3</sub>	16.132	9.947
	NO <sub>2</sub>	7.764	7.945
	NH <sub>3</sub>	2.582	2.352
	pNO <sub>3</sub> <sup>-</sup>	1.305	1.288
	pSO <sub>4</sub> <sup>2-</sup>	0.599	0.598
	pNH <sub>4</sub> <sup>+</sup>	0.421	0.437

Table 39. (concluded)

Santa Barbara	SO <sub>2</sub>	0.704	0.878
	O <sub>3</sub>	17.031	15.389
	HNO <sub>3</sub>	12.326	7.367
	NO <sub>2</sub>	4.461	4.577
	NH <sub>3</sub>	0.407	0.353
	pNO <sub>3</sub> <sup>-</sup>	0.381	0.367
	pSO <sub>4</sub> <sup>2-</sup>	1.058	0.938
	pNH <sub>4</sub> <sup>+</sup>	0.330	0.309
Sequoia	SO <sub>2</sub>	0.329	0.311
	O <sub>3</sub>	29.983	29.015
	HNO <sub>3</sub>	2.913	1.980
	NO <sub>2</sub>	0.038	0.051
	NH <sub>3</sub>	0.524	0.472
	pNO <sub>3</sub> <sup>-</sup>	0.326	0.268
	pSO <sub>4</sub> <sup>2-</sup>	0.318	0.313
	pNH <sub>4</sub> <sup>+</sup>	0.135	0.128
Yosemite	SO <sub>2</sub>	0.257	0.253
	O <sub>3</sub>	33.425	33.471
	HNO <sub>3</sub>	2.460	1.661
	NO <sub>2</sub>	0.007	0.012
	NH <sub>3</sub>	0.293	0.254
	pNO <sub>3</sub> <sup>-</sup>	0.137	0.120
	pSO <sub>4</sub> <sup>2-</sup>	0.284	0.257
	pNH <sub>4</sub> <sup>+</sup>	0.086	0.082

---

**Sigma theta ( $\sigma_{\theta}$ ).** The standard deviation of the wind direction, sigma theta ( $\sigma_{\theta}$ ), enters into the calculation of the aerodynamic resistance (see Equation 14). The deposition velocity (see Equation 13) can be dominated by the aerodynamic resistance under some conditions (low wind speeds, low values of  $\sigma_{\theta}$ , or low values of the transfer resistance,  $R_c$ ). For a reactive species such as  $\text{HNO}_3$ , for which  $R_c$  is typically low, the deposition velocity can be largely determined by  $R_a$ . Thus, the mass flux rate of  $\text{HNO}_3$  and other reactive species can be sensitive to the value of sigma theta.

We examined the sensitivities of the calculated flux rates to sigma theta by both increasing and decreasing all values of  $\sigma_{\theta}$  by ten percent. This calculation only yields the sensitivity of the calculated fluxes to biases in the values of  $\sigma_{\theta}$ ; it does not, of course, test the accuracy of the approximation of  $R_a$  used in Equation (14).

Table 40 shows the resulting sensitivities to  $\sigma_{\theta}$ . The values of the calculated  $\text{HNO}_3$  fluxes changed by about five to ten percent in response to variations of  $\pm 10$  percent in  $\sigma_{\theta}$ . The values of the fluxes of the other chemical species were not sensitive to the ten percent variation in sigma theta.

Table 40. Sensitivity of mean annual dry deposition ( $\text{kg ha}^{-1}$ ) to ten percent decreases and increases in  $\sigma_{\Theta}$ .

Site	Species	$\sigma_{\Theta}$		
		-10 percent	Measured	+10 percent
Azusa	SO <sub>2</sub>	1.915	1.934	1.947
	O <sub>3</sub>	20.726	20.950	21.117
	HNO <sub>3</sub>	78.928	87.636	95.773
	NO <sub>2</sub>	19.028	19.185	19.299
	NH <sub>3</sub>	2.067	2.094	2.113
	pNO <sub>3</sub> <sup>-</sup>	1.442	1.516	1.580
	pSO <sub>4</sub> <sup>2-</sup>	1.451	1.549	1.637
	pNH <sub>4</sub> <sup>+</sup>	0.711	0.753	0.790
Bakersfield	SO <sub>2</sub>	2.712	2.725	2.734
	O <sub>3</sub>	18.602	18.683	18.737
	HNO <sub>3</sub>	29.968	32.174	33.791
	NO <sub>2</sub>	9.263	9.301	9.328
	NH <sub>3</sub>	3.777	3.796	3.809
	pNO <sub>3</sub> <sup>-</sup>	2.851	2.955	3.031
	pSO <sub>4</sub> <sup>2-</sup>	1.058	1.097	1.124
	pNH <sub>4</sub> <sup>+</sup>	0.747	0.773	0.792
Fremont	SO <sub>2</sub>	0.729	0.734	0.737
	O <sub>3</sub>	11.037	11.114	11.161
	HNO <sub>3</sub>	5.394	5.990	6.427
	NO <sub>2</sub>	7.268	7.305	7.329
	NH <sub>3</sub>	1.127	1.137	1.144
	pNO <sub>3</sub> <sup>-</sup>	1.098	1.160	1.209
	pSO <sub>4</sub> <sup>2-</sup>	0.509	0.543	0.568
	pNH <sub>4</sub> <sup>+</sup>	0.192	0.204	0.213
Gasquet	SO <sub>2</sub>	0.229	0.231	0.233
	O <sub>3</sub>	21.262	21.582	21.861
	HNO <sub>3</sub>	0.898	0.946	0.989
	NO <sub>2</sub>	1.595	1.599	1.601
	NH <sub>3</sub>	0.716	0.722	0.727
	pNO <sub>3</sub> <sup>-</sup>	0.099	0.105	0.110
	pSO <sub>4</sub> <sup>2-</sup>	0.278	0.298	0.314
	pNH <sub>4</sub> <sup>+</sup>	0.049	0.053	0.056

Table 40. (continued)

Los Angeles	SO <sub>2</sub>	1.939	1.958	1.974
	O <sub>3</sub>	12.073	12.214	12.320
	HNO <sub>3</sub>	52.554	58.922	64.891
	NO <sub>2</sub>	17.784	17.985	18.135
	NH <sub>3</sub>	2.083	2.111	2.133
	pNO <sub>3</sub> <sup>-</sup>	1.035	1.100	1.161
	pSO <sub>4</sub> <sup>2-</sup>	1.352	1.454	1.546
	pNH <sub>4</sub> <sup>+</sup>	0.652	0.697	0.738
Long Beach	SO <sub>2</sub>	3.070	3.096	3.115
	O <sub>3</sub>	10.493	10.587	10.654
	HNO <sub>3</sub>	19.210	21.235	22.950
	NO <sub>2</sub>	17.892	18.087	18.234
	NH <sub>3</sub>	1.914	1.937	1.954
	pNO <sub>3</sub> <sup>-</sup>	1.912	2.033	2.131
	pSO <sub>4</sub> <sup>2-</sup>	1.478	1.573	1.648
	pNH <sub>4</sub> <sup>+</sup>	0.684	0.726	0.759
Sacramento	SO <sub>2</sub>	1.215	1.224	1.231
	O <sub>3</sub>	12.705	12.795	12.858
	HNO <sub>3</sub>	12.910	13.853	14.649
	NO <sub>2</sub>	8.594	8.650	8.690
	NH <sub>3</sub>	2.762	2.791	2.813
	pNO <sub>3</sub> <sup>-</sup>	1.372	1.439	1.493
	pSO <sub>4</sub> <sup>2-</sup>	0.530	0.557	0.579
	pNH <sub>4</sub> <sup>+</sup>	0.365	0.384	0.400
Sacramento collocated	SO <sub>2</sub>	1.129	1.136	1.142
	O <sub>3</sub>	12.718	12.808	12.872
	HNO <sub>3</sub>	14.442	15.562	16.486
	NO <sub>2</sub>	7.630	7.669	7.695
	NH <sub>3</sub>	2.558	2.580	2.596
	pNO <sub>3</sub> <sup>-</sup>	1.256	1.308	1.347
	pSO <sub>4</sub> <sup>2-</sup>	0.558	0.587	0.610
	pNH <sub>4</sub> <sup>+</sup>	0.395	0.415	0.432

Table 40. (concluded)

Santa Barbara	SO <sub>2</sub>	0.477	0.479	0.481
	O <sub>3</sub>	17.006	17.116	17.191
	HNO <sub>3</sub>	11.134	12.482	13.608
	NO <sub>2</sub>	4.443	4.474	4.495
	NH <sub>3</sub>	0.452	0.455	0.458
	pNO <sub>3</sub> <sup>-</sup>	0.387	0.409	0.425
	pSO <sub>4</sub> <sup>2-</sup>	0.961	1.024	1.077
	pNH <sub>4</sub> <sup>+</sup>	0.301	0.321	0.338
Sequoia	SO <sub>2</sub>	0.329	0.336	0.342
	O <sub>3</sub>	29.257	29.822	30.289
	HNO <sub>3</sub>	2.312	2.715	3.091
	NO <sub>2</sub>	0.046	0.047	0.047
	NH <sub>3</sub>	0.504	0.513	0.520
	pNO <sub>3</sub> <sup>-</sup>	0.291	0.318	0.343
	pSO <sub>4</sub> <sup>2-</sup>	0.293	0.321	0.347
	pNH <sub>4</sub> <sup>+</sup>	0.122	0.133	0.144
Yosemite	SO <sub>2</sub>	0.229	0.233	0.236
	O <sub>3</sub>	32.782	33.113	33.388
	HNO <sub>3</sub>	2.070	2.455	2.868
	NO <sub>2</sub>	0.007	0.007	0.007
	NH <sub>3</sub>	0.276	0.282	0.287
	pNO <sub>3</sub> <sup>-</sup>	0.092	0.101	0.110
	pSO <sub>4</sub> <sup>2-</sup>	0.265	0.295	0.324
	pNH <sub>4</sub> <sup>+</sup>	0.066	0.073	0.080

---



## PART III: SYNTHESIS

### SUMMARY

#### Wet Deposition

Wet sulfate and nitrate deposition were each less than  $8 \text{ kg ha}^{-1} \text{ yr}^{-1}$ ; excess sulfate, ammonium, and calcium deposition were less than  $3 \text{ kg ha}^{-1} \text{ yr}^{-1}$ . For comparison, wet sulfate and nitrate deposition in portions of eastern North America exceed  $25$  and  $15 \text{ kg ha}^{-1} \text{ yr}^{-1}$ , respectively (Sisterson, 1991); ammonium and calcium deposition are less than about  $4$  and  $2.5 \text{ kg ha}^{-1} \text{ yr}^{-1}$  in almost all parts of eastern North America (Sisterson, 1991).

In some areas where sulfate deposition is highest, such as the northwest coast, much of the sulfate had its origin as sea salt.

In most years, wet nitrate deposition was greater in the SoCAB and the southern Sierra Nevada than in other parts of California.

Deposition uncertainties are less than 20 percent in the SoCAB, which has a large number of monitors; uncertainties can be up to 100 percent in portions of northeastern and southeastern California, where little monitoring has been done.

To facilitate comparison with dry deposition estimates, Table 41 summarizes wet deposition rates for sulfur and nitrogen (as S and N).

Table 41. Mean annual wet deposition of sulfate (as S, not adjusted for sea salt), nitrate (as N), ammonium (as N), total nitrogen, and calcium by site ( $\text{kg ha}^{-1} \text{ yr}^{-1}$ ). Data for a given year were included only if CI1 and CI3 were each at least 75 percent. NADP sites are capitalized.

Site	Years	S	$\text{NO}_3^- \text{ (N)}$	$\text{NH}_4^+ \text{ (N)}$	N	Calcium
Anaheim	5	0.62	0.46	0.66	1.12	0.39
Ash Mountain	6	0.75	1.25	1.60	2.85	0.64
Bakersfield	6	0.64	0.44	0.85	1.29	0.41
Berkeley	5	0.94	0.57	0.47	1.03	0.69
Bethel Island	6	0.41	0.43	0.89	1.32	0.35
CHUCHUPATE	5	0.43	0.46	0.30	0.76	0.27
DAVIS	5	0.45	0.49	1.02	1.51	0.16
El Monte	6	1.03	0.82	1.04	1.86	0.51
Escondido	6	0.76	0.50	0.51	1.01	0.80
Eureka	4	1.64	0.30	0.35	0.65	1.21
Gasquet	6	2.23	0.50	0.60	1.10	1.94
GIANT FOREST	5	0.72	1.00	1.15	2.15	0.39
Giant Forest	5	0.82	1.11	1.49	2.59	0.77
HOPLAND	7	0.56	0.38	0.29	0.67	0.23
Lake Isabella	5	0.30	0.35	0.32	0.67	0.33
Lakeport	4	0.56	0.49	0.74	1.23	0.41
Lindcove	3	0.53	0.88	1.52	2.40	0.50
Lynwood	6	1.11	0.60	0.79	1.40	0.44
MONTAGUE	6	0.20	0.23	0.21	0.44	0.12
Mammoth Mountain	1	0.68	0.63	0.69	1.32	0.67
Montague	5	0.23	0.28	0.31	0.59	0.26
Mt Wilson	6	0.87	0.89	0.70	1.59	0.68
Napa	5	1.14	0.74	0.78	1.52	0.49
Nipomo	4	0.57	0.31	0.39	0.70	0.42
ORGAN PIPE	7	0.57	0.36	0.34	0.70	0.34
PALOMAR MT.	4	1.02	0.68	0.42	1.10	0.51
Pasadena	6	1.16	1.16	1.05	2.21	0.64
Quincy	3	0.66	0.66	0.50	1.16	0.67
RED ROCK CANYON	5	0.32	0.40	0.27	0.67	0.71
Reseda	6	0.77	0.80	0.71	1.52	0.43
S Lake Tahoe	6	0.39	0.43	0.36	0.78	0.41
SILVER LAKE	4	0.21	0.19	0.11	0.30	0.16
SMITH VALLEY	6	0.20	0.21	0.27	0.48	0.16
Sacramento	6	0.74	0.82	1.66	2.48	0.41
Salinas	4	0.45	0.27	0.50	0.77	0.33
San Bernardino	6	0.69	0.90	1.57	2.46	0.71
San Jose	6	0.54	0.29	0.50	0.79	0.45
San Nicolas	4	0.65	0.17	0.13	0.30	0.60
San Rafael	3	1.67	0.87	1.08	1.95	0.97
Santa Barbara	6	0.62	0.61	0.34	0.96	0.40
Soda Springs	5	0.92	0.99	0.82	1.81	0.90
TANBARK FLAT	6	0.94	1.05	0.67	1.72	0.37
Tanbark Flat	6	1.01	1.31	1.02	2.33	0.67
Victorville	4	0.36	0.49	0.50	0.99	0.89
YOSEMITE	2	0.93	0.96	0.94	1.90	0.42
Yosemite	4	0.70	0.97	0.98	1.96	0.71

## Dry Deposition

This project has produced new estimates of dry-deposition fluxes at 10 sites in California. These estimates will help improve our understanding of the magnitude of dry deposition in California. However, it is important to recognize that the calculations are limited in numerous important respects and that they could likely be improved over time with additional effort. The dry-deposition flux estimates are subject to uncertainties of approximately 50 percent.

CADMP samples are now collected over 12-hour intervals.  $\text{HNO}_3$  fluxes would be underestimated by 30 to 40 percent at all sites except Gasquet if samples were collected as 24-hour averages rather than 12-hour averages (at Gasquet,  $\text{HNO}_3$  was frequently below detection limits).  $\text{O}_3$  fluxes would be underestimated by seven to 23 percent at all sites except Sequoia and Yosemite if samples were collected as 24-hour averages rather than 12-hour averages (Sequoia and Yosemite showed very weak diurnal variations in ozone concentration).

Estimated deposition of  $\text{HNO}_3$  at the 10 sites ranges from 1 to 87  $\text{kg ha}^{-1} \text{ yr}^{-1}$ . At the urban sites,  $\text{HNO}_3$  deposition accounts for 50 to 80 percent of the deposition of oxidized nitrogen species and 40 to 70 percent of the total nitrogen deposition. ✓

To facilitate comparison with wet deposition fluxes, Table 42 shows estimates for total sulfur and nitrogen dry deposition (as S and N). Annual rates of deposition of oxidized nitrogen species at the three rural sites are about one-tenth to one-half as great as the values reported by Meyers et al. (1991), which ranged from 1.5 to 4.6  $\text{kg ha}^{-1}$  for sites in the eastern United States. The deposition rates calculated for the rural CADMP sites are quite uncertain because many of the measurements were below the limits of quantification (see Tables 15 and 16). The deposition rates at Azusa, Bakersfield, Long Beach, and Los Angeles exceed those reported by Meyers et al. (1991) by factors of 2 to 17.

Table 42. Mean annual dry deposition of sulfur and nitrogen ( $\text{kg ha}^{-1}$ ).

Site	Oxidized Nitrogen	Reduced Nitrogen	Total Nitrogen	$\text{SO}_2(\text{S})$	Sulfate(S)	Total S
Azusa	25.67	2.31	27.97	0.97	0.52	1.49
Bakersfield	10.65	3.72	14.37	1.36	0.37	1.73
Fremont	3.82	1.09	4.91	0.37	0.18	0.55
Gasquet	0.72	0.63	1.36	0.12	0.10	0.22
Los Angeles	18.82	2.28	21.10	0.98	0.49	1.47
Long Beach	10.69	2.16	12.84	1.55	0.53	2.08
Sacramento	6.04	2.59	8.63	0.61	0.19	0.80
Sacramento collocated	6.09	2.44	8.53	0.57	0.20	0.76
Santa Barbara	4.23	0.62	4.85	0.24	0.34	0.58
Sequoia	0.69	0.53	1.21	0.17	0.11	0.28
Yosemite	0.57	0.29	0.86	0.12	0.10	0.21

### Comparison of Wet and Dry Deposition

Six of the 10 dry-deposition sites are collocated with wet-deposition monitors. The dry-deposition sites at Azusa, Fremont, downtown Los Angeles, and Long Beach are not collocated with wet-deposition monitors. For purposes of comparison, we paired these four sites with the precipitation sites at El Monte, San Jose, Pasadena, and Lynwood. Of the 10 locations with paired wet- and dry-deposition data, three are nonurban (Gasquet, Yosemite, and Sequoia).

At the three nonurban sites, wet nitrate and sulfate deposition approximately equalled or slightly exceeded dry deposition of oxidized nitrogen and sulfur species (compare Tables 41 and 42). In contrast, dry sulfur deposition at the urban sites was approximately 1 to 3 times the magnitude of wet sulfur deposition. At the urban sites, dry deposition of oxidized nitrogen species ranged from about 5 to 30 times the magnitude of wet nitrate deposition. At all sites, dry deposition of reduced nitrogen species (ammonia and particulate ammonium) was about a factor of 2 greater than wet ammonium deposition.

Despite the large estimated uncertainties in the dry deposition estimates, dry deposition of sulfur and nitrogen can be seen to range from approximately equal to wet

deposition to many times greater.

### Comparison of Deposition and Emissions Estimates

In this section, we compare our dry-deposition flux estimates to emission estimates. Emission densities of  $\text{NO}_x$  (as  $\text{kg ha}^{-1} \text{ yr}^{-1} \text{ N}$ ) are as follows (California Air Resources Board, Technical Support Division, 1990):

- Sacramento Valley: 4.7;
- San Joaquin Valley: 6.5;
- San Francisco area: 30;
- SoCAB: 49.

Although several pieces of evidence suggest that emissions of volatile organic compounds (VOCs) may typically be underestimated by a factor of 2 (e.g., Fujita et al., 1992),  $\text{NO}_x$  emission estimates are generally thought to be more accurate.

Comparison of the values in Table 42 to these emission densities indicates that the deposition rates of oxidized nitrogen species equal the following percentages of the emissions rates:

- Azusa: 52;
- Fremont: 13;
- Los Angeles: 38;
- Long Beach: 22;
- Bakersfield: 160;
- Sacramento: 130.

Addition of the wet-deposition fluxes would increase these values by 1 to 8 percentage points. The comparison suggests that a substantial portion of the SoCAB emissions of  $\text{NO}_x$  would be deposited within the basin. In contrast, total (wet plus dry) nitrogen deposition within the San Francisco Bay area appears to be less than about 20 percent of emissions. However, only one dry-deposition site was monitored (Fremont); at one time, this site recorded peak ozone concentrations in the Bay area, but, in recent years, the peaks have shifted to Livermore. Thus, concentrations of photochemical reaction products (including  $\text{HNO}_3$ ) may be greater at other locations within the Bay area, implying that deposition rates in parts of the Bay area may also be greater than those calculated for Fremont. As shown, the estimated nitrogen deposition rates at Bakersfield and Sacramento exceed the emissions rates of the San Joaquin and Sacramento air basins. However, these basins are large and they include much rural or mountainous land; emissions would be more concentrated in the urban areas, where the monitoring sites were located. From the limited number of monitoring sites, it does not appear possible to estimate a nitrogen flux from the Bay area to the Central Valley. Transport of  $\text{NO}_x$  from the Bay area to the Central Valley is known to occur (Roberts and Main, 1989).

## LIMITATIONS

Wet-deposition flux estimates are based on data obtained using a proven monitoring technique and a reasonably dense network of stations. The most significant source of potential bias is underestimation of precipitation amounts in alpine regions. As noted, we were unable to make use of data from the alpine network because its period of record barely overlapped that of the CADMP data; however, in future years, the alpine-network data will be available for use. The uncertainties in our regionalized estimates of wet deposition vary spatially and among chemical species; they are typically in the range of 20 to 50 percent for the species and areas of greatest interest.

In contrast, both the measurements and the model used to calculate dry deposition are subject to potentially large uncertainties. At present, outstanding questions remain regarding the accuracy of the denuder difference  $\text{HNO}_3$  concentrations. Moreover, the expected uncertainties in dry deposition flux estimates calculated according to the inferential method are on the order of 50 percent.

It is premature to attempt to regionalize the dry deposition estimates. Because 30 to 70 percent of the dry nitrogen deposition occurred via deposition of  $\text{HNO}_3$ , it is first necessary to establish the accuracy of the  $\text{HNO}_3$  measurements. Measurements of particulate sulfate and nitrate,  $\text{SO}_2$ , and  $\text{NO}_2$  are available from a large number of monitors in California; these measurements may be of use in generalizing the dry deposition estimates. The necessary meteorological measurements do not exist at routine monitoring sites; however, such data might be of use in bounding the dry deposition of rates of these species. In contrast to these routinely available measurements, no routine measurements of  $\text{HNO}_3$  exist. It may prove possible to estimate  $\text{HNO}_3$  concentrations from other measurements, such as ozone, nitrate, ammonium, and meteorological variables. Regression of denuder difference and filter-pack nitrate against ozone, PM10 nitrate,  $\text{NO}_2$ , and PM10 ammonium yielded modest relationships ( $r^2$  of 0.3 to 0.5) with standard errors of 2 to 4  $\mu\text{g m}^{-3}$ , implying that considerable uncertainty would occur in estimating  $\text{HNO}_3$  concentrations unless reasonably exact representation of key physical processes were incorporated into the estimation procedure.

## RECOMMENDATIONS

We offer the following recommendations for consideration:

1. Particular effort should be devoted to resolving the questions pertaining to accurate measurement of nitric acid. At many locations, it is the largest component of total nitrogen deposition. Therefore, accurate measurement is critical.
2. The  $\text{HNO}_3$  fluxes calculated for 24-hour intervals were 30 to 40 percent lower than

those calculated for 12-hour intervals at 9 of the 10 sites. If the CADMP dry-deposition sampling interval were increased from 12 to 24 hours, methods should be developed for correcting the resulting underestimation of  $\text{HNO}_3$  deposition.

3. Comparison of results obtained from application of the inferential method and from micrometeorological studies would be highly desirable. Lacking such a comparison, we cannot evaluate the accuracies of the calculated deposition amounts.
4. Approximately three additional years of wet and dry deposition data, now being validated, will become available soon. Consideration should be given to updating the wet deposition estimates and, pending resolution of measurement questions, the dry deposition estimates as well.
5. If analyses of trends are of interest, they should be carried out for the ambient air concentrations, rather than the calculated dry-deposition fluxes, because many uncertainties are introduced in the process of calculating fluxes.



## REFERENCES

- P. R. Bevington and D. Keith Robinson. Data Reduction and Error Analysis for the Physical Sciences, 2nd ed. New York NY: McGraw-Hill, Inc., 1992. 328 pp.
- D. S. Bigelow. Quality Assurance Report NADP/NTN Deposition Monitoring: Field Operations, July 1978 Through December 1983. Ft. Collins CO: National Atmospheric Deposition Program, 1986.
- D. S. Bigelow, D. L. Sisterson, and L. J. Schroder. 1989. An interpretation of differences between field and laboratory pH values reported by the National Atmospheric Deposition Program/National Trends Network monitoring program. Environ. Sci. Technol. 23: 881-887.
- C. L. Blanchard and K. A. Tonnessen. 1993. Precipitation-chemistry measurements from the California Acid Deposition Monitoring Program, 1985-1990. Atmos. Environ. 27A(11): 1755-1763.
- California Air Resources Board (Monitoring and Laboratory Division). Quality Assurance Report for the 1985 - 86 Hydrological Year (July 1985 - June 1986). Sacramento CA: California Air Resources Board, February 1987.
- California Air Resources Board (Monitoring and Laboratory Division). Quality Assurance Report for the 1986 - 87 Hydrological Year (July 1986 - June 1987). Sacramento CA: California Air Resources Board, June 1988.
- California Air Resources Board (Monitoring and Laboratory Division). Quality Assurance Report for the 1987 - 88 Hydrological Year (July 1987 - June 1988). Sacramento CA: California Air Resources Board, 1989.
- California Air Resources Board (Monitoring and Laboratory Division). Quality Assurance Report on Wet Acid Deposition for the 1988/89 Hydrological Year (July 1988 - June 1989). Sacramento CA: California Air Resources Board, July 1990.
- California Air Resources Board (Technical Support Division). Emission Inventory, 1987. Sacramento CA: California Air Resources Board, March 1990.
- R. M. Cionco. 1972. A wind-profile index for canopy flow. Boundary Layer Meteorology. 3: 255-263.
- R. M. Cionco. 1978. Analysis of canopy index values for various canopy densities. Boundary Layer Meteorology. 15: 81-93.
- J. F. Clarke, E. S. Edgerton, and R. P. Boksleitner. 1992. Routine estimation and reporting

- of dry deposition for the U.S.A. dry deposition network. U.S. Environmental Protection Agency, Research Triangle Park, NC 27711.
- J. F. Collins, J. R. Young, A. A. Huang, M. D. Zeldin, and E. C. Ellis. Analysis of precipitation chemistry variability in southern California. Paper no. 87-35A.3. Presented at the 80th Annual Meeting of the Air Pollution Control Association, New York NY, June 21-26, 1987.
- A. H. El-Shaarawi. 1989. Inferences about the mean from censored water quality data. Water Resources Research 25: 686-690.
- E. Englund and A. Sparks. GEO-EAS 1.2.1: Geostatistical Environmental Assessment Software, User's Guide. EPA 600/8-91/008. Las Vegas, NV: U.S. Environmental Protection Agency, 1991.
- B. P. Eynon. 1988. Statistical analysis of precipitation chemistry measurements over the Eastern United States. Part II: Kriging analysis of regional patterns and trends. J. App. Meteor. 27: 1334-1343.
- V. V. Federov. 1989. Kriging and other estimators of spatial field characteristics (with special reference to environmental studies). Atmos. Environ. 23(1): 175-184.
- E. M. Fujita, B. E. Croes, C. L. Bennett, D. R. Lawson, F. W. Lurmann, and H. H. Main. 1992. Comparison of emission inventory and ambient concentration ratios of CO, NMOG, and NO<sub>x</sub> in California's South Coast Air Basin. J. Air Waste Manag. Assoc. 42: 264-276.
- R. J. Gilliom and D. R. Helsel. 1986. Estimation of distributional parameters for censored trace level water quality data. 1. Estimation techniques. Water Resources Research 22(2): 135-146.
- K. Guertin, J. Villeneuve, and S. Deschenes. 1988. The choice of working variables in the geostatistical estimation of the spatial distribution of ion concentration from acid precipitation. Atmos. Environ. 22(12): 2787-2801.
- T. C. Haas. 1990. Kriging and automated variogram modeling within a moving window. Atmos. Environ. 24A(7): 1759-1769.
- T. C. Haas. 1992. Redesigning continental-scale networks. Atmos. Environ. 26A(18): 3323-3333.
- B. B. Hicks, D. D. Baldocchi, T. P. Meyers, R. P. Hosker, Jr., and D. R. Matt. 1987. A preliminary multiple resistance routine for deriving dry deposition velocities from measured quantities. Wat. Air Soil Pollut. 36:311-330.

- B. B. Hicks, R. P. Hosker, Jr., T. P. Meyers, and J. D. Womack. 1991. Dry deposition inferential measurement techniques - I. Design and tests of a prototype meteorological and chemical system for determining dry deposition. Atmos. Environ. 25A(10): 2345-2359.
- J. A. Horrocks and J. D. Kowalski. 1987. A computerized quality control method for the validation of wet deposition laboratory analysis. Paper no. 87-91.2. American Waste Management Association Annual Meeting.
- A. G. Journel and C. Huijbregts. Mining Geostatistics. New York NY: Academic Press, 1979. 600 pp.
- A. G. Journel. Fundamentals of Geostatistics in Five Lessons. Washington DC: American Geophysical Union, 1989. 41 pp.
- S. Kokoska and C. Nevison. Statistical Tables and Formulae. New York: Springer-Verlag, 1989. 88 pp.
- J. M. Lockard. Quality Assurance Report NADP/NTN Deposition Monitoring: Laboratory Operations, July 1978 Through December 1983. Ft. Collins, CO: National Atmospheric Deposition Program, 1987.
- R. T. McMillen. 1990. Estimating the spatial variability of trace gas deposition velocities. National Oceanic and Atmospheric Administration Technical Memorandum ERL ARL-181.
- T. P. Meyers and T. S. Yuen. 1987. An assessment of averaging strategies associated with day/night sampling of dry-deposition fluxes of SO<sub>2</sub> and O<sub>3</sub>. J. Geophys. Res. 92(D6): 6705-6712.
- 1991.
- T. P. Meyers, B. B. Hicks, R. P. Hosker, Jr., J. D. Womack, and L. C. Satterfield. Dry deposition inferential measurement techniques - II. Seasonal and annual deposition rates of sulfur and nitrogen. Atmos. Environ. 25A(10): 2361-2370.
- G. W. Oehlert. 1993. Regional trends in sulfate wet deposition. JASA 88(422): 390-399.
- J. L. Peden. Quality Assurance Report NADP/NTN Deposition Monitoring: Laboratory Operations, January 1984 Through December 1985. Ft. Collins CO: National Atmospheric Deposition Program, 1988.
- B. D. Ripley. Spatial Statistics. New York NY: John Wiley & Sons, 1981.
- P. Roberts and H. Main. The Measurement of Pollutant and Meteorological Boundary Conditions: Technical Support Study 10. Prepared for San Joaquin Valley Air

- Pollution Study Agency, c/o California Air Resources Board, Technical Support Division, Sacramento CA, 1989.
- P. Saxena, T. D. Arcado, B. L. Marler, and S. L. Altshuler. Acid precipitation chemistry in an urban plume. Paper no. 87-35A.4. Presented at the 80th Annual Meeting of the Air Pollution Control Association, New York NY, June 21-26, 1987.
- R. B. See, L. J. Schroder, and T. C. Willoughby. External Quality-Assurance Results for the National Atmospheric Deposition Program and the National Trends Network During 1987. Water-Resources Investigations report 89-4015. Denver, CO: U.S. Geological Survey, 1989.
- S. K. Seilkop and P. L. Finkelstein. 1987. Acid precipitation patterns and trends in eastern North America, 1980 - 84. J. Climate and App. Meteor. 26: 980-994.
- J. Seinfeld. Atmospheric Chemistry and Physics of Air Pollution. New York: John Wiley & Sons, 1986. 738 pp.
- R. H. Shaw and A. R. Pereira. 1982. Aerodynamic roughness of a plant canopy: a numerical experiment. Agricultural Meteorology 26: 51-65
- A. Sirois. 1990. The effects of missing data on the calculation of precipitation-weighted-mean concentrations in wet deposition. Atmospheric Environment 24A(9): 2277-2288.
- D. L. Sisterson. Deposition monitoring: methods and results. In: Acidic Deposition: State of Science and Technology, Summary Report of the U.S. National Acid Precipitation Assessment Program. P. M. Irving, ed. Washington DC: National Acid Precipitation Assessment Program, 1991.
- P. A. Solomon, T. Fall, L. Salmon, P. Lin, F. Vasquez, and G. R. Cass. Acquisition of Acid Vapor and Aerosol Concentration Data for Use in Dry Deposition Studies in the South Coast Air Basin. ARB Research Contract No. A4-144-32. Sacramento CA: California Air Resources Board, 1988.
- W. Stumm and J. J. Morgan. Aquatic Chemistry: An Introduction Emphasizing Chemical Equilibria in Natural Waters, 2nd ed. New York NY: John Wiley & Sons, 1981. 780 pp.
- A. Venkatram. 1988. On the use of kriging in the spatial analysis of acid precipitation data. Atmos. Environ. 22: 1963-1975.
- J. G. Watson, J. C. Chow, R. T. Egami, J. L. Bowen, C. A. Frazier, A. W. Gertler, D. H. Lowenthal, and K. Fung. Dry Deposition measurements for the California Acid

Deposition Monitoring Program. Contract number A6-076-32. Sacramento, CA: California Air Resources Board, 1991.

- M. L. Wesely. 1989. Parameterization of surface resistances to gaseous dry deposition in regional-scale numerical models. Atmos. Environ. 23: 1293-1304.
- M. L. Wesely and B. M. Lesht. 1989. Comparison of RADM dry deposition algorithms with a site-specific method for inferring dry deposition. Wat. Air Soil Pollut. 44: 273-293.
- M. D. Zeldin and E. C. Ellis. Trends in precipitation chemistry in southern California. Paper no. 84-19.6. Presented at the 77th Annual Meeting of the Air Pollution Control Association, San Francisco CA, June 24-29, 1984.

